The Get3 ATPase Drives Unidirectional Targeting of Tail-Anchored Membrane Proteins

Thesis by
Michael E. Rome

In Partial Fulfillment of the Requirements for the degree
of
Doctor of Philosophy

CALIFORNIA INSTITUTE OF TECHNOLOGY
Pasadena, California
2014
(Defended April 15th)

ACKNOWLEDGEMENTS

I would first like to thank my advisor Shu-ou Shan for providing an outstanding graduate school experience. I regard Shu-ou as one of the best scientists and deepest thinkers I have ever met. During my time at Caltech, I feel I have grown tremendously as a scientist and Shu-ou is primarily responsible for this. I would also like to thank the other members of my committee: David Chan, for serving as my committee chair and for his continued guidance since I first rotated in his lab (also the exciting and fruitful collaboration with both him and Oliver Losón); Judith Campbell, for providing critical feedback on projects and for being a generous lab neighbor; Pamela Bjorkman, for her razor sharp focus (and wit) during my committee meetings; and Bil Clemons, for being an outstanding collaborator and role model. Bil has always been supremely generous, supportive and critical (in a good way!)- for this I am grateful. Additionally, I want to thank Andre Holtz for productive discussions and shenanigans, Ray Deshaies for sharing his vast scientific knowledge, and the entire Caltech biology and chemistry departments- truly world class!

I want to also express my deepest gratitude to the amazing mentors I had during my time at UCLA: Salvatore Stella and Nicholas Brecha, for showing me how much fun bench work can be, and Peter Bradley, for being an incredible mentor and for instilling in me a great work ethic.

I would like to acknowledge the wonderful collaborators I have been fortunate to work with. First, I would like to acknowledge The GET team at Caltech, specifically: Meera Rao, for being an excellent bay mate, providing rigorous scientific discussions and for the very productive collaboration we have enjoyed; Harry Gristick, for his amazing

structural work, sound technical skills and comic relief; Justin Chartron, for solving many important structures in the field and providing countless reagents; Un-Seng Chio, for assistance with the Get3 directionality paper; Amanda Mock, for the Mock Bag domain; and Christian Suloway, for reagents and including me in the first tetramer story.

I would also like to thank the outstanding lab mates I have had throughout the years: Sowmya Chandrasekar, David Akopian, Aileen Ariosa, George Liang, Hwang Fu, Jae Ho Lee, Camille McAvoy, Samantha Piszkiewicz, Xin Zhang, Vinh Lam, Dennis Woo, Peera Jaru-Ampornpan, Dawei Zhang, Nathan Pierce, Thang Nguyen, Kuang Shen, Ishu Saraogi, Natalie Kolawa, Tara Gomez, Kuang-Jung Chang, Willem den Besten, Ruzbeh Mosadeghi, Narimon Honarpour, Senthil Radhakrishnan, Rati Verma, Ethan Emberley, Gary Kleiger, Anjanabha Saha, and Tobias Stuwe. I am really sorry if I left anyone out!

I want to thank the wonderful group of friends and classmates I have had during my time at Caltech: Eric Erkenbrack, Jennifer Wellman, Jon Valencia, Alex Webster, Weston Nichols, Rob Oania, Nate Pierce, Adler Dillman, Ned Perkins, Paul Minor, Brandon Wadas, Arya Khosravi, Chinny Idigo, Kathy Shafer, Danielle Brown, Justin Liu, Anna Abelin, Amit Lakhanpal, the entire 2008 biology and BMB class, Samy Hamdouche, Oliver Losón, Stefan Materna, Andy Ransick, Mike Collins, Sagar Damle. Again, sorry if I left you out!

I want to thank the very accommodating administration and staff at Caltech: Liz Ayala, Margot Hoyt, Santiago, and Joe Drew. Caltech truly has the best personnel I have seen at any institution.

I want to thank my family for their amazing and unwavering support. I cannot begin to express how much I owe my parents. I have so much gratitude that I promise not to put

you both into an old folks' home! Mom, for her love, guidance and for always laughing at my jokes; Lenny (dad), for being the person I look up to the most- Lenny not only inspired me to be the best person I can be, but also showed me the awe-inspiring ways of science; Jordan and Amy, for showing me how awesome married life can be and for just being awesome in general; Zachary, for being a "sizick" dude and for always lending his support; Grandma Allie, for being the best; Odelia, for also being the best; and Maya, for being a big brown chocolate labrador retriever.

Last, but certainly not least, I want to thank Tara Guillozet- she is my wife (in Borat's voice). Tara, you've been my biggest enthusiast and have given me unconditional support throughout my graduate experience. I owe you so much- mainly for putting up with my annoying jokes, character personas, and tendency to steal the blanket. I really could not have done it without you. Thank you for everything, I love you!

ABSTRACT

Efficient and accurate localization of membrane proteins is essential to all cells and requires a complex cascade of interactions between protein machineries. This is exemplified in the recently discovered Guided Entry of Tail-anchored protein pathway, in which the central targeting factor Get3 must sequentially interact with three distinct binding partners (Get4, Get1 and Get2) to ensure the targeted delivery of Tail-anchored proteins to the endoplasmic reticulum membrane. To understand the molecular and energetic principles that provide the vectorial driving force of these interactions, we used a quantitative fluorescence approach combined with mechanistic enzymology to monitor the effector interactions of Get3 at each stage of Tail-anchored protein targeting. We show that nucleotide and membrane protein substrate generate a gradient of interaction energies that drive the cyclic and ordered transit of Get3 from Get4 to Get2 and lastly to Get1. These data also define how the Get3/Tail-anchored complex is captured, handed over, and disassembled by the Get1/2 receptor at the membrane, and reveal a novel role for Get4/5 in recycling Get3 from the endoplasmic reticulum membrane at the end of the targeting reaction. These results provide general insights into how complex cascades of protein interactions are coordinated and coupled to energy inputs in biological systems.

TABLE OF CONTENTS

Chapter 1:

Introduction

Proteins containing transmembrane domains (TM or TMD) comprise ~30% of the proteome and carry out essential functions in all cells. Across all kingdoms of life, conserved protein-targeting machineries ensure the accurate and efficient localization of membrane proteins to various cellular compartments. Although the well-characterized co-translational Signal Recognition Particle (SRP) pathway delivers numerous Endoplasmic Reticulum (ER)-destined proteins, many membrane proteins utilize post-translational targeting pathways whose mechanisms remain elusive. A recent example is tail-anchored (TA) proteins[1,2], which contain a TMD at the end of their C-terminus. TA proteins comprise a significant subset of the eukaryotic membrane proteome and play essential roles in numerous processes including protein translocation, vesicular trafficking, protein homeostasis, and programmed cell death [3]. Due to the location of the TMD at the end of the protein coding sequence, TA proteins cannot utilize the co-translational SRP pathway and instead must use post-translational pathways for correct localization to their cellular compartment.

In the newly discovered Guided Entry of Tail-anchored protein (GET) pathway, a sophisticated set of protein machineries facilitates the delivery of TA proteins to the ER membrane **(**Figure 1**)**. Targeting via the Get pathway results in a topology where the C-terminus of TA proteins is in the lumen of the ER and the N-terminus is facing the cytosol. Once at the membrane, TA proteins are either retained in the ER bilayer or further trafficked to their final destination using the targeting machinery of the secretory pathway.

After protein translation is complete, TA proteins are initially bound by the yeast protein chaperone Sgt2 [4] (or metazoan SGTA, step1). The Get4/5 complex (or

mammalian TRC35/Ubl4a) then enables transfer of the TA substrate from Sgt2 onto Get3 (mammalian TRC40, step 2-3) [4,5]the primary chaperone in the GET pathway. The Get3/TA targeting-complex is then recognized by the Get1/2 receptor on the ER membrane (step 4). After stable association with Get1/2, TA protein is dislodged from Get3 and is inserted into the membrane bilayer [6-9](step 5). Release of Get3 from Get1/2 is then needed to recycle it for further rounds of TA targeting (step 6). The deletion of Get3 significantly compromises growth in budding yeast, and knockout of the Get3 homologue Trc40 results in embryonic death in mammals[6,10,11]. This provides strong evidence that the Get3/Trc40 component is absolutely required for proper cell function.

Figure 1. Overview of Tail-anchored protein targeting by the GET pathway in budding yeast. Details described in text. '?' highlight unresolved questions.

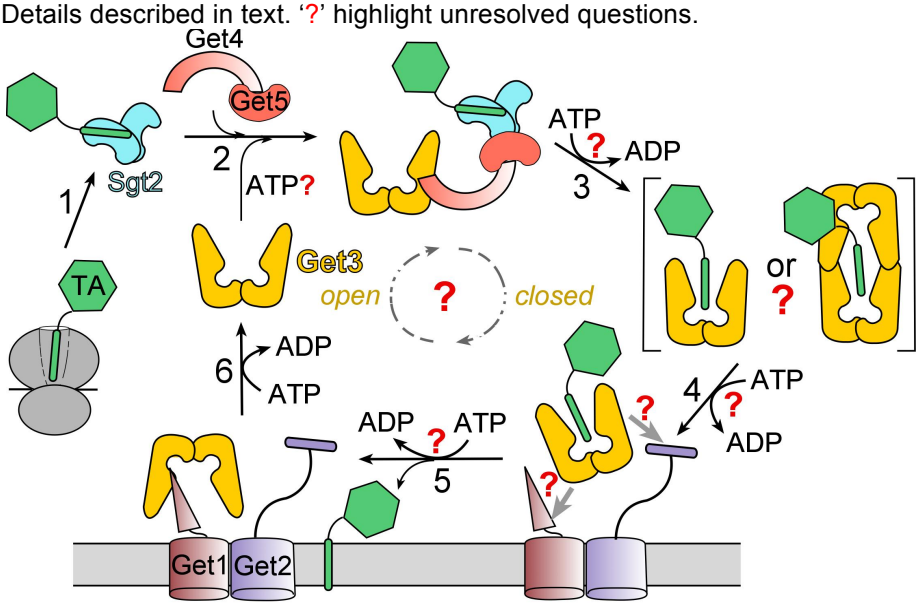

The GET pathway requires a complex cascade of substrate capture, loading, delivery, release, and insertion events, whose underlying molecular basis remains unclear. Many questions arise: given that Get3 has three distinct binding partners with overlapping binding sites (Get4, Get1 and Get2), what drives the unidirectionality of this pathway (Figure 2), and what ensures the spatial and temporal accuracy of these

interactions? How does Get3 detach from Get4/5? How is Get3 recognized by Get1/2? Why are two subunits required in the Get1/2 receptor, and how is Get3 recycled at the end of the targeting reaction?

Figure 2. The GET pathway directionality problem. Cartoon depiction of the molecular events that must take place in order for Get3 to transit from the cytosol to the ER membrane in a unidirectional manner.

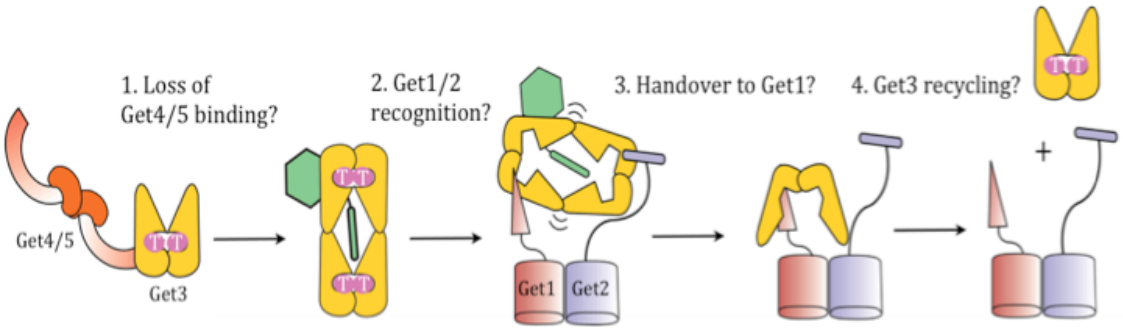

An important clue to addressing these issues is that the energy from ATP hydrolysis is required for TA targeting [6,7]. Through a series of seminal publications from the Hegde and Weissman groups [6,12], the ATP requirement was isolated to the Get3/TRC40 chaperone, a highly conserved ATPase homodimer that coordinates TA delivery in the GET pathway. Extensive structural work has revealed that nucleotide binding to Get3 regulates the conformation of its dimer interface, which leads to closure of its helical domains. This generates a range of structures, from open states in apo-Get3 in which the helical domains are spread apart, to more closed states in AMPPNP- or ADP•AlF4--bound Get3 in which the helical domains form a hydrophobic interface proposed to bind the TMD of TA substrates [2,13,14]. Moreover, the Get1 cytosolic domain has strong affinity for open, nucleotide-free Get3[8,9], demonstrating that Get3's conformational state is subject to regulation by its interaction-partners in the GET

pathway. These results suggest that the Get3 ATPase could couple nucleotide- and effector-induced changes in its dimer conformation to TA protein binding and release.

Despite a plethora of structural and genetic data, the molecular mechanisms responsible for Get3- dependent TA protein targeting are poorly understood. Until a recent publication from our lab[3], even basic information, such as when, where and how ATP binding and hydrolysis occur in this pathway, had not been addressed. Secondly, both open and closed conformations were observed with ADP- and Get2-bound Get3 [8,15], raising questions as to Get3's ability to specifically generate nucleotide- or effector-driven conformational changes. Thirdly, while the predominant model for TA protein binding invokes a closed Get3 dimer, there is also evidence for tetrameric Get3 [16] in which the TA substrate can be enclosed in a large hydrophobic chamber (Fig. 1, brackets). Whether and how a Get3 tetramer functions in TA protein targeting have been unclear. Most importantly, given the complex cascade of molecular events that must be coordinated by Get3, it is difficult to rationalize how Get3 is able to recognize its various effector proteins with a simple two-state (open to closed) conformational model. The goal of this thesis is to address these outstanding questions, in order to gain a deeper understanding of the energetic driving forces and molecular mechanisms that underlie this fundamental and essential cellular process.

Chapter 2

Precise Timing of ATPase Activation Drives Targeting of Tail-anchored Proteins

A version of this chapter was first published in PNAS (2013 May 7;110(19):7666-71), was written by Michael E. Rome, Meera Rao, William M. Clemons and, Shu-ou Shan.

Abstract

Tail-anchored (TA) proteins, whose transmembrane domain resides at their extreme C-terminus, comprise 3–5% of the membrane proteome and perform numerous essential cellular functions. Their proper localization requires sophisticated post-translational targeting mechanisms that are still poorly understood. In eukaryotic cells, the highly conserved ATPase Get3 coordinates the delivery of TA proteins to the endoplasmic reticulum (ER). How Get3 uses its ATPase cycles to drive this fundamental process remains elusive. Using mechanistic enzymology and biophysical methods, we establish a quantitative framework for the Get3 ATPase cycle and show that ATP specifically induces multiple conformational changes in Get3 that culminate in its ATPase activation through tetramerization. For the first time, we demonstrate that upstream and downstream components actively regulate the Get3 ATPase cycle. The Get4/5 TA loading complex, induces Get3 into a conformation in which it is locked in the ATP-bound state and primed for TA protein capture, whereas the TA substrate induces tetramerization of Get3 and activates its ATPase reaction 100-fold. Together, these allosteric regulations ensure the precise timing of ATP hydrolysis in the GET pathway. Our results establish a precise model for how Get3 harnesses the energy from ATP to drive the membrane localization of TA proteins, and provide new insights into how dimerization-activated nucleotide hydrolases regulate diverse cellular processes.

Proper localization of membrane proteins is essential for the structure and function of all cells. Tail-anchored (TA) proteins, which contain a single transmembrane domain at their extreme C-terminus, constitute 3-5% of the membrane proteome [1] and mediate diverse cellular processes including protein translocation, vesicular transport, and protein quality control [1,17]. Due to their topology, TA proteins cannot engage co-translational protein targeting machineries and instead must use post-translational mechanisms for efficient and accurate delivery to the target membrane [1,18].

Recent work identified the GET (Guided Entry of Tail-anchored proteins) pathway, in which a sophisticated protein interaction cascade mediates the delivery of TA proteins to the endoplasmic reticulum (ER) [1,6,12,17]. Following translation, TA proteins are initially captured by the chaperone Sgt2 in yeast [4,5] or the BAG6 complex in mammalian cells [19]. Sgt2 (or Bag6) then interacts with the Get4/5 complex (or its mammalian homologue TRC35/Ubl4a), which also binds the Get3 ATPase (or its mammalian homologue TRC40) [6,20]. Through mechanisms yet to be determined, Get4/5 enables the loading of TA protein from Sgt2 onto Get3, the central ATPase in the pathway [4,7]. The Get3/TA complex then binds its receptor, the Get1/2 complex on the ER membrane, upon which the TA protein is released from Get3 and inserted into the membrane [6,8,9].

TA protein insertion is an ATP-dependent process [18] driven by the Get3/TRC40 ATPase [6,12], a member of the SIMIBI class of nucleotide hydrolases that mediate diverse cellular processes [2]. Twenty-one Get3 structures, solved in various nucleotide states, suggest how nucleotide binding to Get3 can be coupled to TA protein binding and release. Get3 is an obligate homodimer [13,14], and nucleotide occupancy in its ATPase domain allows adjustments at the dimer interface that are amplified into larger displacements of

its helical domains. This leads to various structures, from open conformations in apo-Get3 in which the helical subdomains are separated, to more closed conformations in AMPPNP- or ADP•AlF_4^--bound Get3 in which the helical domains form a contiguous hydrophobic groove proposed to mediate TA protein binding [13,14,21-23]. In addition, the Get1 cytosolic domain preferentially binds apo-, open Get3 [8,9,24], strongly suggesting that Get1 promotes the release of nucleotide and TA proteins from Get3 at the end of the targeting cycle.

Despite rich structural information, many key questions remain regarding how the Get3 ATPase cycle drives the efficient delivery of TA proteins. First, even basic information, such as when, where and how ATP binding and hydrolysis occur in the GET pathway, remain elusive. Second, ADP-bound Get3 has been solved in both open and closed structures [13,23], raising questions as to the specificity of Get3 in recognizing nucleotides and generating nucleotide-driven conformational changes. Third, the nucleotide states of Get3 required for interacting with Get4/5 or for Get4/5-mediated loading of TA proteins remain controversial [4,7,25]. Most importantly, models based on a two-state open ⇔ closed transition are insufficient to explain the complex cascade of protein interactions that must be coordinated by Get3, which requires multiple functional states in this ATPase.

The requirement for the Sgt2•Get4/5 complex in the GET pathway raises additional questions. Why is Get3 unable to directly capture the TA substrate, and why is an upstream TA loading complex needed? How does the Get4/5 complex drive the transfer of TA proteins to Get3? Thus far, Get4/5 has appeared to be nothing more than a

scaffold that brings Sgt2 and Get3 into close proximity. Whether Get4/5 can actively regulate the conformation of Get3 to facilitate TA protein capture is unclear.

Finally, while the predominant model for TA protein binding invokes a closed Get3 dimer [13] there is also evidence that Get3 can form a tetrameric complex: A small population of Get3 appears to be tetrameric, and recombinant Get3/TA complexes are predominantly tetramers on size exclusion chromatography. Further, several archaeal Get3 homologues form obligate tetramers [16,21]. Whether and how a Get3 tetramer functions in TA protein targeting and how tetramerization of Get3 is coupled to its ATPase cycle are unclear.

To address these questions, here we establish a quantitative framework for the ATPase cycle of *Saccharomyces cerevisiae (Sc)* Get3. We demonstrate that Get4/5 and the TA protein substrate actively regulate this cycle to ensure the precise timing of ATP hydrolysis. These results provide an explicit model for how Get3's ATPase cycle is coupled to conformational changes that drive TA protein targeting.

Results

Cooperative ATP binding to Get3 active sites.

We began by establishing a quantitative framework for the Get3 ATPase cycle (Fig. 1). To probe for nucleotide-driven conformational changes, we compared Get3's activity under two conditions: (i) 'Single-site' conditions, in which Get3 is in 10–1000 fold excess over the nucleotide so that statistically, the majority of nucleotide-bound Get3 dimers have a single ATPase site occupied; and (ii) 'multi-site' conditions, in which the nucleotide is in excess over Get3 so that both ATPase sites are occupied. Nucleotide binding by Get3 is measured using both ATPase assays (Fig. 2A and Supporting Information (SI): Fig. S1A) and direct measurements based on changes in anisotropy of the fluorescent ATP analogue 2'-/3'-O-(N'-methylanthraniloyl)-ATP (mantATP; Fig. 2B). Under single-site conditions, Get3 binds ATP weakly and displays no discrimination between ATP and ADP (Fig. 2A, B; Fig. 1 & SI: Table S1, K_1 & K_9). In contrast, under 'multi-site' conditions Get3's ATPase reaction exhibited a cooperative dependence on ATP concentration, giving a Hill co-efficient of 2 and a ~10-fold higher affinity for binding the second ATP (Fig. 2C; Fig. 1 & SI: Table S1, K_3).

To test the specificity of this cooperative effect, we directly measured the kinetics of nucleotide binding and release from Get3 using: (i) environmentally sensitive changes in mantATP under single-site conditions (SI: Fig. S1B); and (ii) FRET between a native tryptophan in Get3 and mantATP under multi-site conditions (SI: Fig. S1C; [9]). These measurements show that ATP binds two-fold faster and dissociates three-fold more slowly under multi-site conditions (Fig. 2D and SI: Fig. S2, black; Fig. 1 & SI: Table S1, k_1, k_{-1} vs. k_3, k_{-3}), providing independent support for cooperative ATP binding to both

active sites of Get3. This cooperativity is specific for ATP: compared to single-site conditions, the rate of mantADP binding was unchanged and ADP release is over three-fold faster under multi-site conditions (Fig. 2D and SI: Fig. S2, gold; Fig. 1 & SI: Table S1, k_8, k_{-8} vs. k_9, k_{-9}), indicating that Get3 disfavors ADP occupancy at both active sites. Together, these results show that ATP specifically induces rearrangements in Get3 that lead to stronger binding of the second ATP molecule (Fig. 1, steps 1 & 3), whereas ADP does not.

Tetramerization of Get3 activates ATP hydrolysis and is required for TA protein targeting

Unexpectedly, the observed ATPase rate constant at saturating ATP concentrations, or k_{cat}, rises with increasing Get3 concentration (Figs. 2C & 3A). This phenomenon was observed even in the presence of BSA, an effective surfactant and crowding reagent, suggesting that it is unlikely to be caused by enzyme loss or inactivation at low concentrations. Instead, this observation suggests that an oligomerization process stimulates Get3's ATPase activity. Quantitatively, these data are most consistent with a model in which dimeric Get3 is in dynamic equilibrium (K_d = 3.5 ± 1.9 μM) with tetrameric Get3 that hydrolyzes ATP faster (Fig. 1, steps 4–7; SI: Eq 9). Analysis of the data based on this model yielded a k_{cat} value for tetrameric Get3 of 1.3 ± 0.4 min^{-1} (Fig. 1, k_6), over 100-fold faster than dimeric Get3 (Fig. 3A and SI: Fig. S3A; Fig. 1, k_4 = 0.012 min^{-1}). This phenomenon has previously escaped detection, likely because it is abolished in less physiological solution conditions (SI: Fig. S3B), whereas our experiments were performed in the same buffer as for protein targeting/translocation

reactions. The transient nature of tetrameric Get3 could also render it susceptible to dissociation during size exclusion chromatography [26].

In a structure of the *Methanocaldococcus jannaschii* (*Mj*) Get3 tetramer, helix 8 plays a key role in stabilizing the tetrameric interface. Mutations of conserved residues in this helix, F192D, M193D and M196D, destabilize the tetramer [16]. To independently test whether tetramerization of *Sc*Get3 is responsible for its ATPase activation, we mutated homologous residues in *Sc*Get3 (PM199DD, ML200DD; Fig. 3B). Given their location, these mutations are unlikely to affect the TA binding groove in the dimer model, but would specifically disfavor the formation or conformation of the tetramer. These mutations reduced activated ATP hydrolysis at high Get3 concentrations to almost the same extent as the mutant Δ181-210, a negative control that lacks a large portion of the putative TA-binding groove (Fig. 3A, B) and completely abolished TA protein capture and targeting by Get3 (SI: Fig. S4D). In contrast, observed k_{cat} values at low Get3 concentrations, where it is primarily a dimer, were largely unchanged in these mutants (Fig. 3A). These results provided independent evidence that formation of a Get3 tetramer is required for activated ATP hydrolysis.

If tetramerization of Get3 and its associated ATPase activation were important, it would also be manifested in a TA protein targeting reaction. To test this hypothesis, we quantitatively measured the targeting and translocation of a TA protein, Sbh1p, to ER microsomal membranes (SI: Fig. S4A). An NXT glycosylation site was engineered into the C-terminus of Sbh1p, whose glycosylation reports on successful translocation across the membrane. Both the translation lysate and ER microsomes were derived from a Δ*get3* yeast strain, so that the targeting of Sbh1p is dependent solely on exogenously added

Get3. Consistent with predictions from ATPase assays, the efficiency of Sbh1p targeting and translocation exhibited a cooperative dependence on Get3 concentration with a Hill coefficient of 2 (Fig. 3C and SI: Fig. S4B), suggesting that efficient TA protein targeting requires two Get3 dimers to further associate to form a tetramer. Additionally, the PM199DD and ML200DD mutants exhibit defects in translocation (Fig. 3D and SI: Fig. S4C) that quantitatively correlate with their defects in tetramerization-induced ATPase stimulation (Fig. 3D). Combined with the previous observation that mutants M200D and L201D are deficient in TA substrate binding and in supporting cell growth [13], these results provide strong evidence that transient formation of a Get3 tetramer is required for efficient TA protein targeting.

Get4/5 enhances ATP binding but inhibits ATP hydrolysis by Get3.

We next asked how the Get4/5 complex, which acts as a scaffold to facilitate TA protein loading from Sgt2 onto Get3, regulates the nucleotide state and ATPase activity of Get3. Intriguingly, Get4/5 quantitatively inhibits the ATPase activity of Get3 (Fig. 4A). Analysis of the ATP concentration dependence of the reaction showed that the average K_M value is lowered to 1.4 ± 0.3 μM in the presence of Get4/5, indicating that Get3 binds ATP more strongly when it is bound to Get4/5 (Fig. 4B & SI: Fig. S5A). In contrast, Get4/5 reduced the value of k_{cat}, indicating specific inhibition of ATP hydrolysis (Fig. 4B). These results strongly suggest that Get4/5 induces Get3 into an alternative conformation in which ATP is bound more tightly but held in a catalytically compromised structure.

To provide independent evidence for this model, we tested how Get4/5 alters nucleotide binding of Get3 using the FRET assay. The analysis showed that Get4/5 did not affect the rate of ATP binding to Get3 (Fig. 4C) but reduced the rate of ATP dissociation from Get3 at least 10-fold (Fig. 4D), providing direct evidence that Get3 binds ATP more tightly when it is bound to Get4/5. This effect is specific for ATP, as under the same conditions ADP release from Get3 remained fast and was largely unaffected by Get4/5 (SI: Fig. S5B).

If Get4/5 induces stronger ATP binding to Get3, then reciprocally, ATP-bound Get3 would bind more strongly to Get4/5. To test this prediction, we measured complex formation between Get3 and Get4/5 using gel filtration chromatography. With apo-Get3, complex assembly was not detected even at micromolar protein concentrations (SI: Fig. S5C). In contrast, in the presence of saturating ATP almost all the Get3 molecules formed a complex with Get4/5 (SI: Fig. S5D). These results, though qualitative, are consistent with previous pull-down experiments in which a stable Get3-4/5 complex was enriched in the presence of nucleotides [4,7,25]. Together, these results demonstrate that Get4/5 preferentially binds ATP-loaded Get3 and reciprocally, interaction with Get4/5 enables ATP to be more tightly bound to Get3.

As the ATPase activity of Get3 is activated upon tetramerization, we further asked whether the Get4/5 complex inhibits this activation. With saturating Get4/5 and ATP, the ATPase rate constant stayed constant at 0.16 ± 0.07 min^{-1} and was independent of Get3 concentration (Fig. 4E), indicating that Get4/5 inhibits formation of the Get3 tetramer or the ATPase activation induced by tetramerization.

TA protein induces rapid ATP hydrolysis and locks Get3 in the ADP-bound state

We next asked how the TA protein substrate regulates nucleotide binding and hydrolysis of Get3. To this end, we co-expressed Get3 with Sbh1p. The Get3/Sbh1 complex purified predominantly as a tetrameric complex (SI: Fig. S6A), consistent with previous observations that co-expression with substrate leads to tetramerization of Get3 [16,21].

To determine the ATP hydrolysis rate from this complex, we carried out pre-steady-state measurements using a high ATP concentration and Get3 active sites in 1:5 stoichiometry relative to ATP. Under these conditions, the ATPase reaction exhibited two distinct kinetic phases: (i) an initial burst whose magnitude increased with increasing Get3 concentration (Fig. 5A & SI: Fig. S6B), representing a rapid first round of ATP hydrolysis; and (ii) a slower linear phase representing subsequent rounds of ATP turnover at steady-state. The rate constant for the first round of ATP hydrolysis is 3.3 ± 1.1 min^{-1} (SI: Eq 10), over 100-fold faster than that for the Get3 dimer. The rate constant for subsequent, steady-state ATP turnover is 0.055 ± 0.001 min^{-1}, 60-fold slower than the first turnover. Thus, loading of TA protein onto Get3 activates one round of ATP hydrolysis, but subsequent ATP turnover is inhibited. Further, ATPase activation in the Get3/TA complex was not observed under single-site conditions (Fig. 5B; cf. Fig. 2A), suggesting that it requires both Get3 active sites to be bound with ATP. Finally, the magnitude of the burst phase is stoichiometric with the concentration of Get3 active sites, suggesting that all four ATPs in the Get3 tetramer are hydrolyzed during the first round of ATP turnover.

To test whether nucleotide binding or release could be rate-limiting for the observed

ATPase rates, we used the fluorescence assays to directly measure these events. MantATP binding to the Get3/Sbh1 complex was slow and concentration-independent at the lowest concentrations tested under both multi-site (Fig. 5C & SI: Fig. S6C) and single-site conditions (SI: Fig. S6D), suggesting that a slow conformational change of the Get3/Sbh1 complex becomes rate-limiting for ATP binding. The rate of the dominant, slow phase in ATP binding is similar to that of the burst phase in the ATPase reaction (5.0 vs. 3.3 min^{-1}), suggesting that the ATPase rate constant observed here may still be limited by a conformational change that precedes hydrolysis.

Nucleotide release was also significantly slowed in the Get3/Sbh1 complex. Remarkably, dissociation of ADP is at least 100-fold slower in this complex compared to free Get3 (Fig. 5D and SI: Table S2) and is indistinguishable from that of ATP or non-hydrolyzable ATP analogues (SI: Fig. S6E and Table S2). This strongly suggests that TA protein loading locks Get3 into a conformation in which the ATPase sites are shielded from solvent and all the nucleotides are bound tightly. Nevertheless, ADP release from the Get3/TA complex is still 200-fold faster than the steady-state ATPase rate and is unaffected by the presence of up to 10 mM inorganic phosphate (SI: Fig. S6E and Table S2), indicating that product release is not rate-limiting for steady-state ATP turnover. Together, these data argue that only one round of ATP hydrolysis occurs in the GET pathway, after which the Get3/TA complex is locked in a catalytically inactive state loaded with ADP, and disassembly of this complex would be needed to reset its ATPase cycle.

Discussion:

Efficient and accurate delivery of membrane proteins often requires energy input from nucleotide triphosphates, which in the GET pathway is harnessed and utilized by the Get3 ATPase [2,27]. When, where, and how ATP binding and hydrolysis occur in the GET pathway have remained elusive. Little is known about how Get3's nucleotide state, conformation and activity are regulated by its upstream and downstream effectors to drive TA protein targeting. Here, quantitative mechanistic analyses define a precise framework for Get3's ATPase cycle and elucidate how it is used to drive this fundamental cellular process.

Previous work showed that Get3's NHD acts as a fulcrum at the dimer interface to generate a variety of structures including 'open', 'semi-open', 'semi-closed', and 'closed' states [2]. The cooperative ATP binding observed here supports a model in which Get3 changes from a largely open conformation in apo-Get3 to increasingly closed conformations upon successive ATP binding (Fig. 1, steps 1 & 3). Importantly, this cooperativity is highly specific to ATP but not ADP. Thus, an ADP-bound Get3 dimer remains in a largely open conformation [14,23], despite the occasional observation of 'closed', ADP-bound Get3 structures [21]. Nevertheless, the amount of cooperativity induced by ATP is fairly modest, ~10-fold. Together with published structures and molecular dynamics simulations [28], we speculate that Get3 exists in an ensemble of conformations that are in close equilibrium with one another, and each ATP binding event induces a modest shift in the conformational landscape. Thus, even the Get3 dimer bound with both ATPs is not completely 'closed', and is termed *semi-closed* here (Fig. 1). Intriguingly, Get3 is catalytically activated through tetramer formation (Fig. 1, steps 5, 6).

Tetramerization of Get3 was previously suggested by the structure of an *Mj*Get3 tetramer and by the formation of tetrameric Get3/TA complexes [16]. Our findings for the first time provide a function for tetrameric Get3, demonstrating that it is the active species for ATP hydrolysis and is crucial for efficient targeting of TA proteins. In support of this model, residues in helix 8 that stabilize the tetramer interface are highly conserved [14,16]; their mutations disrupt ATPase activation and TA protein targeting by Get3 (this work) and lead to defects in cell viability and TA binding [13,16]. Given the location of these residues, these phenotypes are difficult to reconcile with a dimeric model for Get3. The participation of these residues in the formation of an active Get3 tetramer and the associated ATPase activation shown here provide a cohesive model to explain this collection of results.

In vivo, tetramerization of Get3 by itself should be disfavored to minimize futile rounds of ATP hydrolysis. This could be achieved in part by the low *in vivo* concentration of Get3, ~1 μM [29], which is below the K_d value for tetramerization (3.5 μM). The results here further show that futile ATPase cycles of Get3 are minimized by the Get4/5 complex, which mediates the loading of TA proteins from Sgt2 onto Get3 [4,7]. Despite previous reports of Get4/5 binding to apo-Get3 [30], our results demonstrate that Get4/5 preferentially binds ATP-loaded Get3 and locks it in the ATP-bound state (Fig. 6, step 2). This is achieved by tightening Get3's ATP binding but inhibiting its hydrolytic activity, particularly the tetramerization-induced activation of ATP hydrolysis. Get4/5 could exert these effects by inducing Get3 into a distinct, 'occluded' conformation in which its ATPase site is more closed but is incompetent for hydrolysis (Fig. 1). Alternatively or in addition, Get4/5 could prevent Get3's tetramerization. The latter

model is particularly attractive as it explains why Get5 is a stable dimer [31]: a complete Get4/5 complex could hold two closed Get3 dimers in the ATP-bound state, priming them for subsequent tetramer formation once the TA protein is loaded onto Get3 (Fig. 6, step 3). Regardless of the model, our data show that Get4/5 is not a passive scaffold that simply brings Sgt2 and Get3 into close proximity. Rather, Get4/5 actively promotes TA protein loading onto Get3 by locking it in the correct nucleotide state and priming its conformation for TA substrate capture. This also provides a rationale for why Get3 cannot efficient capture the TA substrate by itself, and why an elaborate TA loading complex is required in the GET pathway[4,19] .

In contrast to Get4/5, multiple lines of evidence strongly suggest that the TA protein induces the tetramerization and activation of Get3's ATPase activity (Fig. 6, step 3): (i) co-expression of TA protein with Get3 results in a stable Get3 tetramer (this work; [16,21]); (ii) Rapid ATP hydrolysis was observed with the Get3/TA complex, as would be expected for an activated Get3 tetramer. Several important lessons are learned from analysis of the Get3/TA complex. First, after the first round of ATP hydrolysis, subsequent ATP turnover is 60-fold slower and incompatible with the timescale of protein targeting *in vivo*, arguing that only one round of ATP hydrolysis occurs in the GET pathway. Second, following ATP hydrolysis, Get3 is locked in a catalytically inactive state. Together with observations with the Get3•Get4/5 complex, these results demonstrate that the open-to-closed rearrangement of Get3 can be conceptually and experimentally uncoupled: even when Get3 is globally 'closed' and nucleotide release is slow, additional active site readjustments specifically regulate catalytic activity. We speculate that this relates to local rearrangements of the switch II loops [2], which provide

multiple essential catalytic residues. The ADP-bound *Mj*Get3 tetramer structure possibly provides a view of a closed but catalytically inactive Get3 tetramer, in which the switch II loop is pulled away and incompatible for ATP hydrolysis [16]. Finally, ADP release is significantly slowed in the Get3/TA complex and becomes indistinguishable from that of ATP, suggesting that the TA protein is dominant in inducing a closed Get3 tetramer.

In the context of the targeting cycle, TA-induced Get3 tetramer formation would be beneficial as the hydrophobic TM of the TA substrate can be enclosed in a cage at the tetrameric interface and completely shielded from solvent [16], thus minimizing potential aggregation of the TA substrate (Fig. 6). Our results also strongly suggest that following hydrolysis, ADP release from the Get3/TA complex is delayed until Get3 finds the Get1/2 membrane receptor. Tetramer disassembly by this receptor would be needed to release the TA protein. As ATP- and Get1-binding to Get3 are strongly antagonistic with one another [7-9], the hydrolysis of ATP in the Get3/TA complex likely primes it for disassembly at the membrane.

Collectively, our results lead to a new model for how the energy from ATP binding and hydrolysis is harnessed by Get3 to drive TA protein targeting (Fig. 6). Under cellular conditions, the majority of Get3 cooperatively binds ATP at both active sites, which induces it into a semi-closed conformation (step 1). ATP-loaded Get3 is preferentially captured by Get4/5, which brings Get3 into the vicinity of Sgt2 and induces the Get3 dimer into another conformation in which Get3 is further closed but ATP hydrolysis is inhibited (step 2). In this configuration, Get3 is primed to capture the TA substrate from Sgt2 (step 2). Loading of TA protein induces tetramerization of Get3 (step 3), which might also drive dissociation of Get3 from Get4/5. The tetrameric Get3/TA

complex undergoes a rapid round of ATP hydrolysis, giving a stable ADP-loaded complex which then binds its receptor, Get1/2, at the ER membrane (step 4). Tetramer disassembly, ADP dissociation, and TA protein release into the membrane are likely coupled, resulting in Get1 bound to apo-Get3 in the open conformation (step 5). ATP binding then releases Get3 from Get1 [7-9] and re-initiates the cycle.

Get3 is the only eukaryotic ATPase in the SIMIBI (for SRP, MinD, and BioD) family of deviant P-loop NTPases, including the SRP and SRP receptor (SR) that mediate co-translational protein targeting [32]. Although the details of each system differ, the results here reveal many similarities in the regulatory principles between Get3 and SRP/SR. Both exhibit low nucleotide affinity and forego the need of external exchange factors and NTPase activating proteins as regulatory elements [33]. Instead, both use dimeric complexes as the functional unit. As dimers, both undergo conformational changes on the global (open → closed transitions) and local (catalytic loop repositioning) scale to generate multiple functional states during their NTPase cycle. For both, these rearrangements provide key regulatory points to sense and respond to upstream and downstream components and effect the precise timing of nucleotide hydrolysis in the pathway. For example, the translating ribosome stalls GTPase activation in the SRP/SR complex [34], whereas Get4/5 stalls ATPase activation of Get3. Nucleotide hydrolysis is also activated by downstream factors in both pathways. Based on regulatory mechanisms, Get3 could be placed in the class of NTPases regulated by dimerization [35] whose members, aside from SRP and SR, also include the human GBP1, the septins, HypB, MnmE, and the dynamin family of GTPases [35,36]. Investigation of Get3 undoubtedly enhances our

understanding of the mechanism, regulation, and evolution of this novel class of regulators.

Materials and Methods

Protein Expression and Purification. *Sc*Get3 was expressed and purified according to published procedures [14,25]. Mutant Get3s were generated using Quikchange Mutagenesis protocol (Stratagene), and were purified identically to wildtype Get3. Purification of the Get4/5 and the Get3/Sbh1 complexes is described in SI: Methods.

Fluorescence measurements. All fluorescent nucleotides were from Jena Biosciences. All measurements were carried out at 25 °C in Get3 assay buffer (50mM HEPES pH 7.4, 150mM potassium acetate, 5mM magnesium acetate, 1mM DTT and 10% glycerol) using a Fluorolog-3-22 spectrofluorometer (Jobin Yvon) or a Kintek stopped-flow apparatus. Determination of the individual rate and equilibrium constants is described in SI.

ATPase assays. All reactions were performed in Get3 assay buffer at 25 °C with [γ-^{32}P]-ATP (MP Biomedicals). Reactions at Get3 concentrations below 0.5 μM also included 0.2 mg/mL BSA. Reactions were quenched in 0.75 M potassium phosphate, pH 3.3, analyzed by PEI cellulose thin layer chromatography (TLC) in 1 M formic acid and 0.5 M LiCl, and quantified by autoradiography. Observed rate constants were obtained as described [37]. Determination of individual rate and equilibrium constants in ATPase assays is described in SI.

TA protein Targeting and Translocation. Yeast translation extracts were prepared as described in [16,38], except that an additional centrifugation step (SW55Ti, 30 min at 49,000 rpm) was included prior to loading the clarified lysate on the G25 Superdex column.

Yeast microsomes were prepared as described in [6,39]. Translation and translocation of TA protein was carried out as described in [16] and detailed in SI.

Acknowledgements.

We thank J. Chartron, H. Gristick and C.J.M. Suloway for expression constructs, purification protocols, and critical discussions, M. Sachs and C. Wu for help with yeast translation extracts, R. Schekman for help with yeast microsomes, and D.C. Rees and members of the Shan and Clemons groups for helpful comments. This work was supported by career awards from the David and Lucile Packard foundation and the Henry Dreyfus foundation to S.S., NSF graduate research fellowship DGE-1144469 to M.E.R, NIH training grant 5T32GM007616-33 to M.R., and NIH grant R01 GM097572 to W.M.C.

Supplementary Materials and Methods

Protein Expression and Purification. Get4/5 and the Get3/Sbh1 complexes were expressed and purified according to previously published protocols with slight modifications [16,25]. For Get4/5, the tetrameric fractions from MonoQ and size-exclusion chromatography were collected and used for all assays. For Get3/Sbh1, N-terminally tagged MBP-thrombin-Get3 and His_6-tagged Sbh1 were purified by affinity chromatography using Ni-NTA, followed by the amylose resin (NEB). Proteins eluted

from amylose resin were treated with thrombin overnight at room temperature. The resulting thrombin digest was separated by size exclusion chromatography (Superdex 200, GE Healthcare) and the tetrameric Get3/Sbh1 fractions were collected and pooled. All proteins were exchanged into Get3 assay buffer in the gel filtration step.

Fluorescence measurements.

Equilibrium nucleotide binding under single-site conditions. Measurements were based on a fluorescence anisotropy readout with identical numerical processing as described previously [40]. Samples were excited at 355 nm and fluorescence emission at 448 nm was monitored. For all titrations, mantATP/ADP was held constant at 0.3 μM and Get3 was varied as indicated. Incubation time was calculated based on the nucleotide binding rate under the same conditions, and varied from 5 to 10 minutes depending on Get3 concentration. Observed anisotropy values (A_{obsd}) were plotted as a function of Get3 concentration and fit to Eq 1,

$$A_{obsd} = A_0 + (A_1 - A_0) \times \frac{[\text{Get3}]}{[\text{Get3}] + K_d} \qquad (1)$$

in which A_0 is the anisotropy value of free mantATP/ADP, A_1 is the anisotropy when mant-ATP/ADP is bound to Get3, and K_d is the equilibrium dissociation constant of Get3 for mantATP/ADP.

Competition of ATP with mantATP. To test whether the mant group perturbs the binding affinity of ATP to Get3, 1.5 μM Get3 and either 8 or 11 μM mantATP were pre-incubated for 10 minutes and titrated with ATP. The observed fluorescence (F_{obsd}) were fit to Eq 2,

$$F_{obsd} = F_0 \times \frac{K_{i,app}}{[\text{ATP}] + K_{i,app}} + F_1 \times \frac{[\text{ATP}]}{[\text{ATP}] + K_{i,app}} \qquad (2)$$

in which F_0 is the fluorescence in the absence of the competitor, F_1 is the fluorescence in the presence of saturating competitor, and $K_{i,app}$ is the apparent inhibition constant of ATP at the specified mantATP concentration, determined to be 14.2 μM at 8 μM mantATP and 18.5 μM at 11 μM mantATP. These $K_{i,app}$ values are related to the true inhibition constant of ATP, K_i, by Eq 3,

$$K_{i,app} = K_i \times (1 + \frac{[\text{mantATP}]}{K_d}) \quad (3)$$

in which K_d is the equilibrium dissociation constant of mantATP. The value of K_i determined from these experiments is 4.6 ± 0.1 μM, the same within error as the K_d value determined for mantATP, indicating that the mant group does not perturb the binding of ATP to Get3.

Nucleotide association and dissociation kinetics. All rate measurements were performed on a Kintek stopped-flow apparatus. Under single-site conditions, the environmental sensitivity of mantATP/ADP was used as a readout. Samples were excited at 355 nm and fluorescence emissions were collected at 445 nm. MantATP/ADP concentration was held constant at 0.3 μM and Get3 concentration was varied as indicated. Observed rate constants (k_{obsd}) were plotted as a function of Get3 concentration and fit to Eq 4,

$$k_{obsd} = k_{on}[\text{Get3}] + k_{off} \quad (4)$$

in which k_{on} is the association rate constant, and k_{off} is the dissociation rate constant.

Under multi-site conditions, FRET between a native tryptophan in Get3 and mantATP/ADP was used. Samples were excited at 280 nm and fluorescence emission was collected at 445 nm. For association rate measurements, Get3 was held constant at 1.5 μM and mant-ATP/ADP concentration was varied as indicated. The data were fit to

Eq 4 above, except that the concentration of Get3 was replaced with that of mantATP/ADP. For dissociation rate measurements, a pulse-chase setup was used. A complex between Get3 and mantATP/ADP (at 30 μM) was preformed by incubation for 10 minutes, followed by addition of unlabeled ATP•Mg^{2+} or ADP•Mg^{2+} at 2-4 mM as the chase to initiate mantATP/ADP dissociation. The time course for change in acceptor fluorescence (F_{obsd}) was fit to either a single (Eq. 5) or double (Eq. 6) exponential function, in which F_e is the fluorescence when reaction reaches equilibrium, ΔF_1 and k_{fast} are the magnitude and rate constant of the fluorescence change in the fast phase, and ΔF_2 and k_{slow} are the magnitude and rate constant of the fluorescence change in the slow phase,

$$F_{obsd} = F_e + \Delta F_1 \times e^{-k_{fast}t} \quad (5)$$

$$F_{obsd} = F_e + \Delta F_1 \times e^{-k_{fast}t} + \Delta F_2 \times e^{-k_{slow}t} \quad (6)$$

Eq 6 was often needed to fit kinetic data, because the time courses for mantATP/ADP binding or dissociation were biphasic in most cases (Figure S7). We cannot rule out the possibility of enzyme conformational changes or heterogeneity that might in part give rise to the biphasic behavior. Nevertheless, the following strongly suggests that this behavior is primarily caused by heterogeneity in the mant nucleotides (where the mant group isomerizes between the 2'- and 3'-position). (i) The relative magnitude of the two kinetic phases, in the absence of perturbation by enzyme, is ~35%:65%, comparable to the equilibrium distribution of the two isomers [41]. (ii) In single-site binding measurements, while the observed rate constants from the fast phase showed a linear concentration dependence expected for bi-molecular association, the rate constants for the slow phase are concentration independent and occur at a time scale (k_{slow} ~ 0.005 s^{-1}) consistent with the time scale for conversion of one mant isomer to the other

[42]. (iii) The relative magnitudes of the two kinetic phases in binding measurements are unchanged by varying Get3 concentration, but the magnitude of the fast phase increases with increasing concentration of ATP or mantATP. This is inconsistent with enzyme heterogeneity giving rise to the biphasic behavior (as the faster binding enzyme population would sequester most of the ATP and dominate the signal if this were the case). Instead, these observations are expected if the faster-binding mant-isomer sequesters most of the enzyme and dominates the signal at higher concentrations. Further, unlabeled ATP also increases the magnitude of the fast phase, suggesting that the faster-binding isomer favors the same binding mode as that for ATP. For these reasons, and because the kinetics and equilibrium derived from the fast phase were in excellent agreement with those from direct ATPase assays, the faster-binding isomer faithfully reports on the nucleotide binding and release kinetics of Get3 and were used for determination of binding constants in this work (Figure 1 and Table S1).

Although it is theoretically possible to remove one of the mant isomers by substituting 3'-OH with 3'-H, we found that this substitution itself significantly weakens nucleotide binding to Get3 and hence could not be used to obtain the correct rate and equilibrium constants.

ATPase measurements.

Single-site, single turnover ATPase rate (k_2). Get3 was in excess over a trace amount of ATP* (<0.1nM) and titrated at indicated concentrations. The data were fit to eq 7.

$$k_{obsd} = k_{cat} \times \frac{[\text{Get3}]}{[\text{Get3}] + K_M} \qquad (7)$$

Here, k_{cat} is the rate constant at saturating Get3 concentration, and K_M is the concentration of Get3 required to reach half saturation.

Multi-site, multiple turnover Get3 ATP hydrolysis rate. In this assay, a fixed amount of Get3 was titrated with excess ATP as indicated. The data were fit to an allosteric sigmoidal curve with a Hill coefficient of two (eq 8).

$$k_{obsd} = \frac{k_{cat} \times [\mathrm{ATP}]^2}{K_M^2 + [\mathrm{ATP}]^2} \tag{8}$$

Here, k_{cat} is the rate constant at saturating Get3 concentrations, and K_M^2 is the product of ATP binding affinities for the first and second active site, i.e., $K_M^2 = K_1 \times K_3$.

ATPase activation through tetramerization of Get3. Observed k_{cat} values were determined under multi-site conditions as above, at a series of Get3 concentrations. The plot of observed k_{cat} as a function of Get3 concentration were fit to Eq 9,

$$observed\ k_{cat} = k_6 + (k_4 - k_6) \times \frac{\left(-K_5 + \sqrt{K_5^2 + 4K_5[\mathrm{Get3}]}\right)}{2[\mathrm{Get3}]} \tag{9}$$

where k_4, k_6, and K_5 are defined in Figure 1.

ATPase rate constants in the Get3/Sbh1 complex. Pre-steady-state measurements were carried out with Get3 active sites in 1:2.5 – 1:10 stoichiometry relative to saturating ATP (1 mM), so that both the first and subsequent ATP turnovers can be visualized. The reaction time course is bi-phasic, as explained in the text, and was fit to Eq 10,

$$Fraction(\mathrm{ATP}) = (a - b)e^{-k_{burst}t} - k_{linear}t + b \tag{10}$$

where a is the fraction of ATP before initiation of the reaction, b is the reaction end point, k_{burst} is the rate constant associated with the burst phase and k_{linear} is the rate associated with the slower, linear phase.

TA protein targeting and translocation. For translation, a model substrate (N-Sbh1p) was used, which contains an N-terminal flag tag, a fragment of MBP (to facilitate separation on SDS-PAGE) fused to yeast Sbh1p, a C-terminal bovine opsin tag for glycosylation, and optimized methionine content to increase signal:

MDYKDDDDKMENAQKGEIMPNIPQMSAFWYAVRTAVINAASGRQTVDEAL
KDAQTNSSSNNNNNNNNNNLGLVPRGSISEFGSSSPTPPGGQRTLQKRKQ
GSSQKVAASAPKKNTNSNNSILKIYSDEATGLRVDPLVVLFLAVGFIFSV
VALHVISKVAGKLFRMNGTEGPNMYMPMSNKTVD

The coding sequence for this protein was cloned into a transcription plasmid [43] under control of an SP6 promoter. mRNAs were transcribed using the SP6 Megascript kit (Ambion). All translation and translocation assays were carried out as described in [16]. ^{35}S-methionine labeled pre- and glycosylated proteins were separated by 15% SDS-PAGE and quantified by autoradiography using a Typhoon (GE Healthcare) phosphoimager and Image QuantTL (GE Healthcare). Translocation efficiency (%glycosylated protein) was plotted as a function of Get3 concentration and fit to Eq 11,

$$T_{obsd} = T_0 + T_{\max} \times \frac{[\text{Get3}]^{\text{h}}}{[\text{Get3}]^{\text{h}} + K_d{}^{h}} \qquad (11)$$

in which T_0 is the fraction of translocation in the absence of Get3, $T_{\max}$ is the maximal amount of translocation with saturating Get3, K_{d} is the concentration of Get3 at half saturation, and h is the Hill co-efficient.

TA protein capture by Get3 in translation extract. A Get3 pull-down assay in translation extract was performed. A 50 µl translation reaction in Δ*get3* lysate was initiated for 1 minute at 26 °C, at which time His_6-tagged Get3 was added. After 40 min, the reaction mixture was adjusted with 20 mM imidazole and 1 mM cyclohexamide (final concentrations), followed by the addition of 10 µl Ni-NTA beads. After incubation on a rotating wheel at room 25 °C for 40 minutes, the beads were washed 3 times for 5 minutes in Get3 assay buffer with 30 mM imidazole and 0.5 mM ATP, and eluted with SDS-PAGE buffer containing 200 mM DTT and 300 mM imidazole.

Complex formation by gel filtration: Complex formation between Get3 and Get4/5 was assayed using size exclusion chromatography (Superdex 200, GE Healthcare). To generate the complex, 13.3 μM of Get3 was incubated with 13.3 μM of Get4/5 in Get3 assay buffer for 30 min at room temperature, with or without 200 μM ATP. Complex formation was assayed by following the depletion of the Get3 peak at ~14.8 ml.

Table S1. Summary of the rate and equilibrium constants during Get3's ATPase cycle, related to Figures 1–3. The individual constants are defined in Figure 1. The values reported are the mean ± SD, with n = 3.

Rate or equilibrium constants	
K_1	12.4 ± 0.1 μM
k_1	(2.0 ± 0.1) × 10^5 M^{-1} s^{-1}
k_{-1}	4.0 ± 0.3 s^{-1}
k_2	Not determined
K_3	1.3 μM
k_3	≥ (4.3 ± 0.4) × 10^5 M^{-1} s^{-1}
k_{-3}	1.6 ± 0.1 s^{-1}
k_4	≥ 0.012 min^{-1}
K_5	3.5 ± 1.9 μM
k_6	1.3 ± 0.4 min^{-1}
k_8	(3.1 ± 0.3) × 10^5 M^{-1} s^{-1}
k_{-8}	14.4 ± 0.9 s^{-1}
K_9	11.7 ± 1.3 μM
k_9	(2.9 ± 0.2) × 10^5 M^{-1} s^{-1}
k_{-9}	4.5 ± 0.6 s^{-1}

Table S2. Summary of nucleotide dissociation rate constants from Get3 with and without effector proteins, related to Figures 4 and 5. The values reported are the mean ± SD, with n = 3.

Nucleotide	Effector	1st Phase		2st Phase	
		rate constant (s^{-1})	amplitude (%)	rate constant (s^{-1})	Amplitude (%)
ATP (k_{-3})	–	1.6	60	0.012	40
ADP (k_{-8})	–	14.4	56	0.015	44
ATP	+ Get4/5	0.15	40	0.0086	60
ADP	+ Get4/5	11.3	38	0.012	62
ATP	+ Sbh1	0.18	24.5	0.022	75.5
ADP	+ Sbh1	0.15	34.5	0.033	65.5
ADP + P_i	+ Sbh1	0.14	39	0.036	61
AMPPNP	+ Sbh1	0.214	40	0.032	60

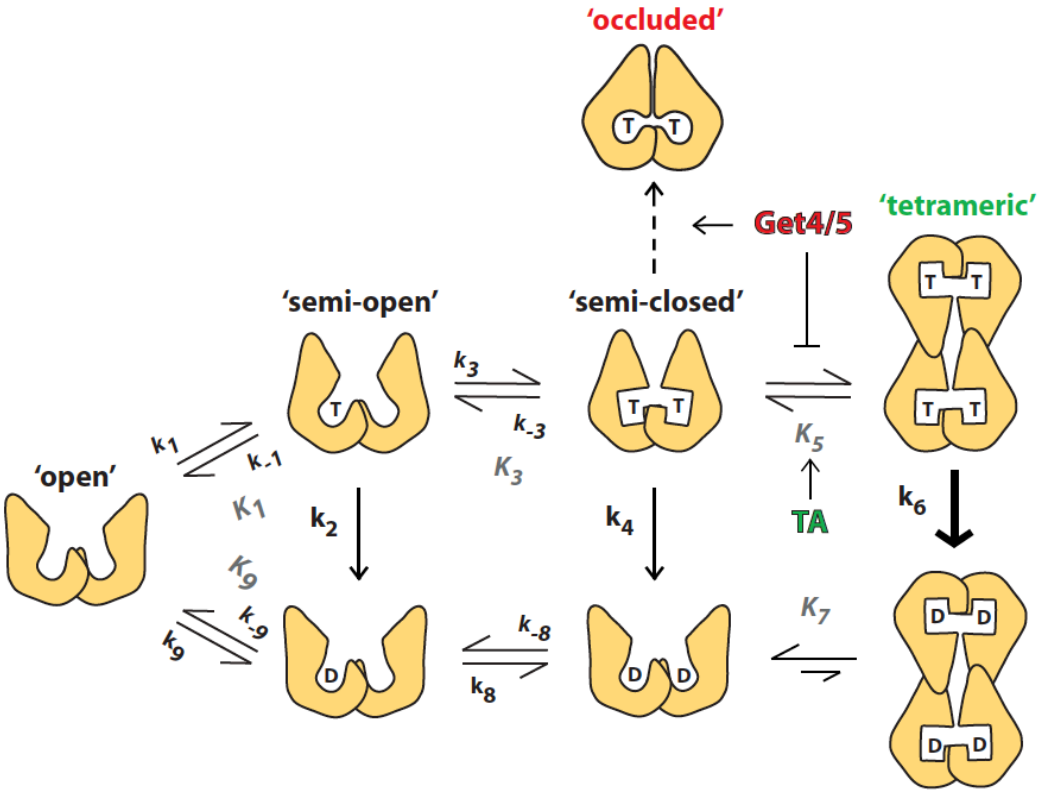

Figure 2.1 Model for the ATPase cycle of Get3. T denotes ATP, D denotes ADP. Different shapes depict different Get3 conformations. Steps 1–2, ATP binding and hydrolysis by a single active site in Get3. Step 3, ATP binding to a second active site of Get3. Step 4, ATP hydrolysis from dimeric Get3. Step 5, formation of the Get3 tetramer. Steps 6–7, ATP hydrolysis and ADP release from tetrameric Get3. Steps 8–9, release of ADP from the two active sites of Get3. The individual rate and equilibrium constants are listed in SI: Table S1.

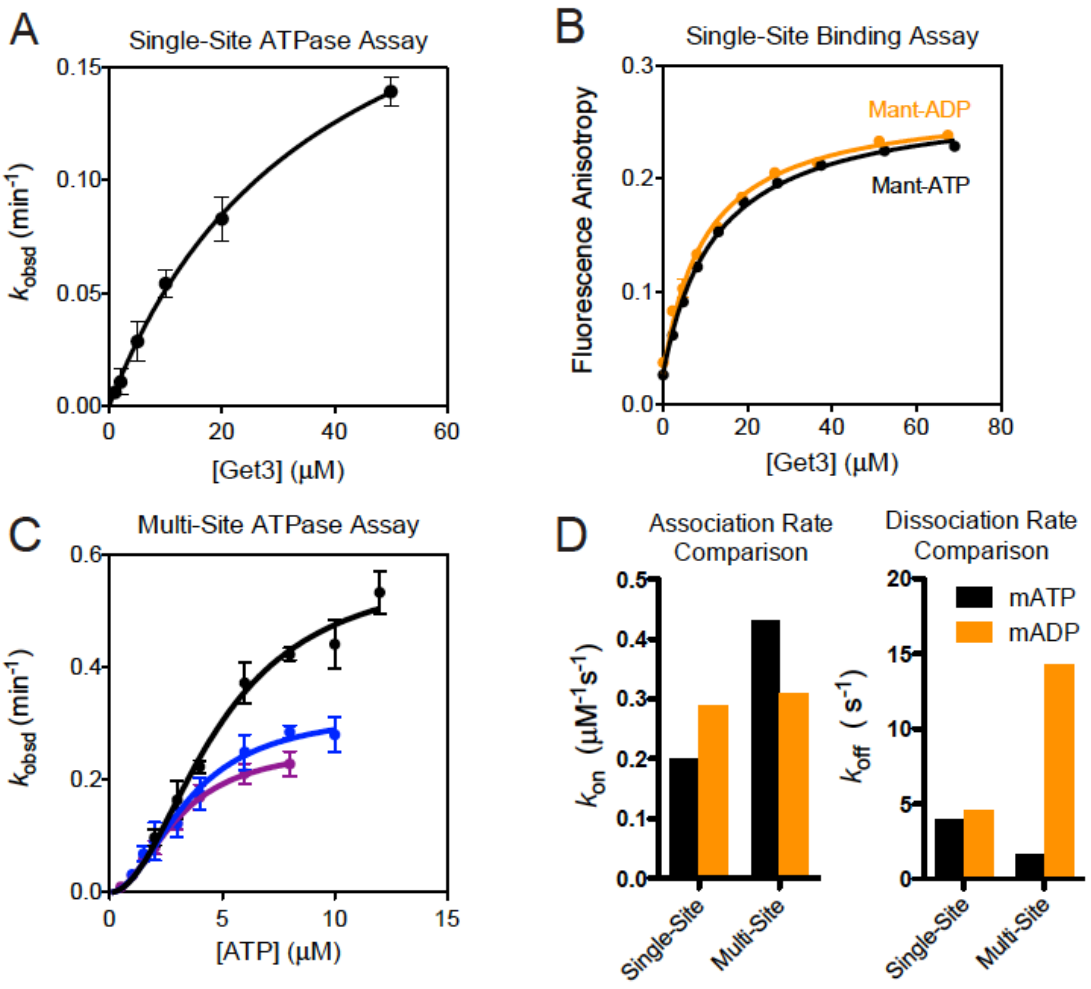

Figure 2.2 Cooperative ATP binding to the two active sites of Get3. (**A**) Single-site ATP hydrolysis by Get3. The data were fit to SI: Eq 7 and gave a K_M of 37 ± 6.7 μM. (**B**) Equilibrium titration of mantATP (0.3 μM, black) and mantADP (0.3 μM, gold) binding to Get3 under single site conditions. The data were fit to SI: Eq 1. (**C**) ATP hydrolysis by Get3 under multi-site conditions. The data were fit to SI: Eq 8 and gave a Hill coefficient of 2, average K_M values of 3.0 ± 0.2, 3.6 ± 1.0 and 4.8 ± 0.2 μM, and observed k_{cat} values of 0.26 ± 0.02, 0.33 ± 0.03 and 0.58 ± 0.03 min^{-1}, respectively, for reactions with 0.2

(purple), 0.5 (blue), or 1.0 (black) μM Get3. (**E**) Summary of nucleotide association and dissociation rate constants under single and multi-site conditions. See also SI: Table S1.

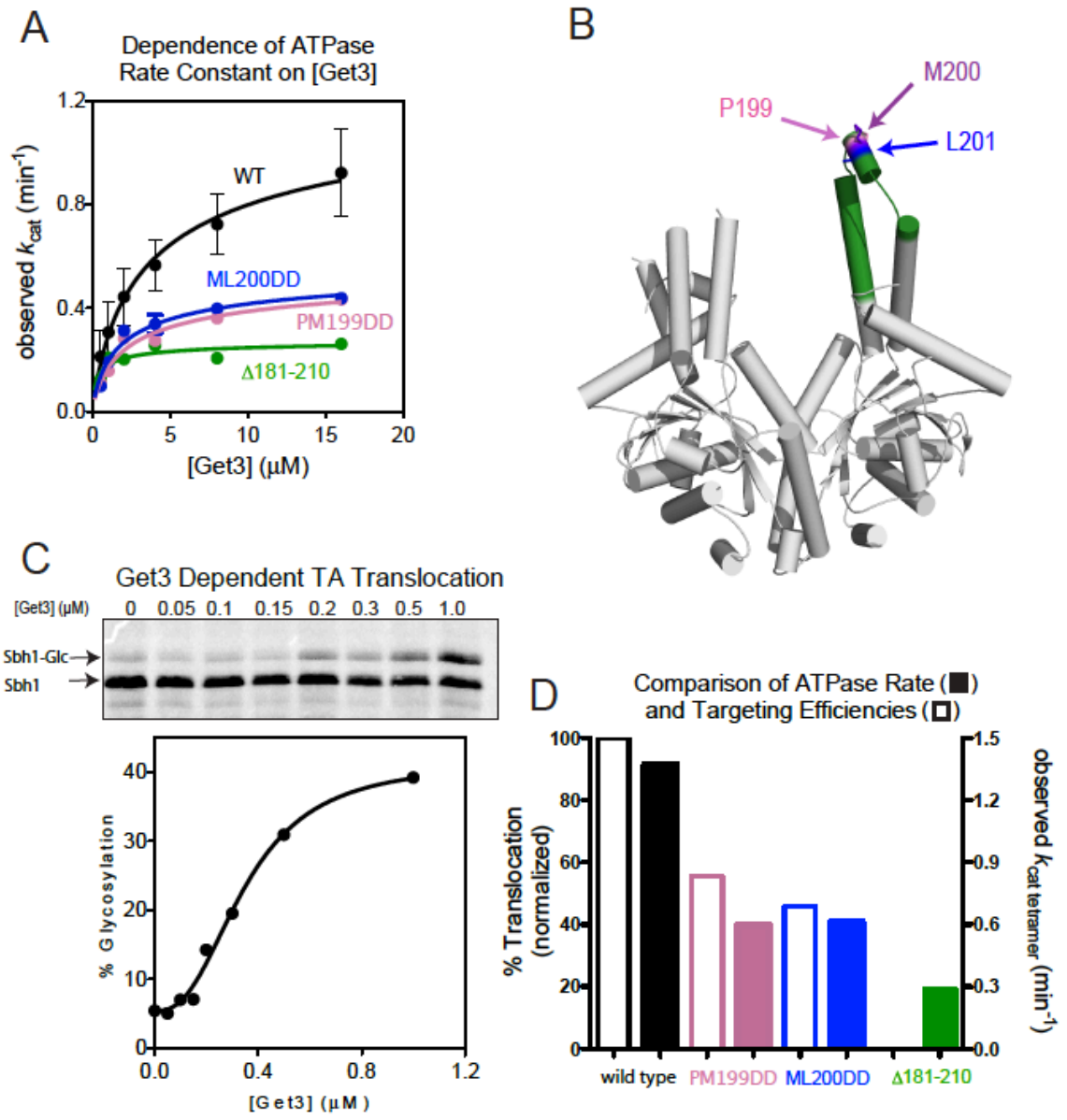

Figure 2.3 Tetramerization stimulates Get3's ATPase activity and is required for TA protein targeting. (**A**) Observed k_{cat} values as a function of Get3 concentration. The data were fit to SI: Eq 9, which gave tetramer ATPase rate constants of 1.3 ± 0.4, 0.31±0.03, 0.60±0.012, and 0.6±0.02 min^{-1}, respectively, for wildtype Get3 (black) and mutants Δ181-210 (green), PM199DD (pink), and ML200DD (blue). (**B**) Structure of *Sc*Get3 (PDB: 3A36) highlighting the residues mutated: P199 (pink), M200 (violet), L201(blue). The remainder of residues 181-210 is in green. (**C**) Targeting and integration of Sbh1p by wildtype Get3. The data were fit to SI: Eq 11, which gave a $K_{1/2}$ of 0.35 ± 0.029 μM and a Hill coefficient of 2. (**D**) Comparison of TA protein targeting efficiencies (open) and tetramer ATPase rate constants (filled) for wildtype Get3 (black) and mutants PM199DD

(pink), ML200DD (blue), and Δ181-210 (green). %translocation was normalized to wildtype Get3.

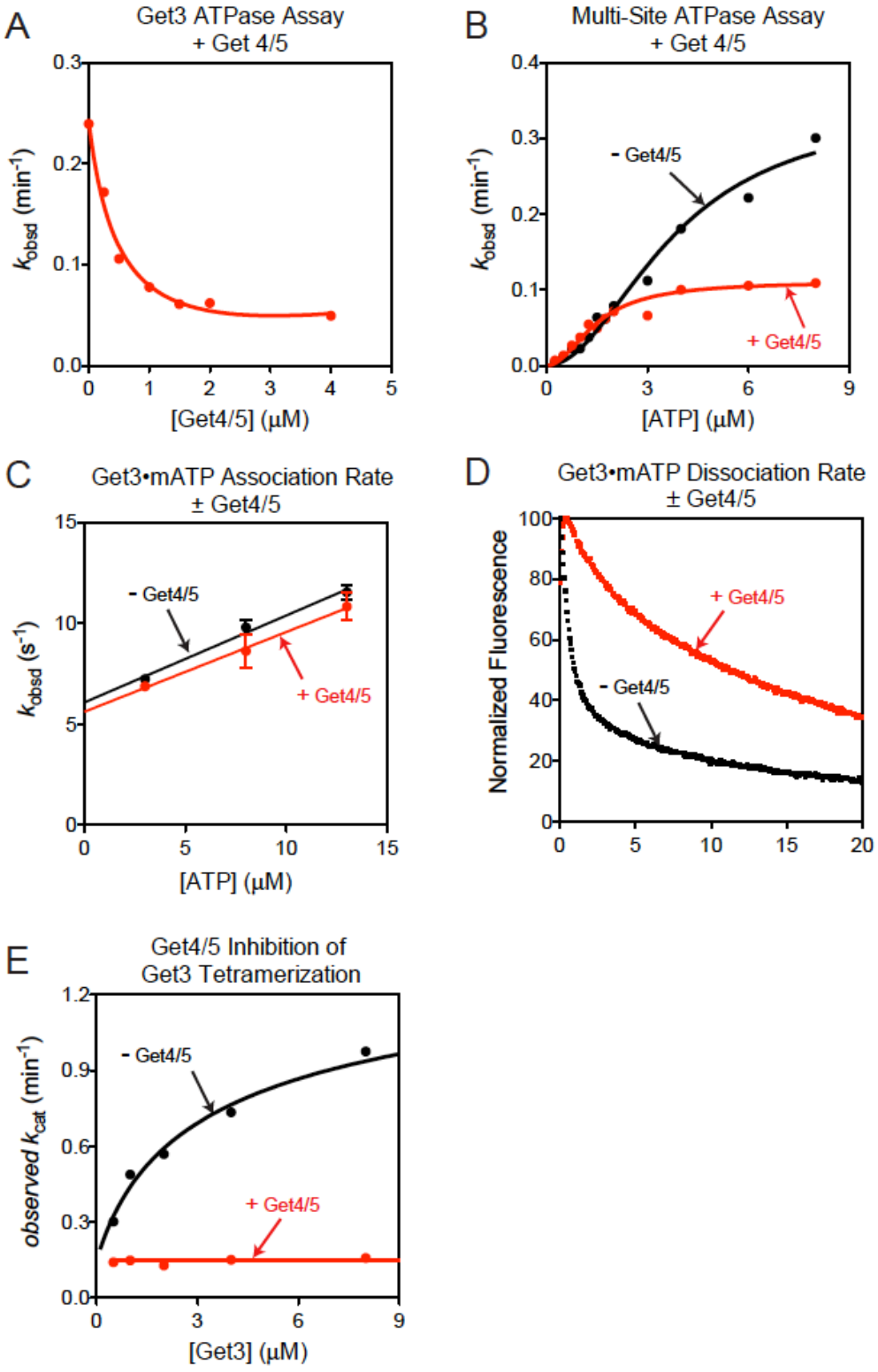

Figure 2.4 Get4/5 strengthens ATP binding to Get3 and inhibits its ATPase activity. (**A**) Get4/5 quantitatively inhibits the ATPase activity of Get3. Reaction contained 0.5 μM

Get3 and 10 μM ATP. (**B**) ATP concentration dependence of observed ATPase activity at 0.5 μM Get3, in the absence (black) and presence (red) of 5 μM Get4/5. The data were fit to SI: Eq 8 and gave average K_M values of 3.7±0.2 and 1.4 ± 0.3 μM, and k_{cat} values of 0.40±0.1 and 0.12±0.05 min^{-1} with and without Get4/5, respectively. (**C**) Association rate constants of mantATP binding to Get3 in the presence (red) and absence (black) of 3.0 μM Get4/5. The data were fit to SI: Eq 4 and the k_{on} values are reported in Table S1. (**D**) Dissociation of mantATP from Get3 was slowed in the presence (red) of 3.0 μM Get4/5. obtained k_{off} values are reported in Table S2. (**E**) Observed k_{cat} values were determined as a function of Get3 concentration with (red) or without (black) 50 μM Get4/5 present. The data with Get3 was analyzed as in (A), and the data with the Get3•Get4/5 complex were fit to a linear function.

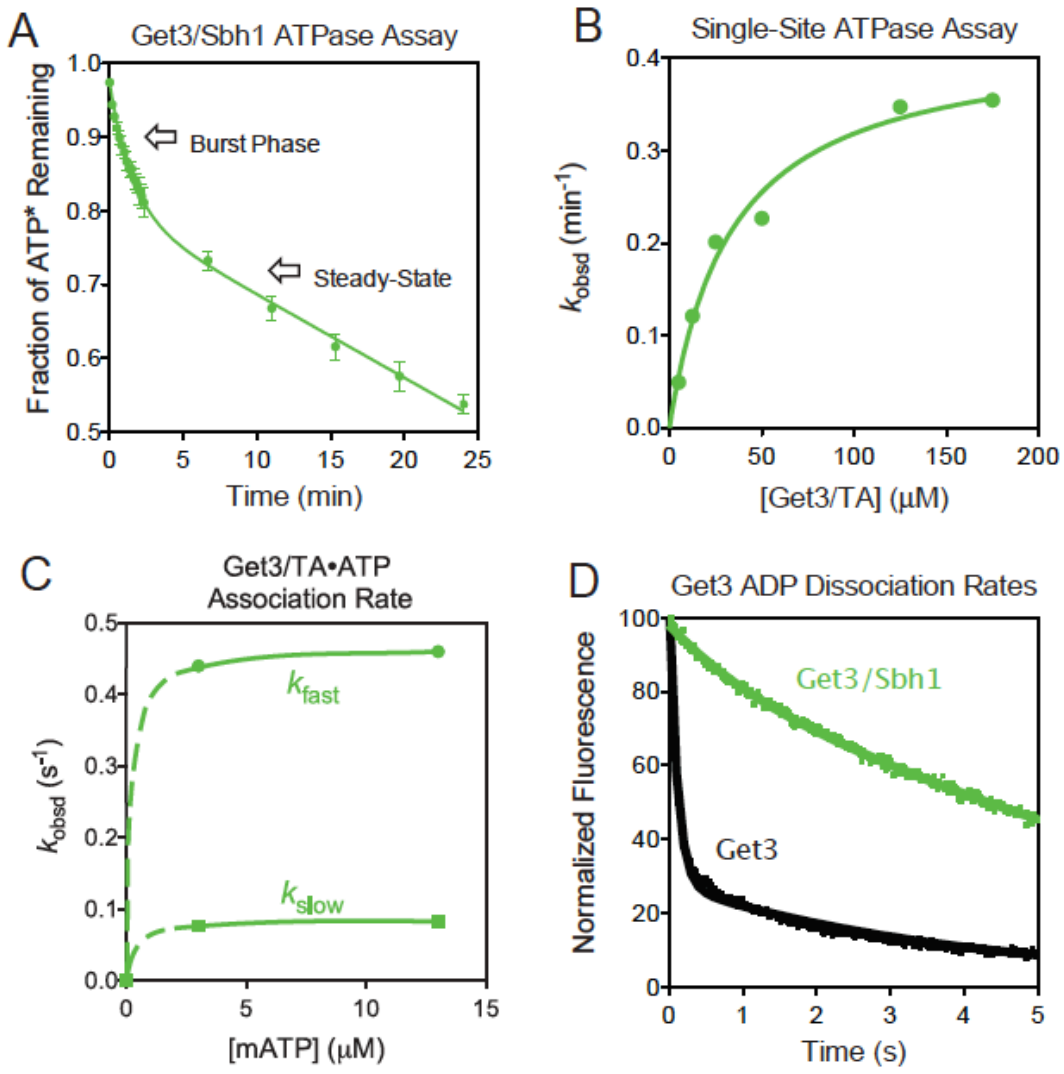

Figure 2.5 TA protein induces rapid ATP hydrolysis. (**A**) Pre-steady-state ATPase measurement at a stoichiometry of Get3/TA:ATP of 1:5. The data were fit to SI: Eq 10 and gave ATPase rate constants of 3.3 ± 1.1 and 0.055 ± 0.001 min^{-1} for the burst- and steady-state phase, respectively. (**B**) ATP hydrolysis from the Get3/TA complex under single-turnover conditions. The data were fit to SI: Eq 7 and gave a k_{cat} value of 0.42 min^{-1} and a K_M value of 33 μM. (**C**) Kinetics of mantATP binding to the Get3/TA complex. Two phases were observed during the binding; both are invariant at 0.45 s^{-1} and 0.08 s^{-1} over a range of mantATP concentrations. The dashed part of the curve depicts theoretical increases in binding rates at lower ATP concentrations where bi-molecular association is rate-limiting, but which was inaccessible in our experiments. (**D**) Dissociation of

mantADP from the Get3/TA complex, measured with 2 μM Get3/TA complex (green) and 20 μM mantADP. The data with Get3 (black) were from Figure S2F (black) and shown for comparison. All rate constants are reported in Table S2.

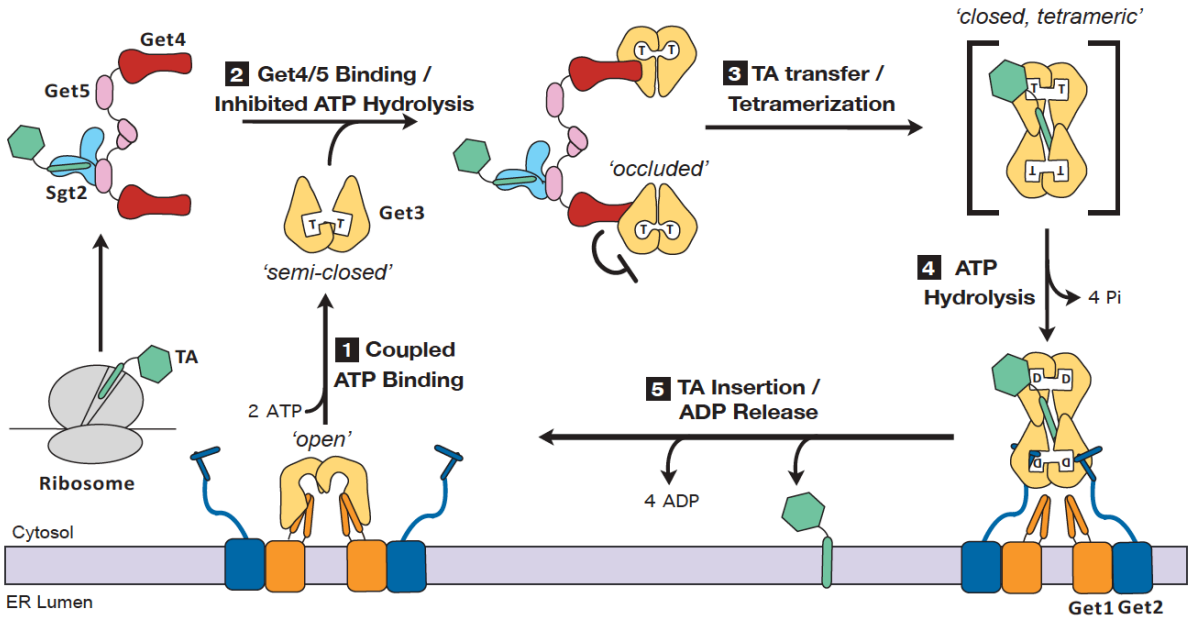

Figure 2.6: Model for TA protein targeting driven by the ATPase cycle of Get3, as described in the text.

Chapter 3

A gradient of interaction affinities drives efficient targeting and recycling in the GET pathway

A version of this chapter is currently in revision at the journal eLife (2014), was written by Michael E. Rome, Un Seng Chio, Harry B. Gristick Meera Rao, and, Shu-ou Shan.

Abstract:

Efficient and accurate localization of membrane proteins requires a complex cascade of interactions between protein machineries. This is exemplified in the GET pathway, where the central targeting factor Get3 must sequentially interact with three distinct binding partners to ensure the delivery of Tail-Anchored (TA) proteins to the endoplasmic reticulum (ER) membrane. To understand the molecular principles that provide the vectorial driving force of these interactions, we developed quantitative fluorescence assays to monitor protein-protein interactions at each stage of targeting. We show that nucleotide and substrate generate a gradient of interaction energies that drive the ordered transit of Get3 to successive effectors. These data also define how the targeting complex is captured, handed over, and disassembled by the ER receptor, and reveal a novel mechanism for how Get3 is recycled. These results provide general insights into how complex protein interaction cascades are coupled to energy inputs in biological systems.

Introduction:

Membrane proteins comprise ~30% of the proteome; their efficient and accurate localization is crucial for the structure and function of all cells. Although the well-studied co-translational Signal Recognition Particle (SRP) pathway delivers numerous ER-destined proteins [27], many membrane proteins utilize post-translational targeting pathways whose mechanisms are far less well understood. A well-known example is tail-anchored (TA) proteins, which comprise 3-5% of the eukaryotic membrane proteome and play essential roles in numerous processes including protein translocation, vesicular trafficking, quality control, and apoptosis [1,44-46]. As their sole transmembrane domain (TM) is at the extreme C-terminus, TA proteins cannot engage the co-translational SRP machinery and instead must use post-translational pathways for localization [47].

In the Guided Entry of Tail-anchored protein (GET) pathway, TA proteins are initially captured by the yeast co-chaperone Sgt2 (or mammalian SGTA)[1,4]. The Get4/5 complex then enables loading of the TA substrate from Sgt2 onto Get3 (or mammalian TRC40), the central targeting factor [2,4,25]. The Get3/TA complex binds a receptor complex on the ER membrane, comprised of Get1 and Get2, via which the TA protein is released from Get3 and inserted into the membrane [6,8,9]. Dissociation from Get1/2 is then needed to recycle Get3 for additional rounds of targeting [7-9]. Knockout of Get3 (or TRC40) confers stress sensitivity in yeast and embryonic lethality in mammals, underscoring its essential role in the proper functioning of the cell [6,10,11].

TA protein targeting is driven by the ATPase cycle of Get3, a member of the SIMIBI (Signal recognition particle, MinD and BioD) class of nucleotide hydrolases [2,15]. Crystallographic studies revealed that Get3 is an obligate homodimer in which the

ATPase domains bridge the dimer interface and are connected to helical domains [13,14]. Notably, the conformation of Get3 can be tuned by its nucleotide state, the TA substrate, and its binding partners [3,8,9,13]. Apo-Get3 is in an *open* conformation in which the helical domains are disconnected [14]. ATP biases Get3 to more *closed* structures in which the helical domains form a contiguous hydrophobic surface implicated in TA protein binding [13,14,21]. The Get4/5 complex further locks Get3 into an *occluded* conformation, in which ATP is tightly bound but its hydrolysis is delayed, priming Get3 into the optimal state to capture the TA substrate [3,48]. TA proteins induce further association of Get3 dimers to form a closed tetramer, which stimulates rapid ATP hydrolysis and delays ADP release [3,16]. Finally, Get1 strongly binds apo-Get3 in the *open* conformation (see also below), likely at the end of the targeting reaction [8,9,24].

The GET pathway demands a sequential cascade of interactions of Get3 with three distinct binding partners: the Get4 subunit in the Get4/5 complex and the Get1 and Get2 subunits in the Get1/2 receptor complex. All three partners share overlapping binding sites on Get3 (Fig. S1 and [48]). This raises intriguing questions as to the mechanisms that ensure the high spatial and temporal accuracy of these protein interactions. For example, Get3 must first interact with Get4/5 in the cytosol to facilitate the loading of TA substrate [4,25]. It is unclear what then drives the release of Get3 from Get4/5 and enables its transit to the ER membrane, where it interacts with the Get1/2 receptor instead.

Similarly, how Get3 and the Get3/TA complex transit between different subunits of the Get1/2 receptor at the ER membrane remain unclear. Get1/2 (WRB/CAML in mammals) is necessary and sufficient for TA protein insertion at the ER membrane [7,9,49,50]. High-resolution crystal structures revealed that Get1 binds strongly to apo- or

ADP-bound Get3 in the *open* conformation [8,9,24]. In contrast, Get2 has been co-crystalized with Get3 in both *open* and *closed* states [8,9]. *In vitro* reconstitution experiments suggest that Get2 helps bind Get3, whereas Get1 plays a more active role in triggering the release of TA protein from Get3 [7-9]. This led to the proposal that Get2 first captures Get3 whereas Get1 disassembles the targeting complex [1,7]. However, which subunit is responsible for capturing the Get3/TA targeting complex has not been experimentally addressed, nor whether Get1 or Get2 can discriminate different substrate-bound states of Get3. When and how Get1 and Get2 compete or collaborate to bind Get3, and how Get3 is transfered from one subunit to the other in the receptor complex remain ambiguous. It is also unclear why the receptor has two distinct proteins, both of which bind Get3 and are conserved throughout eukaryotic evolution.

At the end of targeting, Get1 is bound to apo-Get3 in a tight complex [7-9]. Experiments with the cytosolic domain of Get1 show that its interaction with Get3 is strongly antagonized by ATP, leading to the current model that ATP drives the recycling of Get3 from the ER membrane [8,9]. However, two observations raise difficulties with this minimal model. In experiments with intact ER membranes or Get1/2 proteoliposomes, ATP is not sufficient to completely release Get3 from the membrane [7,9]. Further, the tight interaction of Get1 with Get3 would lead to slow kinetics of their dissociation [8] that are incompatible with the timescale required *in vivo* for multiple rounds of TA protein targeting.

To address these issues, we developed fluorescence assays to report on the interaction of Get3 with its effectors. Quantitative measurements show that both substrate and nucleotide regulate the interaction of Get3 with Get4/5 and Get1/2, generating

differential gradients of interaction energies that drive the ordered transit of Get3 from one binding partner to the next. During the insertion reaction, interactions with Get1/2 are controlled by the substrate and nucleotide occupancy of Get3, with Get3 ‘handover’ occurring upon nucleotide release from the Get3/TA complex. Finally, ATP actively displaces Get3 from Get1, which together with Get4/5 ensure the effective recycling of Get3 back to the cytosol.

Results:

Nucleotide and substrate govern how Get3 interacts with Get4/5

To characterize the interaction of Get3 with full-length heterotetrameric Get4/5 [25], we developed a sensitive fluorescence-based binding assay (Fig. 1A). Get4 contains two cysteines, one of which is buried, and the other was mutated to threonine without affecting function. Using this 'cyslite' Get4/5, we detected its binding to Get3 based on a 70% increase in the fluorescence of acrylodan-labeled Get4 at C48 (Fig. S2A). Labeled Get4/5 is functional in regulating Get3's ATPase activity (Fig. S2B). This assay enables us to quantitatively measure the kinetics and equilibrium of Get3's interaction with the Get4/5 complex, and test how their interaction is regulated in the GET pathway.

We and others have previously shown that Get4/5 specifically enhances ATP binding to Get3 [3] and vice versa [7,25,48]. In support of this model, equilibrium titrations based on the fluorescence assay show that ATP-bound Get3 binds the Get4/5 complex 80-fold more strongly than apo-Get3 (Fig. 1B and Table 1). Interestingly, the equilibrium dissociation constant (K_d) for Get3-Get4/5 binding in ATP is 3.2 nM, over 40-fold tighter than the values obtained using a Get4/5 complex with a truncated Get5 (Get4/5N) **(**Table 1 and [30,48]). Thus, although Get5 is distant from the Get3-Get4 binding interface, full-length Get5 greatly strengthens the association of Get4 with Get3.

Once the TA substrate is loaded onto Get3, it must detach from Get4/5 and contact the Get1/2 receptors instead. The timing and sequence of these interactions are challenging to understand, given that Get4, Get2 and Get1 share overlapping binding sites on Get3. We asked whether the TA substrate or nucleotide state of Get3 were sufficient to provide the vectorial driving force for these events. We co-expressed Get3

with a model TA substrate, Sbh1, and purified recombinant Get3/Sbh1 complex [3,16]. Our results show that in the ATP-bound state, the interaction with Get4/5 is weakened in the Get3/Sbh1 complex compared to free Get3 (K_d = 25.45 nM vs. 3.2 nM; Fig. 1C, D and Table 1A). Remarkably, no interaction could be detected between Get4/5 and the apo-Get3/Sbh1 complex (Fig. 1C, D and Table 1A). Thus, the combination of substrate loading and nucleotide release drive the dissociation of Get3 from Get4/5.

Given the extremely tight interaction of Get3 with Get4/5 in ATP, the question arises as to how Get3 samples various Sgt2•Get4/5 complexes for the presence of the TA substrate. Kinetic measurements show that Get3-Get4/5 association in ATP is extraordinarily fast and at the diffusion-limit of macromolecular interactions (~10^8 $M^{-1}s^{-1}$; Fig. 2A and B; Table 1B). Further, the association kinetics exhibits a strong dependence on ionic strength (Fig. 2C and Table 1B), demonstrating that the rapid initial Get3-Get4/5 association is in part driven by electrostatic attractions. Although all the rate measurements showed two kinetic phases (Fig. 2 and S2; Table 1B & C), the difference between the two phases is modest (≤10-fold in rates and ≤2-fold in equilibrium) and does not affect the conclusions herein. Interestingly, dissociation of the complex is also fast (Fig. 2D and Table 1C), indicating that the Get3•Get4/5 complex is highly dynamic.

Collectively, these results show that in the ATP-bound state, the interaction of Get3 with Get4/5 is tight yet highly dynamic, allowing Get3 to sample multiple Get4/5 complexes on a short timescale. Further, TA substrate loading and nucleotide release collectively drive the dissociation of Get3 from Get4/5, enabling the transit of the targeting complex to the ER membrane.

Capture and handover of Get3/TA by the Get1/2 receptor

To test how the Get3 targeting cycle is completed at the ER membrane, we began by examining the cytosolic domains of Get1 and Get2 (Get1-CD and Get2-CD, respectively), both of which bind Get3 via overlapping sites (Fig. S1; [8,9]). To directly measure the interaction of Get3 with Get1-CD and Get2-CD, we developed a fluorescence-based assay. Both Get1 and Get2 are cysteineless, in which engineered single cysteines were introduced for fluorescence labeling. We monitored the binding of Get3 to Get1-CD or Get2-CD based on robust increases in the fluorescence anisotropy of fluorescein labeled at Get1(C62) or Get2(C34) (Fig. 3A). In addition, Get3 binding strongly enhances the fluorescence of Coumarin-labeled Get1(C62) (Fig. S3A), providing an independent assay to measure the Get3-Get1-CD interaction. The cysteine mutants of Get1-CD and Get2-CD are functional in binding Get3 (Fig. S3B and data not shown). Using these assays, we tested how the interactions of Get3 with Get1 and Get2 are regulated during targeting.

The equilibrium binding affinities of Get3 for Get1-CD and Get2-CD were determined as a function of the substrate- and nucleotide-bound state of Get3 (Fig. 3, B & C), and summarized in the order by which the Get3/TA complex proceeds through its ATPase cycle during the targeting reaction (Fig. 4A and Table 2). Prior to nucleotide release, Get2 has a much higher affinity for the Get3/TA complex than for Get1, suggesting that Get2 is responsible for initial capture of the targeting complex (Fig. 4A, Get3/TA complex). Whereas the Get2-Get3 interaction is relatively insensitive to the nucleotide state and substrate binding of Get3, Get1 strongly prefers to bind free, apo-Get3 such that in this state, Get3 has a 10-fold higher affinity for Get1 than Get2 (Fig. 4A,

red vs purple bars). Thus, nucleotide- and substrate-induced conformational changes allow Get3 to sequentially interact with Get2 and then Get1 at the membrane.

Interestingly, once ADP is released, Get1-CD binds the Get3/TA complex with an affinity similar to that of Get2-CD (Fig. 4A, apo-Get3/TA; Table 2). This strongly suggests that nucleotide release is a key event upon which the targeting complex initiates contact with Get1. In addition, it suggests that the Get2 and Get1 subunits of the receptor complex cooperate in binding Get3/TA at this stage. To test this model, we utilized a Get1/2-mini construct [7], in which Get1-CD and Get2-CD are fused to a pair of oppositely charged α-helices that stably dimerize (Fig. 4B cartoon, and Fig. S4). If the Get1 and Get2 subunits cooperate in binding the Get3/TA complex, then mini-Get1/2 will bind Get3/TA more strongly than either Get1-CD or Get2-CD. Indeed, mini-Get1/2 labeled with DACM at Get1(C62) bound the Get3/TA complex ~6 fold more tightly than Get1-CD or Get2-CD (Fig. 4B, closed circle, Fig. S4B, and Table 2). As a control, a mini-Get1/2 containing a mutant Get2 defective in Get3 binding (mini-Get1/2RERR, [7]) yielded a binding constant identical to Get1-CD (Fig. 4B, open circles; Table 2), confirming the contribution of Get2 to Get3/TA binding in the fusion protein. These results suggest that once ADP is released from the Get3/TA complex, both subunits in the Get1/2 receptor bind the targeting complex synergistically. This not only enhances the efficiency of capture, but could also provide a productive mechanism for the Get3/TA complex to be transferred from the Get2 to Get1 subunit.

Get3 interactions with the full-length receptor in proteoliposomes

To test the insights from measurements with Get1-CD and Get2-CD in the context of the full-length proteins in the membrane environment, we expressed and purified full-length Get1 and Get2 and incorporated them either individually or together into proteoliposomes (PL) (Fig. S5). Using a semi-quantitative proteoliposome sedimentation assay (Fig. 5A), we varied the nucleotide and substrate occupancy of Get3 and measured the amount of Get3 bound to either Get1- or Get2-PL (Fig. 5B). In general, we found that Get3 binds to Get1-PL and Get2-PL at much lower concentrations than what was needed for binding Get1-CD and Get2-CD, suggesting that the transmembrane domain of Get1/2 and/or the presence of the phospholipid membrane enhances the interaction of Get3 with its membrane receptors.

In agreement with results obtained with the cytosolic domains, Get2-PL indiscriminately bound to Get3 with modest sensitivity to the nucleotide state or the presence of TA substrate (Fig. 5B). Get1-PL bound most strongly to apo-Get3; the interaction is weaker with the Get3/TA complex in the apo-state, and is completely abolished if Get3/TA is loaded with ATP (Fig. 5C). Surprisingly, although ATP is expected to completely antagonize Get1 binding to Get3 based on the results with Get1-CD ([7-9] and the results above), significant albeit weakened binding of Get3 to Get1-PL was observed in the presence of ATP (Fig. 5). In summary, binding of Get3 to full-length Get1 and Get2 in the membrane qualitatively recapitulates the trends observed with Get1-CD and Get2-CD, with one notable exception for Get1 interaction with ATP-bound Get3.

ATP actively displaces Get3 from Get1

At the end of the targeting reaction, Get3 is locked into a tight complex with Get1 ([7-9] and Fig. 4). It has been reported that Get1 and ATP compete with one another for binding Get3 [8,9], which we also observed in our fluorescence assays (Fig. 4A). However, available data only support the role of ATP as a competitor that prevents Get3 re-binding to Get1-CD. Whether ATP actively displaces Get3 from the ER membrane is unclear. To test this hypothesis, we compared the kinetics of Get3 dissociation from Get1-CD driven either by ATP, or by unlabeled Get1 that simply traps spontaneously dissociated Get3 (Fig. 6A cartoon). We found that the Get3•Get1-CD complex is kinetically stable, with a lifetime exceeding 200 s (Fig. 6A, black). Remarkably, ATP accelerates the release of Get3 from Get1-CD at least 30-fold, reducing the lifetime of the complex to <5 sec (Fig. 6A, orange; Table 2). This demonstrates that ATP does not act as a passive trap, but rather actively displaces Get3 from Get1.

Independent evidence for an active displacement mechanism was obtained by monitoring the reciprocal reaction, release of mant-ATP from Get3 [3]. To test whether Get1 actively displaces ATP from Get3, we compared the kinetics of mant-ATP release from Get3 driven either by Get1-CD, or by unlabeled ATP that simply traps spontaneously released Get3 (Fig. 6B cartoon). The data show that reciprocally, Get1 accelerates ATP release from Get3 >30-fold (Fig. 6B). Together, these results demonstrate a highly active disassembly process in which Get1 and ATP 'push' each other from Get3.

Get4/5 is required for recycling Get3 from the ER membrane

The tight binding of Get3 to full-length Get1/2 at the ER membrane poses a fundamental challenge for TA trafficking: how is Get3 effectively recycled back to the cytosol for additional rounds of TA targeting? Although ATP can displace Get3 from Get1, our results with Get1-PL indicate that ATP alone is insufficient to drive the complete release of Get3 from the full-length receptor at the membrane (Fig. 5). To address this problem, we pre-incubated Get3 with Get1-PL and tested which combination of factors is required for complete removal of Get3 from Get1 (Fig. 7A cartoon). Given the high affinity of Get4/5 for ATP-bound Get3 (K_d = 3.2 nM, Fig. 1), we suspected that both ATP and Get4/5 would be required to partition Get3 back to the cytosol. Although super physiological levels of ATP could remove a substantial fraction of Get3 from Get1-PL, we found that a combination of ATP and Get4/5 at physiological concentrations were able to completely displace Get3 from Get1-PL (Fig. 7A). Similar results were obtained with yeast ER microsomes derived from a Get3 deletion strain (Δget3 yRM): the combination of ATP and Get4/5 are necessary and sufficient for complete removal of Get3 from the ER membrane, whereas either component alone is not (Fig. 7B). Together, these results strongly suggest that Get4/5 is needed to efficiently recycle Get3 from the ER membrane at the end of TA targeting. Consistent with an additional role for Get4/5 in the GET pathway beyond mediating TA substrate transfer from Sgt2 to Get3, an *in vivo* assay based on Kar2p secretion [6] showed that *Δget4* causes a much stronger defect in TA protein biogenesis than *Δsgt2* (Fig. S6).

Discussion:

The GET pathway demands a complex cascade of substrate capture, loading, delivery, release, and insertion events, whose underlying molecular basis remains enigmatic. This process requires the highly ordered interaction of Get3 with distinct partners that contact Get3 at overlapping binding sites (Fig. S1 and [48]), raising intriguing questions as to how the correct sequence and timing of these molecular interactions is ensured. In this work, quantitative analyses using fluorescence and biochemical assays resolve these questions, provide more detailed models for the targeting and insertion of TA proteins at the membrane, and suggest a new role for Get4/5 in the recycling of Get3 from the membrane.

Get4/5 samples and discriminates different Get3 states.

The Get4/5 complex is required for Get-dependent TA targeting and facilitates the transfer of TA proteins from Sgt2 to Get3 [4]. Remarkably, association between Get3 and Get4/5 occurs at diffusion-limited rates (Fig. 2) and is among the fastest association rates observed between proteins. This is achieved in part by electrostatic attractions, a recurring theme that has also been observed with the barnase-barstar interaction [51], ubiquitin ligases binding to ubiquitin-conjugating enzymes [52], and ribosomal binding proteins [53]. This allows Get3 to form a tight complex with Get4/5, while still being able to sample multiple Get4/5 complexes on a short timescale until it finds its cognate TA substrate. Notably, the TA-binding chaperone Sgt2 also binds the Get4/5 complex with rapid association and dissociation rates [54]. These examples likely underlie a common

principle whereby factors involved in membrane protein biogenesis continuously sample their environments.

Get4/5 displays an exceptional ability to discriminate between distinct nucleotide and substrate states of Get3. ATP binding to Get3 enhances the interaction with Get4/5 80-fold, whereas TA substrate occupancy weakens this interaction 8-fold, and nucleotide release from the Get3/TA complex abolishes the interaction. This enables Get4/5 to strongly bind and pre-organize Get3 in the correct nucleotide and conformational state to capture the TA substrate, but also to detach readily from Get3 once the TA substrate is loaded. The latter also implies that Get3 transits to the ER membrane to interact with the Get1/2 receptor only when it acquires its TA substrate. How Get4/5 generates this exquisite molecular discrimination awaits to be determined.

Differential interactions with Get1 and Get2 drive the capture and remodeling of the targeting complex.

The mechanism of TA protein insertion at the ER membrane remains enigmatic with several outstanding questions: 1) Why are two ER membrane proteins, Get1 and Get2, required? 2) When do Get1 and Get2 interact with the targeting complex, and how is this decision made? 3) How is Get3 recycled from the ER membrane at the end of the targeting cycle? Quantitative analysis of Get3's interaction with Get1/2 shed new light on these issues.

We previously showed that ADP release from the Get3/TA complex is 100-fold slower than free Get3, and ATP-rebinding to the Get3/TA complex is delayed >10,000-fold compared to free Get3 [3]. This suggests that Get3/TA complexes encounter the

Get1/2 receptor in the ADP state. In this work, we found that Get2 binds with little discrimination as to the nucleotide or substrate occupancy of Get3. In contrast, Get1 has a much lower affinity for the Get3/TA complex before nucleotide release and instead strongly prefers apo-, free Get3. Coupled with the tight binding of Get3/TA to Get2-PL, this provides energetic evidence that Get2 is the first subunit to capture the Get3/TA targeting complex in the ADP-bound state (Fig. 8A, step 2). On the other hand, Get1 acts only at late stages, and its stronger binding to free Get3 compared to Get3/TA provides the driving force for the disassembly of the Get3/TA complex. This model is consistent with experiments showing that high concentrations of Get1 can trigger substrate release from Get3 [9].

Interestingly, nucleotide release from the Get3/TA complex induces distinct changes in the interaction of Get3 with multiple partners. Upon ADP release, the interaction of Get4/5 with Get3/TA is completely abolished, whereas Get1 attains substantial affinity for Get3/TA. Further, the anisotropy values of both the Get1•Get3/TA and Get2•Get3/TA complexes increase substantially when ADP dissociates (Fig. S3C). These results strongly suggest that the Get3/TA complex transitions to a new conformational state after ADP release, which we term a '*strained tetramer*' (Fig. 8A, step 2). At this stage, the affinities of Get1 and Get2 for the Get3/TA complex become approximately equal. Coupled with the strong preference of Get1 for apo-Get3, we propose that ADP-release represents a key switch point at which Get3 is transferred from Get2 to Get1 to initiate remodeling and disassembly of the Get3/TA complex (Fig. 8A, steps 2-3).

Experiments in which Get1 and Get2 are simultaneously presented to Get3 (Fig. 4B) further demonstrate that both subunits co-bind once the Get3/TA complex reaches the apo-stage (strained tetramer conformation). Co-binding provides a productive pathway that minimizes loss of the Get3/TA complex during its transfer from Get2 to Get1 at the membrane. It also raises the possibility that Get2 can help retain any Get3/TA complexes that fail to be successfully disassembled by Get1 and allow for additional rounds of remodeling, thus enhancing the efficiency of this process.

ATP and Get4/5 cooperate in the recycling of Get3 from the membrane.

Once the TA substrate is inserted into the membrane, Get3 must partition back to the cytosol to begin a new round of protein targeting. Our pre-steady state kinetic analysis shows that dissociation of Get1 from Get3 is very slow and poses a kinetic barrier for multiple rounds of targeting *in vivo.* Although previous work showed that ATP strongly antagonizes the binding of Get1-CD to Get3 [1,7,8], whether ATP passively traps free Get3 or actively disassembles the Get3•Get1 complex was unclear. Here we provide strong evidence that ATP actively displaces Get3 from Get1 and brings the kinetics of Get3 recycling to a much faster timescale. This result also implies the existence of a transient Get3•Get1•ATP intermediate during disassembly, in which ATP and Get1 'push' one another to accelerate release (Fig. 8B, steps 4-5).

Which factor wins this 'tug of war' depends both on their respective affinities for Get3 and concentrations in cells. With Get1-CD, the cellular concentration of ATP (4 mM) is sufficient to drive the unidirectional release of Get3 from Get1. However, binding assays with full-length Get1/2 in proteoliposomes or ER-microsomes indicate that

additional factors are needed. Full-length Get1 binds to Get3 much more tightly than Get1-CD, such that complete Get3 dissociation cannot be achieved even at super physiological concentrations of ATP. These results are consistent with previous observations that Get3 could only be competed off Get1/2-PL or ER microsomes under conditions when ATP and excess Get3 competitor were used [7], or when Get1PL-Get3 complexes are subjected to rapid pull-downs in the presence of ATP [9].

The finding that both Get4/5 and ATP are required for Get3 ER recycling (Fig. 7) resolves the conundrum for how the pathway overcomes the tight binding of Get3 to Get1 to achieve effective recycling. These results reveal that Get4/5 is required for maintaining a cytosolic pool of Get3, and explain why deletion of Get4/5 lead to phenotypes more similar to that of *Δget3* rather than *Δsgt2* cells [4,11]. If the sole function of Get4/5 is to facilitate TA transfer from Sgt2 to Get3, then deletion of Get4/5 should phenocopy that of Sgt2. Instead, Δ*get4/5* mutations are significantly more deleterious than Δ*sgt2*, supporting the role of Get4/5 as an essential factor in controlling the cellular localization of Get3 (Fig. S6 and [4,55]).

Taken together, our results provide a new model for how Get3/TA complexes are captured, processed, and recycled at the ER membrane (Fig. 8A). Get3/TA complexes transit to the ER in the ADP state and are first tethered to the membrane by binding Get2 (step 1). ADP release induces a strained conformation in the Get3/TA tetramer, allowing the complex to be transferred from Get2 to Get1 in a coordinated mechanism (step 2-3). The strong preference of Get1 for apo-Get3 over Get3/TA and its ability to insert into the hydrophobic cavity of Get3 [8,9,24] drive the disassembly of the targeting complex (step 3). After TA insertion, ATP binding to the Get1•Get3 complex produces a highly unstable

intermediate, leading to facile displacement of Get3 from the membrane (step 4-5). Once Get3•ATP complexes dissociate from Get1, they rapidly form a tight complex with Get4/5, preventing re-binding of Get3 to Get1 (step 5). The protein targeting cycle then resets as Get3 waits to bind a new TA substrate (step 6).

Collectively, the results herein demonstrate that the TA substrate and nucleotide generate differential gradients of interaction affinities between Get3 and its binding partners (Fig. 8B), providing the vectorial driving force for the ordered capture, remodeling and disassembly of the targeting complex during TA protein targeting. These results also rationalize why two distinct subunits are required in the Get1/2 receptor: it resolves the conflicting requirement of the membrane receptor to both effectively capture and destabilize the targeting complex, by using Get1 and Get2 to fulfill these two opposite functions. Effectively, Get2 bridges the gap during Get3's interaction cycle, after Get3/TA dissociates from Get4 and before it can interact effectively with Get1 (Fig. 8B). This principle shares conceptual parallels to the machineries mediating vesicular tethering and fusion [56,57]. Analogous to the role of Rabs in tethering nascent vesicles to target organelles, Get2 acts to capture and tether Get3/TA complexes to the ER membrane. Analogous to the role of v-/t-SNAREs as remodeling machines that destabilize membrane bilayers and induce fusion [58,59], Get1 acts to remodel and disassemble the targeting complex to enable membrane insertion of the TA substrate. Such 'two-component' systems may be a general strategy during protein targeting processes.

Materials and Methods

Protein Expression and Purification. *Sc*Get3, *Sc*Get3/TA, and *Sc*Get4/5 were expressed and purified according to published procedures [3,14,16,25]. All mutant proteins were generated using Quikchange Mutagenesis protocol (Stratagene), and were purified identically to the wildtype protein. His_6-tagged Get1-CD and Get2-CD (both in a pET33b expression vector) were induced at log phase for 3 hours at 37°C with 0.8mM Isopropyl β-D-1-thiogalactopyranoside (IPTG). Overexpressed protein in clarified lysate was purified by Ni-NTA affinity chromatography followed by thrombin digestion to remove the affinity tag. Get2-CD was further purified by gel filtration chromatography on a Superdex200 column (GE healthcare). Get1-CD was further purified by gel filtration chromatography on a superpose 12 column (GE healthcare). His6-tag Get1/2-mini [7] was expressed for 3 hours at 37°C, and purified by Ni-NTA affinity chromatography. To obtain stoichiometric complex, partially purified proteins were further purified with a 125ml Superdex75 gel filtration column (GE healthcare). Full-length Get1 and Get2 were expressed identically to [9] using the overnight auto induction system (Novagen) in TB media [60]. For purification, Get1 and Get2 (approximately 20-30 g of dry weight cell pellet) were re-suspended in buffer A (50 mM HEPES, pH 8.0, 500 mM NaCl, 10% Glycerol) containing protease inhibitor cocktail (Roche), and lysed by French cell press. Unbroken cells were removed by centrifugation at 12000g for 20 minutes, and the supernatant was subjected to ultracentrifugation in a Ti45 at 200,000 x g for 50 minutes. The resulting membrane pellet was washed in buffer A, resuspended in buffer A with 0.5% LDAO and 20mM Imidazole using a dounce homogenizer, and incubated for 1 hour under gentle agitation. Detergent-solubilized membrane was clarified by

ultracentrifugation in a Ti45 as above, and the supernatant was subjected to Ni-NTA chromatography in buffer A with 0.1% LDAO and 20 mM Imidazole. Following extensive washing, His_6-tagged Get1 or Get2 was eluted in buffer A with 0.1% LDAO and 200 mM Imidazole, and immediately flash frozen in liquid nitrogen. All proteins (with the exception of Get1/2 full-length) were exchanged into Get3 assay buffer (50mM HEPES pH 7.4, 150mM potassium acetate, 5mM magnesium acetate, 1mM DTT and 10% glycerol) in the gel filtration step.

Fluorescence labeling. Get4/5 (C177T/S48C) was labeled with thiol-reactive acrylodan. Get1CD-Q62C, Get2CD-T34C, and Get1/2 mini (with a Get1 Q62C mutation) were labeled with maleimide derivatives of either coumarin (DACM) or fluorescein. Protein was dialyzed in labeling buffer (50 mM KHepes, pH 7.0, 300 mM NaCl) and treated with 2 mM TCEP to reduce the disulfide bonds. The labeling reaction was carried out using a 10-30 fold excess of dye over protein. The reaction was incubated overnight at 4 °C and stopped by adding 2 mM DTT. Excess dye was removed by gel filtration using Sephadex G-25 (Sigma) [43].

Fluorescence measurements

All measurements were carried out at 25 °C in Get3 assay buffer using a Fluorolog-3-22 spectrofluorometer (Jobin Yvon) or a Kintek stopped-flow apparatus.

Get4/5 equilibrium measurements. Measurements using acrylodan-labeled Get4/5 were based on an environmental sensitive readout. Samples were excited at 370 nm and fluorescence emission at 490 nm was monitored. For all titrations, Get4/5FL was held

constant (50 – 200 nM) and Get3 concentration was varied. Incubation time was 10 minutes and nucleotide was present at 2 mM wherever applicable. Observed fluorescence values (F_{obsd}) were plotted as a function of Get3 concentration and fit to Eq 1,

$$F_{obsd} = F_0 + F_1 \times \frac{K_d + [\text{Get4/5}] + [\text{Get3}] - \sqrt{(K_d + [\text{Get3}] + [\text{Get4/5}])^2 - 4[\text{Get3}][\text{Get4/5}]}}{2[\text{Get4/5}]} \quad (1)$$

in which F_{obsd} is the observed fluorescence, F_o is the initial fluorescence value, F_1 is the maximum fluorescence change at saturating Get3 concentrations, and K_d is the equilibrium dissociation constant of the complex.

Get4/5 association and dissociation kinetics. All rate measurements were performed on a Kintek stopped-flow apparatus. For association rate measurements, acrylodan-labeled Get4/5 was held constant at 0.2 μM, Get3 concentration was varied as indicated, and ATP was present at 2 mM. Observed rate constants (k_{obsd}) were plotted as a function of Get3 concentration and fit to Eq 2,

$$k_{obsd} = k_{on}[\text{Get3}] + k_{off} \quad (2)$$

in which k_{on} is the association rate constant, and k_{off} is the dissociation rate constant.

For dissociation rate measurements, a pulse-chase experiment was used. A complex between acrylodan-labeled Get4/5 (at 0.15 μM) and Get3 (at 0.3 μM) was preformed by incubation in 2 mM ATP for 10 minutes, followed by addition of unlabeled Get4/5 at 6 μM as the chase to initiate Get3-Get4/5 dissociation. The time course for change in fluorescence (F_{obsd}) was fit to a double exponential function (Eq. 3),

$$F_{obsd} = F_e + \Delta F_1 \times e^{-k_{fast}t} + \Delta F_2 \times e^{-k_{slow}t} \quad (3)$$

in which F_e is the fluorescence when the reaction reaches equilibrium, ΔF_1 and k_{fast} are the magnitude and rate constant of the fluorescence change in the fast phase, and ΔF_2 and k_{slow} are the magnitude and rate constant of the fluorescence change in the slow phase,

Equilibrium measurements of Get3 binding to Get1- and Get2-CD. Measurements using fluorescein-labeled Get1- or Get2-CD were based on a fluorescence anisotropy readout (Fig. 3). Samples were excited at 450 nm and fluorescence emission at 518 nm was monitored. For all titrations, Get1-CD or Get2-CD was held constant at 200 nM and Get3 or Get3/TA concentration was varied. Incubation time was 5-10 minutes depending on protein concentration, and nucleotide was present at 2mM. Observed anisotropy values were plotted as a function of Get3 concentration and fit to Eq 1, with anisotropy values replacing the fluorescence values.

Equilibrium measurements of Get3/TA binding to Get1/2-mini. Measurements are based on the fluorescence change of DACM-labeled Get1 (denoted by *) in Get1*/2-mini. Samples were excited at 380 nm and fluorescence emission at 470 nm was monitored. For all titrations, Get1*/2-mini was held constant at 200 nM and Get3/TA concentration was varied. Incubation time was 10 minutes. Observed fluorescence values (F_{obsd}) were plotted as a function of Get3/TA concentration and fit to Eq 1.

Get1-CD dissociation kinetics from Get3. Measurements used a pulse-chase setup on the stopped-flow apparatus (Kintek). 150 nM DACM-labeled Get1-CD was pre-incubated with 350 nM Get3 for 15 minutes, and chased by addition of either 2 mM ATP or 8.5μM unlabeled Get1-CD to initiate complex dissociation. Samples were excited at

380 nm and fluorescence emission at 470 nm was monitored. The time course for change in fluorescence (F_{obsd}) was fit to Eq. 3.

Kinetics of mant-ATP dissociation from Get3. Measurements are based on FRET between mant-ATP and a native tryptophan in Get3 [3], using a pulse-chase setup on a stopped-flow apparatus (Kintek). A complex between mant-ATP (at 15 μM) and Get3 (1.5 μM) was preformed by incubation for 20 minutes, followed by addition of either Get1 (at 2.5 μM) or excess ATP (2 mM) to initiate complex dissociation. The time course for change in donor (mant-ATP) fluorescence (F_{obsd}) was fit to Eq. 3.

Reconstitution of Get1/2 into proteoliposomes. Proteoliposomes containing Get1, Get2, or the Get1/2 complex were prepared as previously described [9] with modifications. The following mixture was assembled in a volume of 300-400 μl: 2-3 μM of membrane protein, 87 mg of washed biobeads (SM-2, Bio-Rad), 30 μl of 20 mg/ml lipids (4:1 PC:PE), 300 μl of reconstitution buffer (50 mM HEPES-KOH, pH 7.4, 500 mM potassium acetate, 5 mM magnesium acetate, 250 mM sucrose, 1 mM DTT, 0.25% DBC). The mixture was incubated overnight with gentle agitation at 4 °C. For Get2-only proteoliposomes, half the amount of biobeads was added for the overnight incubation and a second incubation was included with 87 more mg of biobeads for 2 hours. Following biobead removal, 5 volumes of cold water was added to the reaction, and then pelleted at 311,000g for 30 minutes. The resulting proteoliposome-containing pellet was resuspended in 70 μl of membrane buffer (50 mM HEPES-KOH pH 7.4, 100 mM potassium acetate, 5 mM magnesium acetate, 250 mM sucrose, and 1 mM DTT).

Proteoliposome concentration was determined by SDS-PAGE with a known amount of recombinant Get1 or Get2 protein using silver stain (Thermo).

Proteoliposome sedimentation assay. The experiments described in Figure 5 were performed using the following setup. For Get2-PL binding assays, 96 nM of Get2-PL or equivalent volume of empty-PL were mixed with 500 nM Get3 or Get3/TA in Get3 assay buffer and 2 mM ATP (optional), in a total volume of 150 µl. For Get1-PL binding assays, 20 nM of Get1-PL or equivalent volume of empty-PL were mixed with 40 nM Get3 or Get3/TA Get3 assay buffer and 2 mM ATP (optional), in a total volume of 150 µl. The reactions were incubated for 10 minutes at room temperature, and then ultracentrifuged at 434,000g for 30 minutes. The resulting pellet was resuspended in gel loading dye, and analyzed by SDS-PAGE and silver-staining. The protein bands were quantified using Image QuantTL (GE Healthcare). All values were normalized to the strongest binder in each data set (i.e., ATP-Get3 for Get2-PL, and apo-Get3 for Get1-PL). When comparing Get3 to Get3/TA binding, the values obtained for Get3/TA were multiplied by 1/2 to account for the fact that Get3/TA is a tetramer whereas Get3 is a dimeric.

Get3 recycling assay. Experiments using Get1-PL (Figure 6C) were initiated by pre-incubating the following mixture for 10 minutes at room temperature: 100 nM of Get1-PL or equivalent volume of empty-PL, 100 nM His_6-Get3, and ATP (at indicated concentrations) in a total volume of 150 µl in Get3 assay buffer. Get4/5 (at indicated concentrations) was then added for an additional 10 minutes and the reaction was pelleted as described for the sedimentation assay. Get3 was detected by Western blotting using an

anti-His antibody (Qiagen). Experiments with yRM were initiated by pre-incubating the following mixture for 10 minutes at room temperature: 0.26 U/mL of Δ*get3* yRM, 50 nM His_6-Get3, and ATP (at indicated concentrations) in a total volume of 150 µl in Get3 assay buffer. Get4/5 (at indicated concentrations) was then added for an additional 10 minutes and the reaction was pelleted as described for the sedimentation assay. Equivalent amounts of the soluble and pellet fractions were analyzed by western blot against His_6.

Kar2 secretion assay. Kar2 secretion assays were carried out as described in [6]. For western blot analysis, Kar2 anti-rabbit antibody was used at 1/3000 dilution. The protein bands were quantified using Image QuantTL (GE Healthcare).

Table 1 Summary of the equilibrium binding affinities and kinetics of Get3's interaction with Get45.

A. Equilibrium affinity of the interaction of Get3 with Get4/5.

Get4/5 construct	Get3 complex	Nucleotide	K_d (nM)
Full-length Get4/5	Get3	Apo	233.5 ± 47.3
		ATP	3.20 ± 1.97
	Get3/TA	Apo	Not detectable
		ATP	25.5 ± 4.31
		ADP	19.32 ± 1.37
Get4/5N	Get3	Apo	6.0×10^3
		ATP	127 ± 5.6

B. Summary of the kinetics of Get3-Get4/5 association in ATP.

Ionic Strength Buffer	1st Phase		2st Phase	
	k_1 ($\mu M^{-1} s^{-1}$)	amplitude (%)	k_2 ($\mu M^{-1} s^{-1}$)	amplitude (%)
150 mM KOAc	143.8 ± 11.5	57	43.5 ± 5.0	43
350 mM NaCl	8.9 ± 0.419	64	32.9 ± 6.28	36
100 mM NaCl	145.3 ± 5.88	59	39.2 ± 4.05	41
No Salt	271.9 ± 8.42	59	38.9 ± 9.86	41

C. Summary of the kinetics of Get3 dissociation from Get4/5 in ATP.

Ionic Strength Buffer	1st Phase		2st Phase	
	k_{-1} (s^{-1})	amplitude (%)	k_{-2} (s^{-1})	amplitude (%)
150 mM KOAc	1.10 ± 0.061	50	0.092 ± 0.004	50

Table 2. Summary of the equilibrium binding affinities of Get3's interaction with Get1-CD and Get2-CD.

Receptor	Get3 complex	Nucleotide	K_d (μM)
Get1	Get3	apo	0.055 ± 0.015
		ADP	0.616 ± 0.183
		ATP	Not detectable
	Get3/TA	apo	2.20 ± 0.28
		ADP	2.74 ± 0.003
		ATP	Not detectable
Get2	Get3	apo	0.469 ± 0.09
		ADP	0.444 ± 0.126
		ATP	0.90 ± 0.170
	Get3/TA	apo	1.61 ± 0.006
		ADP	2.74 ± 0.003
		ATP	2.77 ± 0.822
Mini-Get1/2	Get3/TA	apo	0.328 ± 0.006
Mini-Get1/2RERR		apo	1.85 ± 0.353

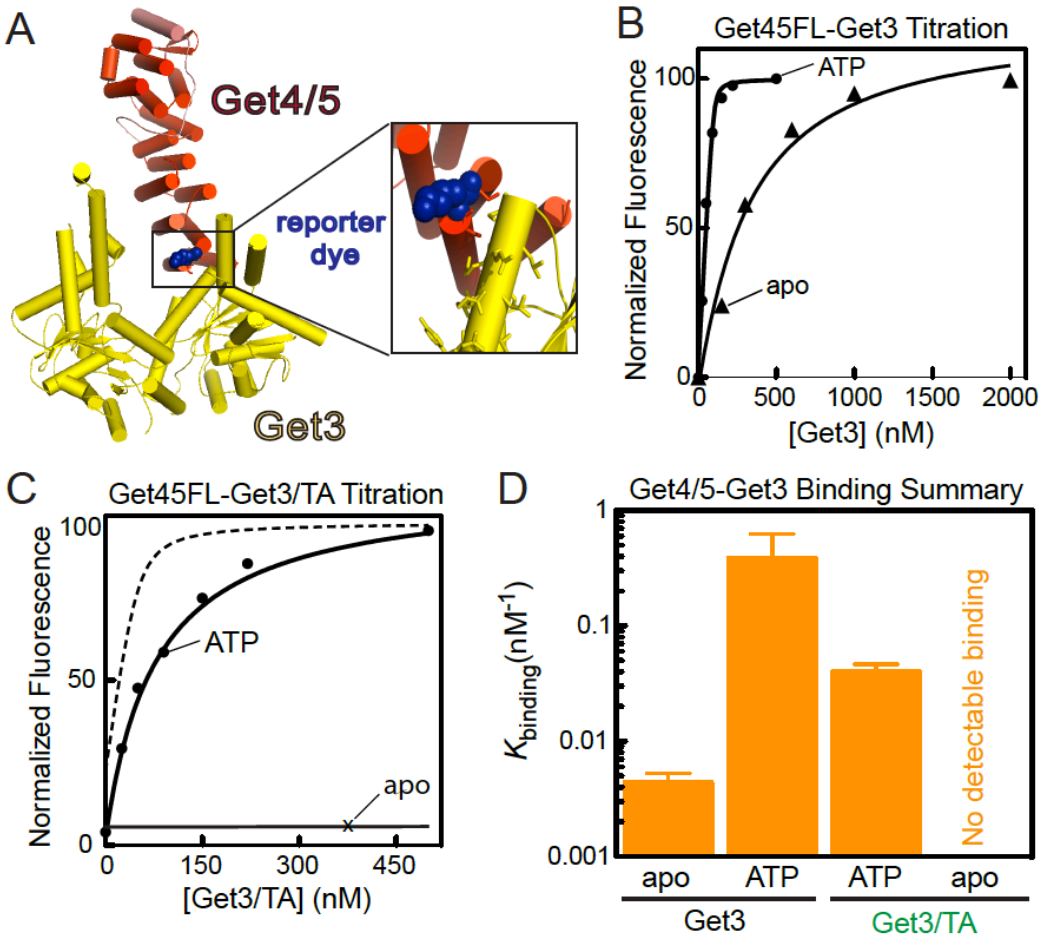

Figure 3.1. Nucleotide and substrate govern how Get3 interacts with Get4/5. (**A**) Structure of Get3 (yellow) bound to Get4/5N (red) [48]. The zoom in shows the placement of the reporter dye on Get4. (**B**) Equilibrium titrations for the binding of Get3 to Get4/5 in the apo- (triangle) and ATP-bound (closed circles) states. Data are fit to equation 1 and the K_d values are summarized in Table 1A. (**C**) Equilibrium titrations for binding of the Get3/TA complex to Get4/5 in the apo- (cross) and ATP-bound (closed circles) states. The data are fit to equation 1 and the K_d values are summarized in Table 1A. The dotted line depicts Get4/5 binding to ATP-bound Get3 from part B and is shown for comparison. (**D**) Summary of the binding constants ($K_{binding} = 1/K_d$) of Get4/5 to Get3 and Get3/TA.

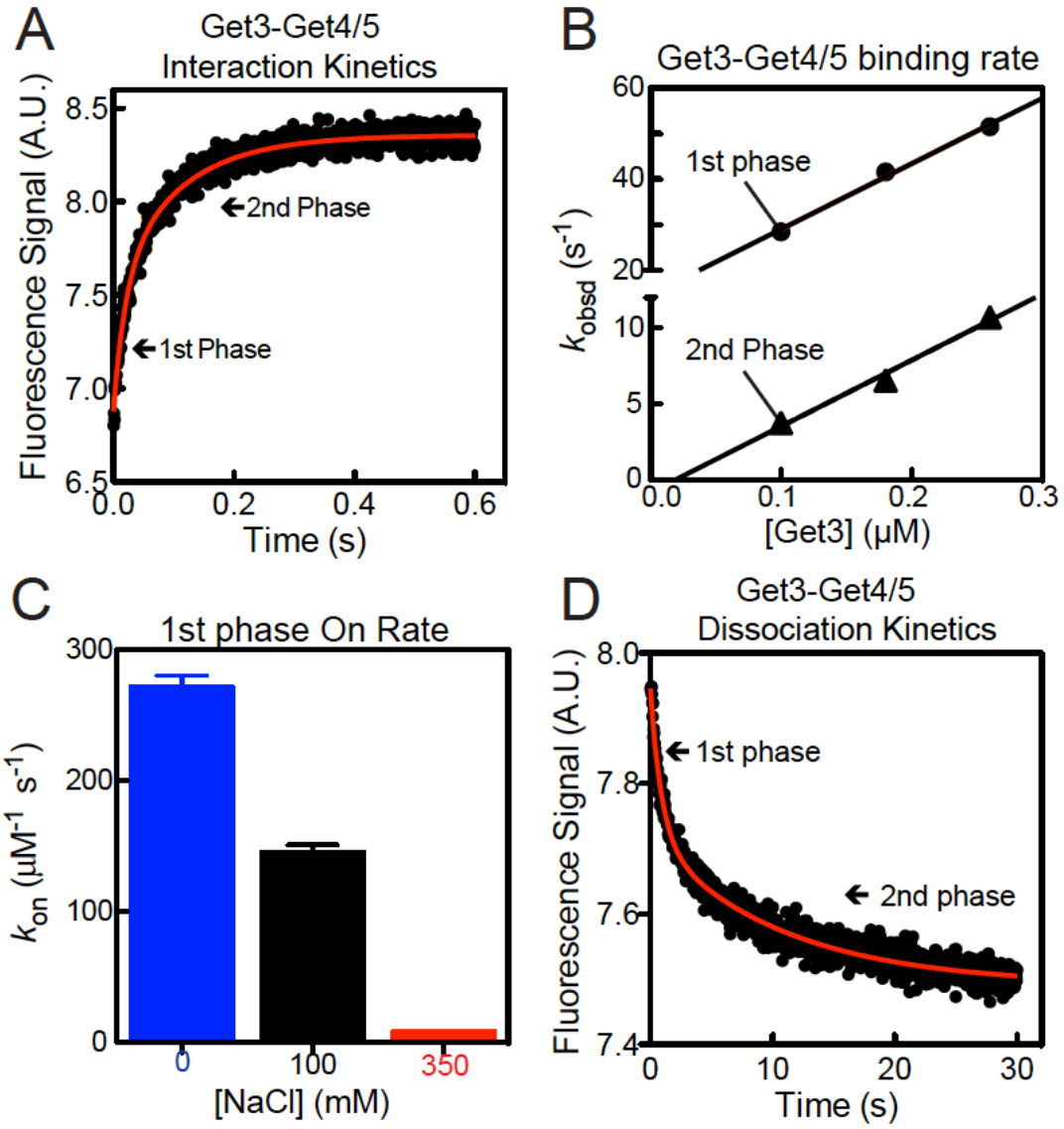

Figure 3.2. Get3 binds to Get4/5 with rapid dynamics. (**A**) Time course of Get4/5 binding to ATP-bound Get3. Arrows indicate the two kinetic phases. (**B**) Observed association rate constants (k_{obsd}) are analyzed as a function of Get3 concentration to determine the association rate constant k_{on} for both the first (circles) and second (triangles) kinetic phases. The data were fit to equation 2, and the k_{on} values are reported in Table 1B. (**C**) Get3-Get4/5 association rates are highly salt-sensitive. See also Table 1B. (**D**) Dissociation rate constants of Get3-ATP from Get4/5. See also Table 1C.

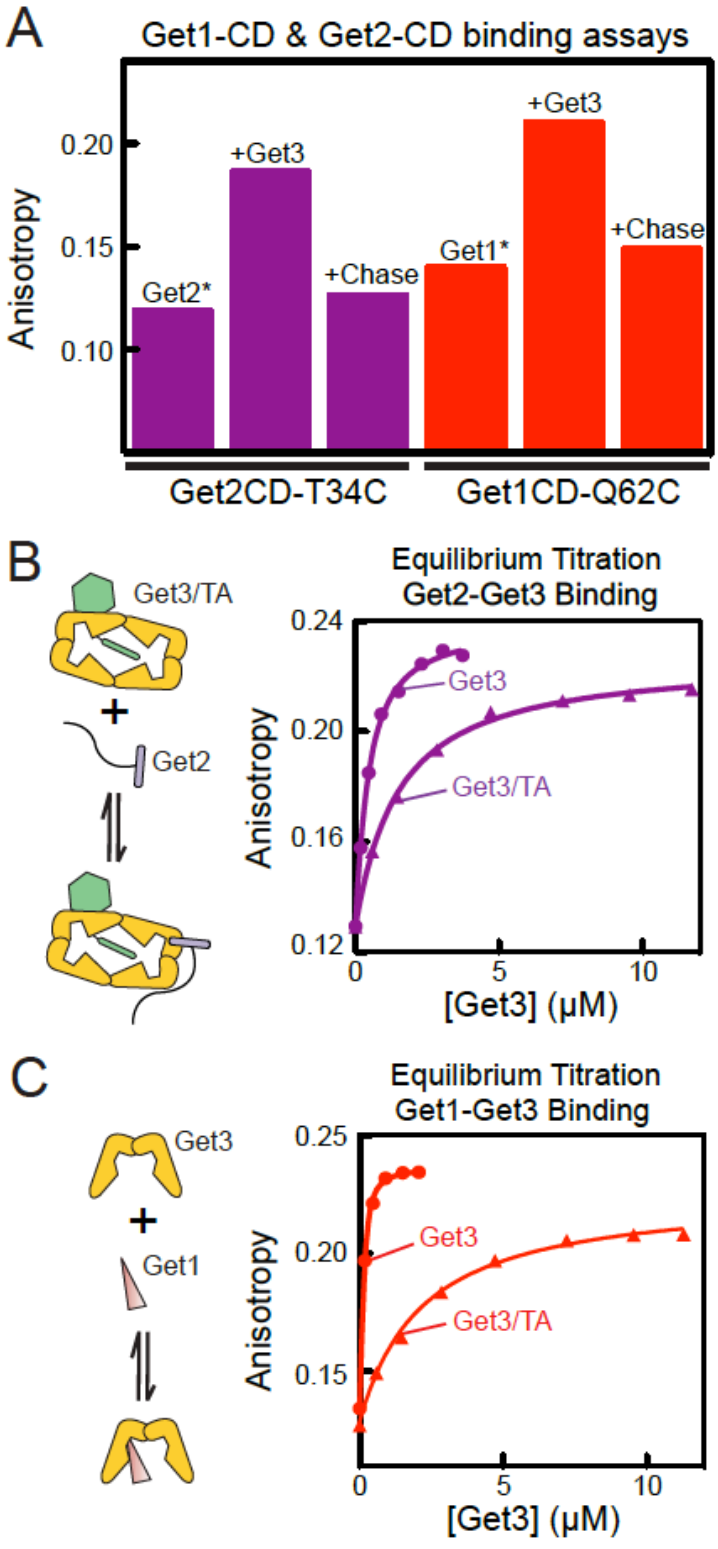
A
Get1-CD & Get2-CD binding assays
Anisotropy
0.20
0.15
0.10
Get2*
+Get3
+Chase
Get1*
+Get3
+Chase
Get2CD-T34C
Get1CD-Q62C
B
Get3/TA
+
Get2
Equilibrium Titration
Get2-Get3 Binding
Anisotropy
0.24
0.20
0.16
0.12
Get3
Get3/TA
0
5
10
[Get3] (μM)
C
Get3
+
Get1
Equilibrium Titration
Get1-Get3 Binding
Anisotropy
0.25
0.20
0.15
Get3
Get3/TA
0
5
10
[Get3] (μM)

Figure 3.3. Interaction of Get3 with Get1-CD or Get2-CD is modulated by nucleotide state and TA loading. (**A**) Fluorescence anisotropy of 200 nM fluorescein-labeled Get2CD-T34C (Get2*) and Get1CD-Q62C (Get1*) by itself, in the presence of 2 μM Get3 (+Get3), or in the presence of Get3 and excess unlabeled Get1- or Get2-CD (+chase). (**B** – **C**) Representative equilibrium titrations for binding of Get1* (B) and Get2* (C) to apo-Get3 and apo-Get3/TA.

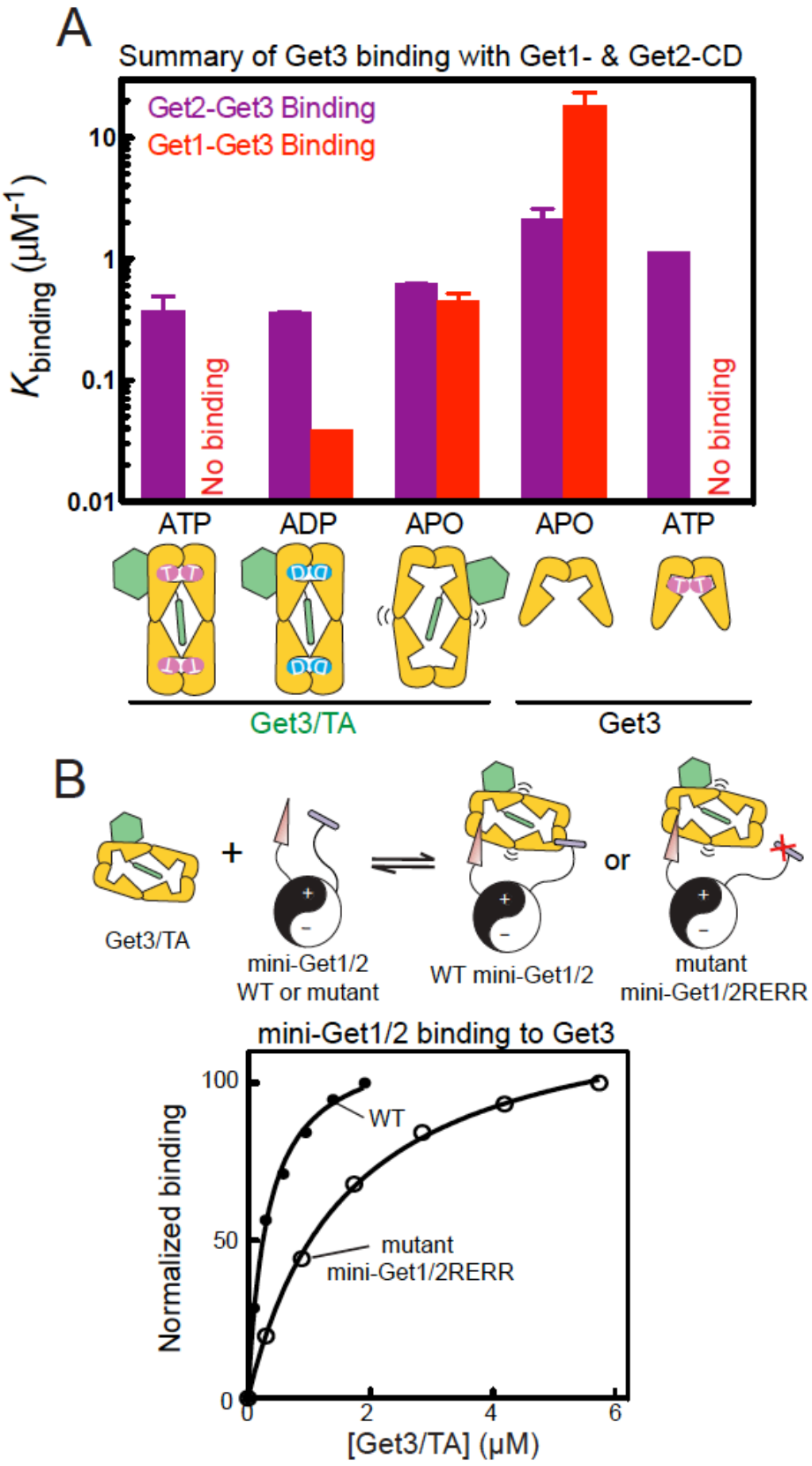

Figure 3.4. Capture and handover of Get3/TA by the Get1/2 receptor. (**A**) Summary of

the binding affinity ($K_{binding} = 1/K_d$) of Get3 for Get2-CD (purple) and Get1-CD (red) in different substrate occupancy and nucleotide states. See also Table 2. (**B**) Binding of the Get3/TA complex to 200 nM DACM labeled wildtype mini-Get1/2 (closed circles) or mutant mini-Get1/2RERR (open circles). The data were fit to equation 1 and the values of K_d are reported in Table 2. Cartoon depicts co-binding of both receptor subunits to the Get3/TA complex when a functional Get2 is present.

Figure 5

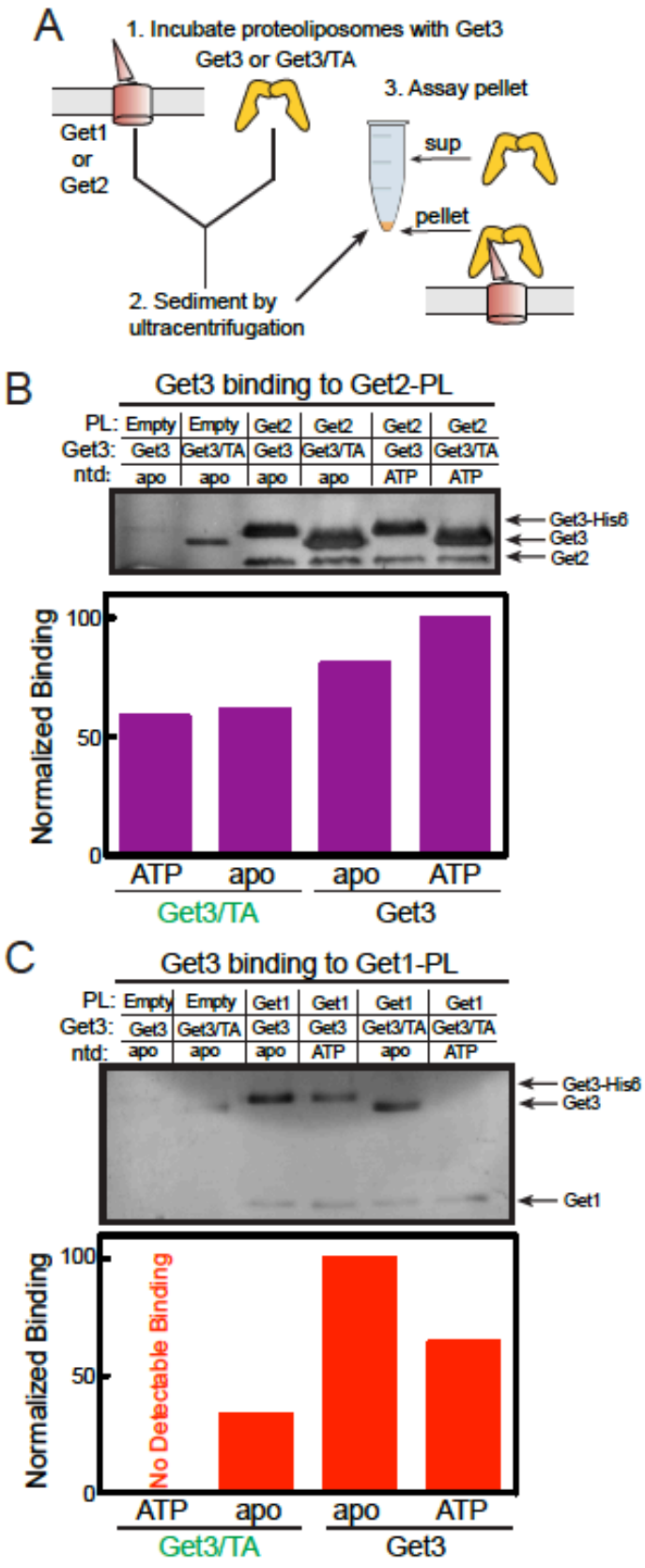
A
1. Incubate proteoliposomes with Get3
Get3 or Get3/TA
3. Assay pellet
Get1
or
Get2
sup
pellet
2. Sediment by
ultracentrifugation
B
Get3 binding to Get2-PL
PL: Empty Empty Get2 Get2 Get2 Get2
Get3: Get3 Get3/TA Get3 Get3/TA Get3 Get3/TA
ntd: apo apo apo apo ATP ATP
Get3-His6
Get3
Get2
Normalized Binding
100
50
0
ATP apo apo ATP
Get3/TA Get3
C
Get3 binding to Get1-PL
PL: Empty Empty Get1 Get1 Get1 Get1
Get3: Get3 Get3/TA Get3 Get3 Get3/TA Get3/TA
ntd: apo apo apo ATP apo ATP
Get3-His6
Get3
Get1
Normalized Binding
100
50
0
No Detectable Binding
ATP apo apo ATP
Get3/TA Get3

Figure 3.5. The interaction of Get3 with the full-length receptor in proteoliposomes. (**A**) Cartoon depicting the proteoliposome sedimentation assay as described in the Methods. (**B,C**) Results of the sedimentation assay with Get1-PL (part B) and Get2-PL (part C) are analyzed by silver-stain of the pellet fraction (upper panel; cf. part A) and quantified (lower panel). Get3 contains a 6HIS tag and can therefore be distinguished from Get3/TA complexes (untagged). The substrate-loading and nucleotide state of Get3 are indicated. See methods for quantification details.

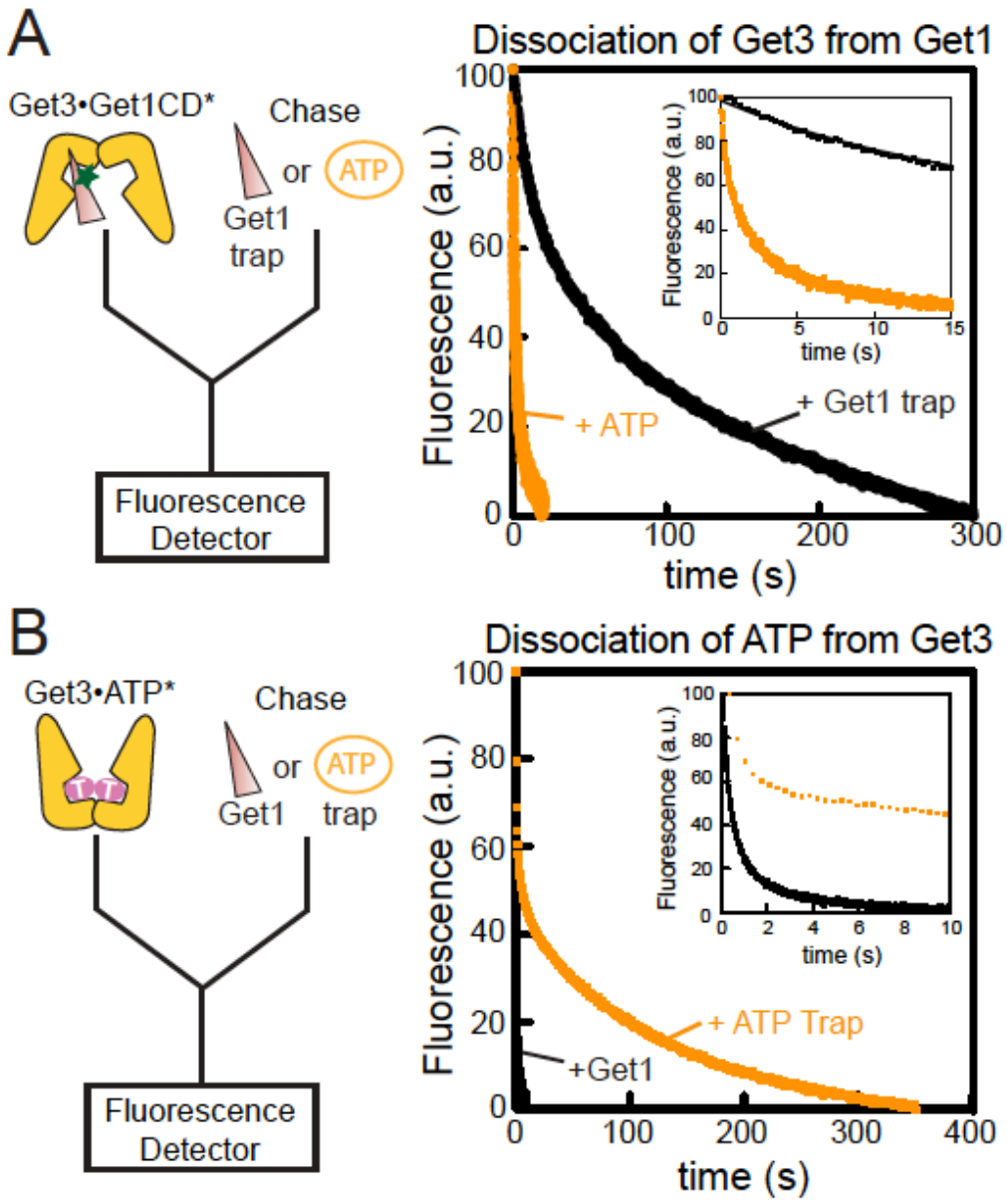

Figure 3.6: ATP actively displaces Get3 from Get1. (**A**) Rate constants for dissociation of a preformed Get3•Get1-CD(DACM-labeled) complex, driven by either 2 mM ATP (orange) or 8.5 µM unlabeled Get1-CD (black). (**B**) Rate constants for dissociation of the Get3•mant-ATP complex, driven by either 2 mM ATP (orange) or 2.5 µM Get1-CD (black).

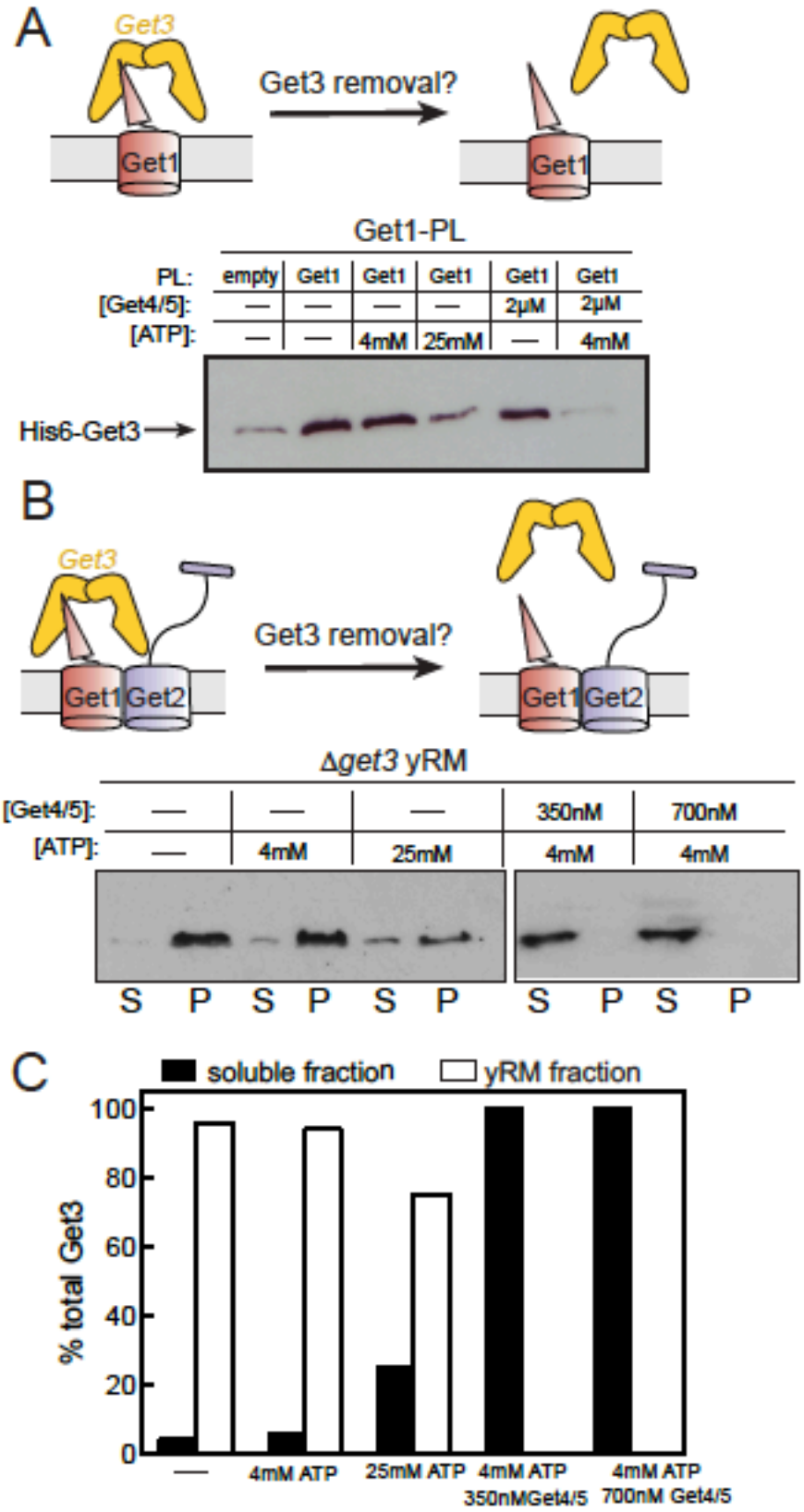
A
Get3
Get3 removal?
Get1
Get1
Get1-PL
PL:
empty
Get1
Get1
Get1
Get1
Get1
[Get4/5]:
—
—
—
—
2μM
2μM
[ATP]:
—
—
4mM
25mM
—
4mM
His6-Get3
B
Get3
Get3 removal?
Get1
Get2
Get1
Get2
Δget3 yRM
[Get4/5]:
—
—
—
350nM
700nM
[ATP]:
—
4mM
25mM
4mM
4mM
S
P
S
P
S
P
S
P
S
P
C
soluble fraction
yRM fraction
% total Get3
100
80
60
40
20
0
—
4mM ATP
25mM ATP
4mM ATP
350nM Get4/5
4mM ATP
700nM Get4/5

Figure 3.7 Get4/5 is necessary for recycling Get3 from the receptor complex in the membrane. (**A**) Release of Get3 from full-length Get1-PL. 50 nM His6-Get3 was pre-incubated with Get1-PL for 15 minutes and chased with the indicated factors for 10 minutes. Proteoliposomes were sedimented as in Figure 5, and His6-Get3 was detected by western blot using anti-His antibody. (**B**) Same as in (A) except that *Δget3* microsomal membranes were used instead of proteoliposomes, and both the soluble and pellet fractions were analyzed. (**C**) Quantification of the results in (B).

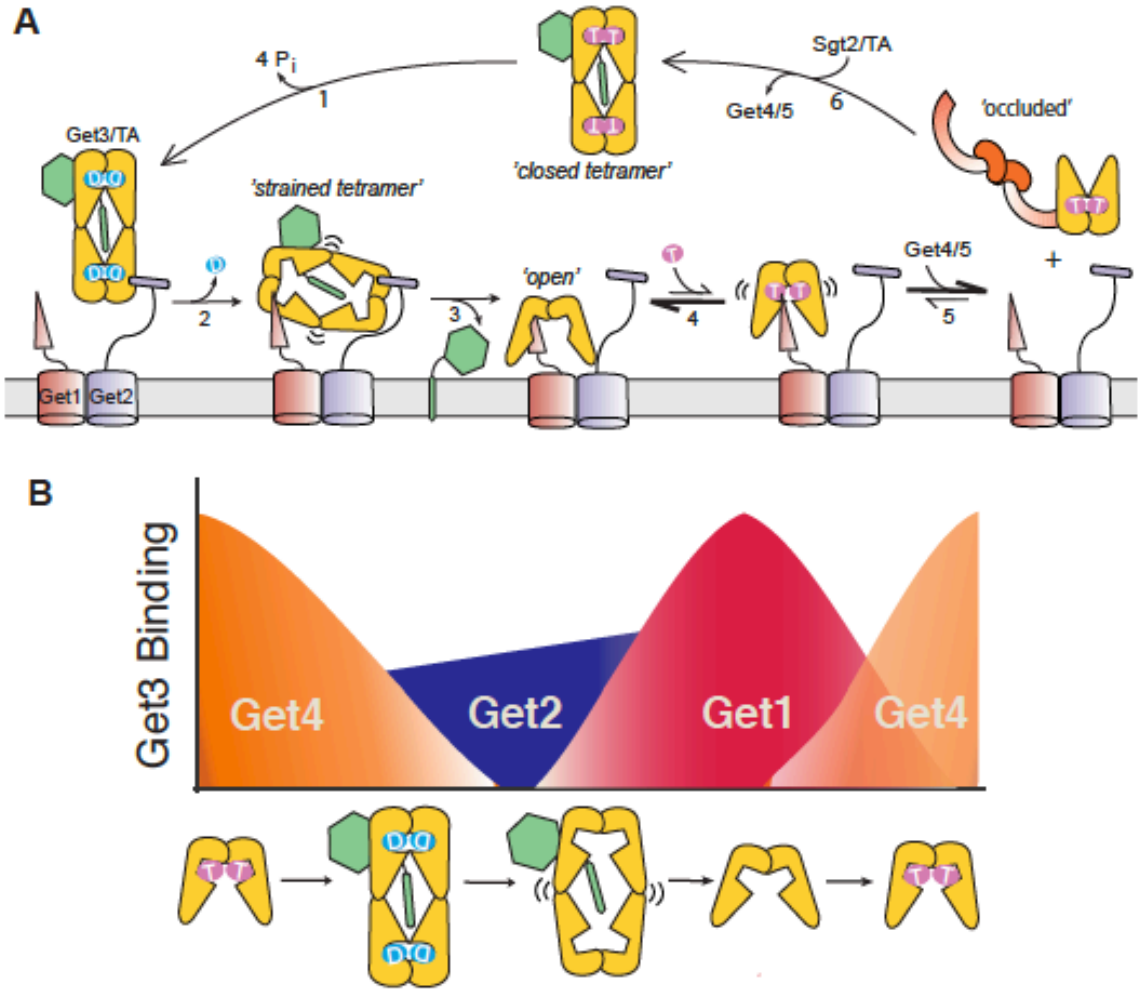

Figure 3.8: (**A**) Model for TA targeting, insertion and Get3 recycling at the ER membrane, as described in the text. (**B**) Cartoon depicting the differential binding affinities of Get3 for Get4, Get2 and Get1 in different substrate and nucleotide states, as described in the text.

Chapter 4

The mechanism of Get3 binding to Get4/5

Get3 binds to Get4/5 in an asymmetric configuration

Given the configuration of Get4/5 as a heterotetramer (2 copies of Get4 and Get5), it is strongly expected that both arms of Get4 are accessible for binding Get3. Surprisingly, the equilibrium titration data for Get3-Get4/5 binding can only fit to a stoichiometry in which each Get3 monomer binds two copies of Get4 and Get5 (1:2), i.e., a Get4/5 tetramer (Fig. 1A), but not to a 1:1 stoichiometry that allows Get3 to bind both copies of Get4 in the Get4/5 complex (Figure 1B). This strongly suggests an asymmetry in the full length Get4/5 complex, in which only one arm of the Get4/5 tetramer is functional in binding Get3.

To directly test the asymmetry in Get4/5 during Get3 binding, we developed an alkylation assay coupled with mass spectrometry to assess the accessibility of an engineered cysteine, Get4(C48), at the Get3-Get4/5 interface (Fig. 2A, Fig. S1A; [61]). In the free Get4/5 complex, Get4(C48) is solvent exposed [25] and rapidly alkylated to completion by N-ethyl-maleimide (NEM; Fig. 2B, black). If both copies of Get4 in the Get4/5 complex can bind Get3, C48 is rendered solvent inaccessible (Fig. 2A) and will be completely protected from alkylation. In contrast, if only one copy of Get4 in Get4/5 is bound to Get3, only half of the Get4 molecules can be protected. Consistent with expectations from the latter model, only 50% of Get4(C48) was protected from alkylation by Get3 throughout the time course relative to free Get4/5 (Fig. 2B, red). This protection pattern was observed at a Get3 concentration nearly 1000 fold above the dissociation constant for the Get3•Get4/5 complex, indicating that the 50% protection did not arise from incomplete Get3-Get4/5 binding. These results strongly suggest that one arm of a

Get4/5 tetramer is able to bind to Get3, while the other arm becomes either allosterically inactivated.

We followed up the results of the alkylation assay by probing accessibility of Get4/5 using PEG- Maleimide 10kDa. To rule out the possibility that Get4 S48 is partially exposed to solvent when bound to Get3, we picked a position on Get4 (Q34C) that is completely occluded in the Get3-Get4/5N closed structure (Fig. 2C). Substitution of Q34 does not impair binding to Get3 and has little sequence conservation [25]. As expected, when Get4(Q34C/C177T)/Get5 is incubated with PEG-Maleimide, a 10kDa shift is observed in the molecular mass of the Get4/5 complex (Figure S1B). Carrying out this reaction over a two-minute time course in the absence of Get3 resulted in 100% Get4/5 pegylation, whereas the addition of Get3 resulted in 50% pegylation (Fig. 2D). This provides corroborating evidence that only one arm of the Get4/5 heterotetramer is able to bind Get3.

Sequential binding of two Get4/5 molecules to Get3

We recently showed that Get3 binds full-length Get4/5 with tight affinity (K_d = 3.2 nM) yet fast dynamics (k_{on} = ~ 10^8 M^{-1} s^{-1}, k_{off}= ~0.5 s^{-1}) (Chapter 3). Moreover, association rate measurements showed two distinct concentration dependent phases that differed by ≤6-Fold. The first kinetic phase was extremely sensitivity to buffer ionic strength (Chapter 3), demonstrating that electrostatic contacts drive fast complex formation. Surprisingly, analysis of the second slower kinetic phase revealed no changes in association rate constants when buffer ionic strength was varied (Fig. 2A). The simplest model to account for the presence of biphasic kinetics, differences in salt

sensitivity, and two distinct crystallographic binding interfaces would be the sequential interaction of two Get4/5 molecules on opposite interfaces of the Get3 dimer (Fig. 5). We propose a three-step binding model: 1) Ge4/5 initially forms a rapid electrostatically driven encounter complex with the first interface in a semi-open Get3 dimer. 2) Get4/5 binding to the semi-open Get3 complex induces a fast unimolecular rearrangement to an 'occluded' conformation. 3) Binding of the second Get4/5 molecule then occurs to the available binding interface on Get3.

The full-length Get4/5 protein is a heterotetrameric complex containing two copies of Get4 each associated with a one half of a Get5 dimer [25]. This raises the possibility that the observed biphasic kinetics is due to binding of another Get3 dimer to the Get4/5 heterotetramer. In order to test this possibility, we carried out association rate measurements with tetramerization-deficient Get4/5N. The results show that Get4/5N binds Get3 with identical kinetics to full-length Get4/5 (Fig. 3 B,C). Importantly, the first concentration dependent phase was sensitive to differences in buffer ionic strength **(**Fig. 3D**)**. Since these distinct binding trends are perfectly recapitulated with the monomeric Get4/5N, this rules out the alternative model that the second phase arises from a second Get3 dimer binding to the other arm in the full-length Get4/5 heterotetramer. Coupled with the above stoichiometry data, this provides additional evidence that distinct Get4/5 molecules sequentially bind to the Get3 dimer.

Binding of the first Get4/5 molecule induces a conformational change in Get3

For the faster-binding population of Get3, the initial association with Get4/5 is unstable, with a dissociation rate constant of 15 s^{-1} (Chapter 3). The equilibrium stability

of this initially assembled complex, derived from the k_{off} and k_{on} values, is 107 nM, approaching the K_d value of the apo-Get3•Get4 complex (~200nM). However, both the equilibrium and kinetic stability of the stably assembled Get3•Get4/5 complex are >15-fold higher than these values. Thus a conformational change must occur after the rapid initial assembly of Get3 with Get4/5 to give a more stable complex. The detection of a conformation change in our kinetic data is consistent with previous results showing that Get4/5 biding induces Get3 into an occluded conformational state, leading to Get3 ATPase inhibition and delayed ATP dissociation kinetics [62].

Since the binding of the second Get4/5 molecule is not sensitive to changes in buffer ionic strength (Fig. 3A), the preceding conformational change must rearrange the Get3-Get4/5 binding interface (corroborating structural evidence provided in the next section). The model thus predicts that once Get3 has transitioned to the occluded conformation, complex dissociation would be insensitive to buffer ionic strength. In order to test this idea, we measured the dissociation rate of the ATP bound Get3-Get4/5 complex in buffer containing either no salt or 350 mM NaCl. In agreement with predictions from association rate measurements, complex dissociation was insensitive to buffer ionic strength (Fig. 4A), demonstrating that the stable Get3-Get45 complex is held together largely by hydrophobic interactions.

In order to rule out a model where two different populations of Get3 give rise to the observed binding and dissociation kinetics, we analyzed the magnitude of each kinetic phase as a function of Get3 concentration and salt concentration (Fig. 4B). The % amplitude of the two kinetic phases during Get3-Get4/5 association is not altered by changes in ionic strength, despite the >30-fold changes in the relative association rates of

the salt-sensitive and -insensitive phases (Fig. 4B). This behavior is not expected if these two phases arise from heterogeneity *among* Get3 dimers (as the faster-binding population will become more dominant in magnitude), but can be explained if the salt-sensitive phase is an obligatory initial association step that must precede binding of the second Get4/5 to a Get3 dimer.

Further evidence for a conformational change is evident when analyzing dissociation of Get3 from Get4/5 in different nucleotide states. The magnitude of the slow phase during dissociation increases successively when apo-Get3 is compared with ADP- and ATP-bound Get3 (Fig. 4C). This indicates that the two phases are governed in part by a reversible conformational change that can be induced by nucleotides, with ATP being more effective than ADP. This is consistent with previous structural, kinetic and molecule simulations data, showing that ATP is more effective than ADP in inducing Get3 into a closed conformation [3,25].

Kinetic modeling of Get3's interaction with Get4/5

Combining our structural, biochemical and quantitative binding data, we sought to model the Get3-Get4/5 interaction using kinetic simulation software [63]. We assigned individual rate constants to each step in the Get3-Get4/5 binding model based off simulations from the modeling algorithm (Fig 5). Using the experimentally derived values for k_{on} and k_{off} from both the salt and salt-insensitive phases, we were able to completely reproduce the biphasic trends observed in association/dissociation rate measurements, and equilibrium titrations (Fig. 6A,B,C). These trends were only found when we modeled a conformational change in Get3 upon binding the first Get4/5

molecule. Since these simulations completely recapitulate experimental data, this provides strong evidence for the binding model presented in Figure 5.

Preliminary data: The Get3-Get4/5 interface is remodeled once Get3 acquires TA substrate

Together with the ~20-fold weaker binding of Get3/TA complex to Get4/5, this suggests a change in the conformation at the Get3-Get4 interaction interface. In support of this notion, in the Get4/5•Get3/TA complex Get4(C48) is alkylated by NEM as efficiently as in free Get4/5, (Figure 3D, green). Together, these data support a model in which each copy of Get3 in a Get3 dimer first binds one copy of Get4 in the Get4/5 heterotetramer, rendering the other arm of Get4/5 unoccupied. The loading of the TA substrate (by Sgt2 or other chaperones) drives tetramerization of Get3, forcing the other arm of Get4/5 to also bind Get 3. This could generate a 'strained' conformation in the Get4/5 heterotetramer that explains its weakened affinity to the Get3/TA complex than to free Get3, thus enabling the facile release of the targeting complex from Get4/5.

Table 1

Summary of the kinetics of Get3 dissociation from Get4/5 in ATP.

Ionic Strength Buffer	1st Phase		2st Phase	
	k_{-1} (s^{-1})	amplitude (%)	k_{-2} (s^{-1})	amplitude (%)
350 mM NaCl	0.924 ± 0.029	32.7	0.100 ± 0.001	67.3
No Salt	0.769 ± 0.037	41.7	0.080 ± 0.003	58.3

Table 2

Summary of the kinetics of Get3-Get4/5-N association in ATP.

Ionic Strength Buffer	1st phase	2nd Phase
	k_1 (μM^{-1} s^{-1})	k_2 (μM^{-1} s^{-1})
150 mM KOAc	101.5 ± 3.2	12.6 ± 0.291
350 mM NaCl	8.3 ± 1.7	5.6 ± 0.90
90 mM NaCl	117 ± 15.5	5.6 ± 0.92
5 mM NaCl	238 ± 35	N/A

Table 3

Comparison of experimental and simulation data

Experimental Association Rate		**Simulated Association Rate**	
1st phase	**2nd Phase**	**1st phase**	**2nd Phase**
k_1 ($\mu M^{-1} s^{-1}$)	k_2 ($\mu M^{-1} s^{-1}$)	k_1 ($\mu M^{-1} s^{-1}$)	k_2 ($\mu M^{-1} s^{-1}$)
143.8	43.5	175	40.6

Experimental Dissociation Rate		**Simulated Dissociation Rate**	
1st phase	**2nd Phase**	**1st phase**	**2nd Phase**
k_1 (s^{-1})	k_2 (s^{-1})	k_1 (s^{-1})	k_2 (s^{-1})
0.64	0.10	0.79	0.075

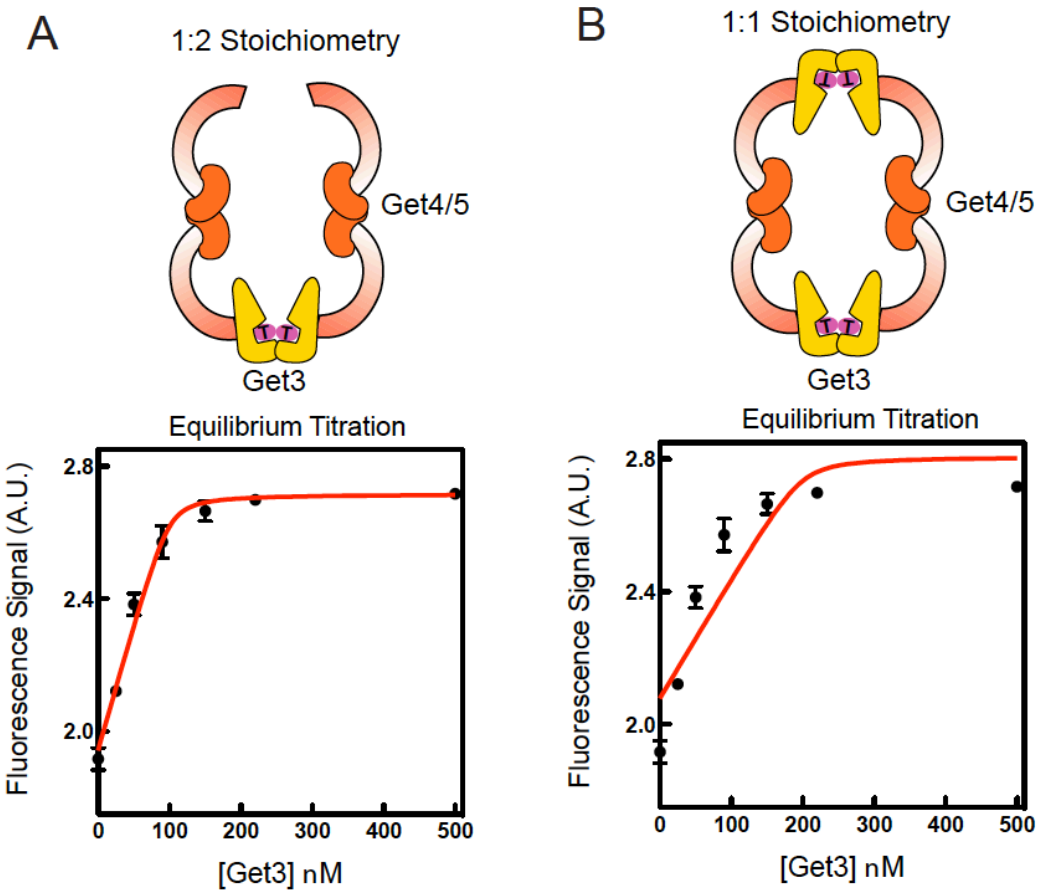

Figure 4.1. Stochiometry of the Get3-Get4/5 complex. (A) Cartoon depicting a 1:2 binding stoichiometry of Get3 with Get4/5. This configuration was used to fit an equilibrium titration of ACR-labeled Get4/5-FL (100nM) with Get3 in 2mM ATP. (B) Same as in A, but with a 1:1 binding stoichiometry.

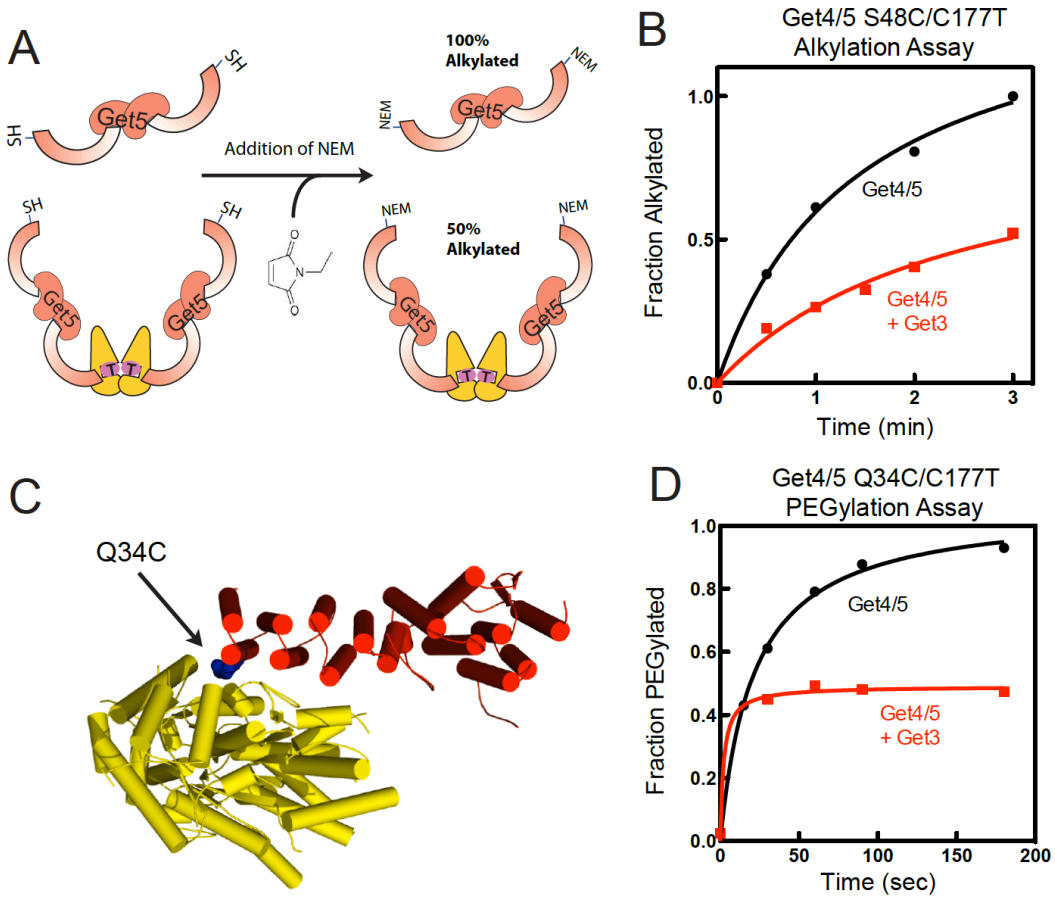

Figure 4.2. Probing the stoichiometry of the Get3-Get4/5 complex using chemical modification. (A) Cartoon depicting the NEM accessibility of a solvent exposed Cys (C48)residue on Get4/5 alone or when in complex Get3. (B) Results of the Alklyation assay, setup shown in A. (C) PDB image depicting the location of Q34C on the Get3-Get4/5 structure. (D) Results of a PEGylation assay with Cys (Q34C) residue on Get4/5 alone or when in complex with Get3.

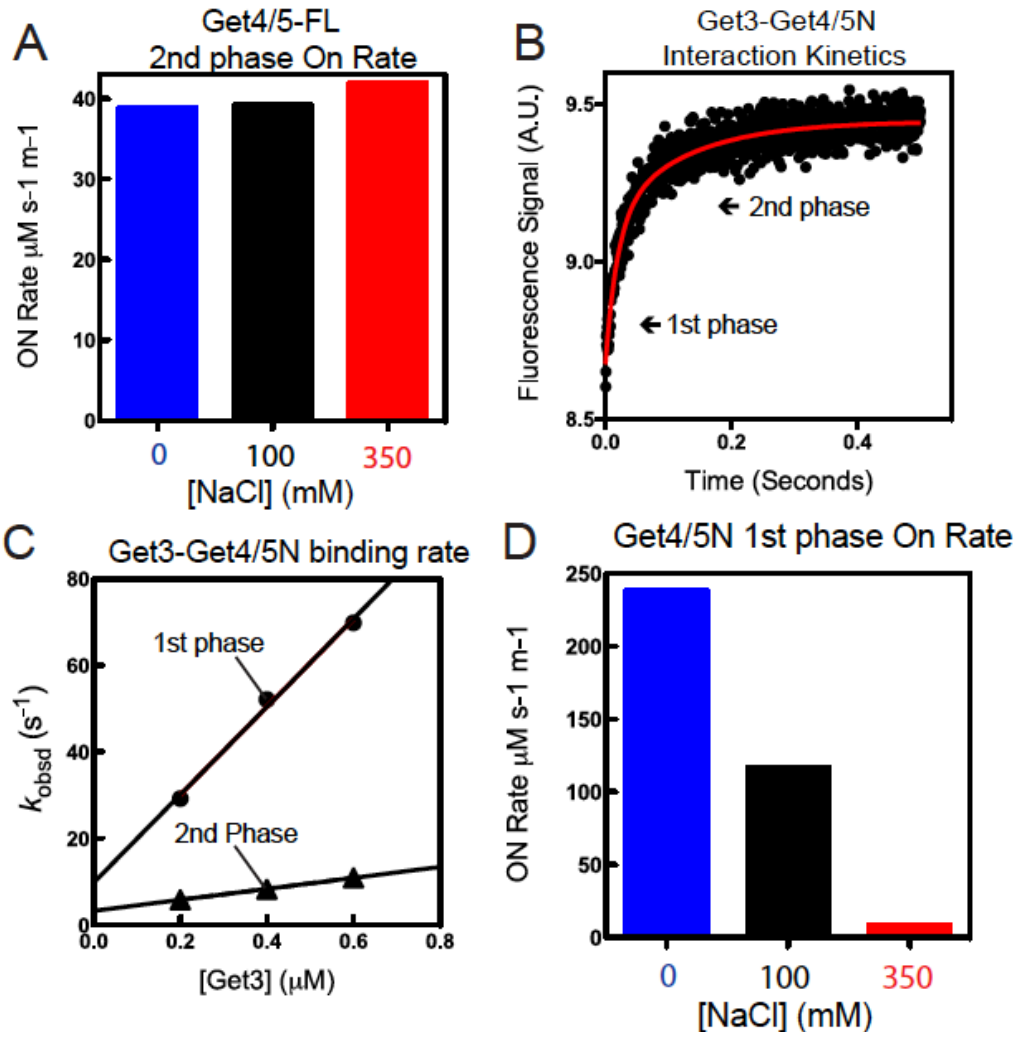

Figure 4.3. Sequential binding of two Get4/5 molecules to Get3. (A) Summary of association rate constants in different salt concentrations for the 2nd kinetic phase in Get3-Get4/5 ON rate measurements. (B) Time course of Get4/5N binding to ATP-bound Get3. Arrows indicate the two kinetic phases. (C) Observed association rate constants (k_{obsd}) are analyzed as a function of Get3 concentration to determine the association rate constant k_{on} for both the first (circles) and second (triangles) kinetic phases. (D) Get3-Get4/5N association rates are highly salt-sensitive.

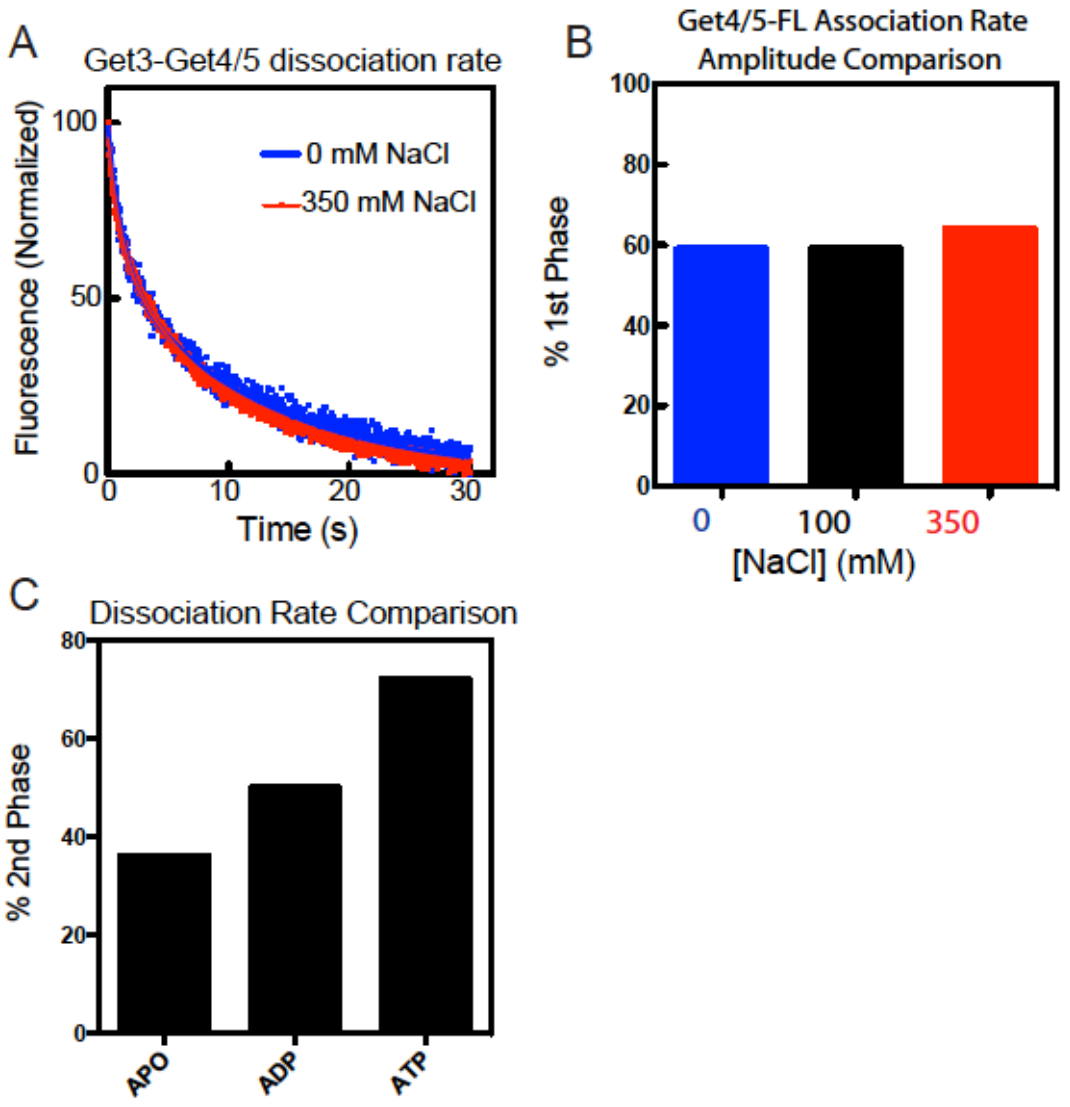

Figure 4.4. Get4/5 undergoes a conformational change upon binding Get3. (A) Dissociation rate measurement of Get3 from Get4/5 in 350mM NaCl (red) and no salt (blue). (B) The amplitude of the 1st kinetic phase for Get3-Get4/5 association in different salt concentrations is invariant to buffer ionic strength. (C) Percent amplitude of the 2nd kinetic phase for Get3 dissociation from Get4/5N in different nucleotide states.

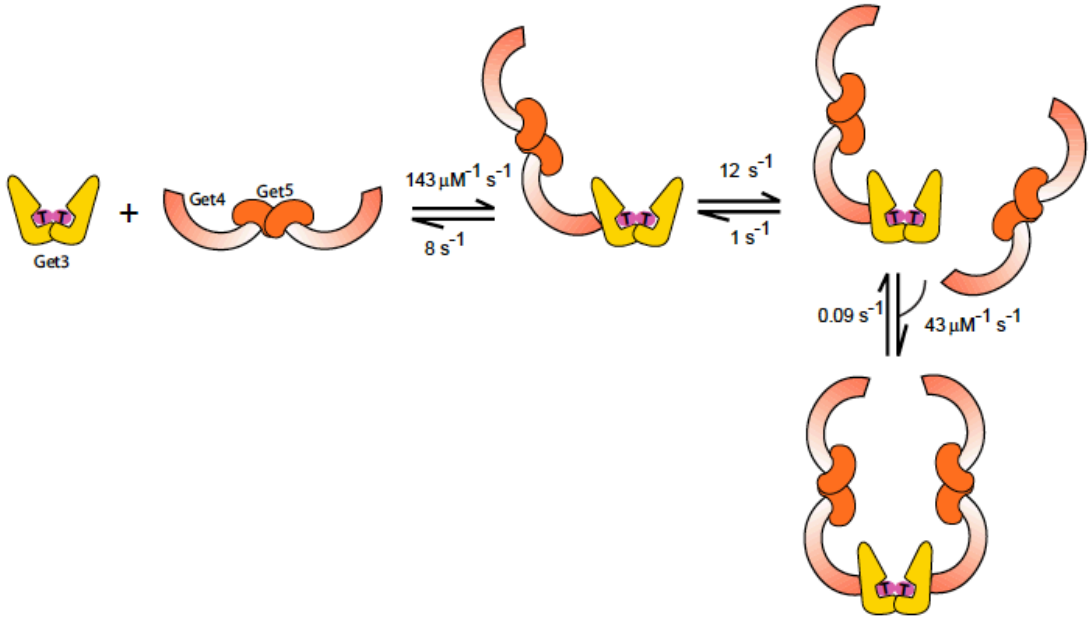

Figure 4.5. Kinetic model for the interaction of Get3 with Get4/5 as described in the text. All steps simulated with Kintek modeling software.

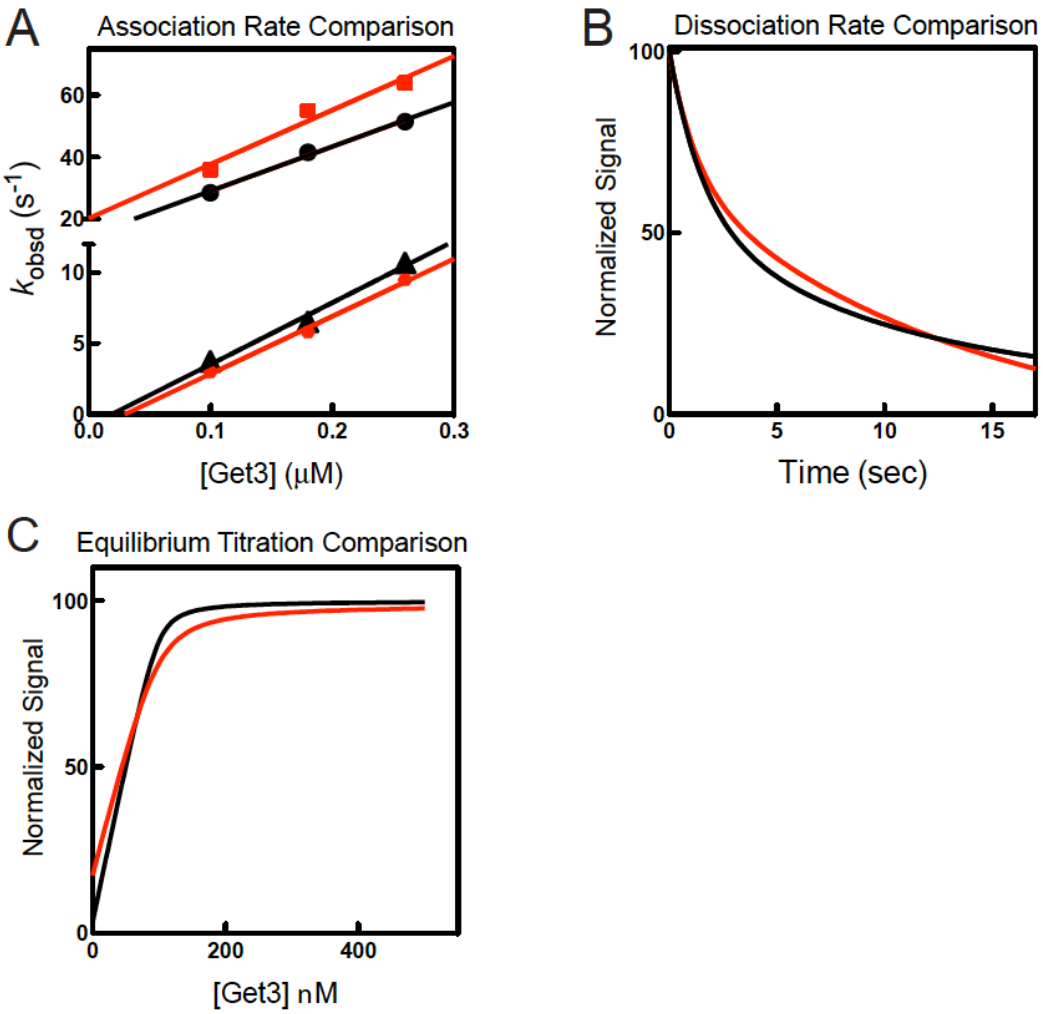

Figure 4.6. Comparison of experimental (black) and theoretical (red) biding data for the Get3-Get4/5 complex. Values report in Table 3. (A) Association rate measurements, (B) Dissociation rate measurements, (C) Equilibrium titrations.

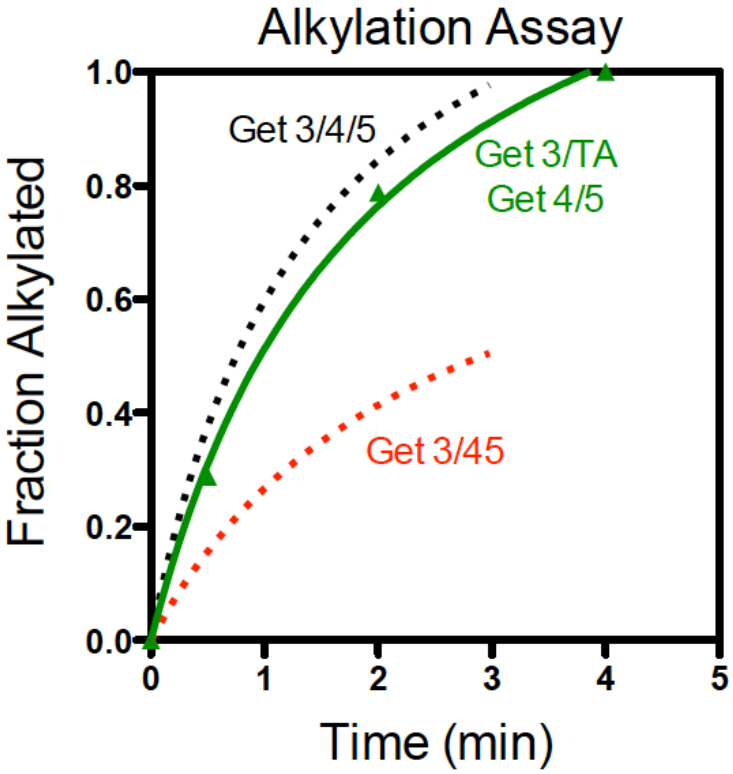

Figure 4.7. Probing the stoichiometry of the Get3/TA-Get4/5 complex using chemical modification. NEM accessibility of a solvent exposed Cys (C48)residue on Get4/5 alone or when in complex Get3/TA .

Appendix A: Supplemental Data for Chapter 2

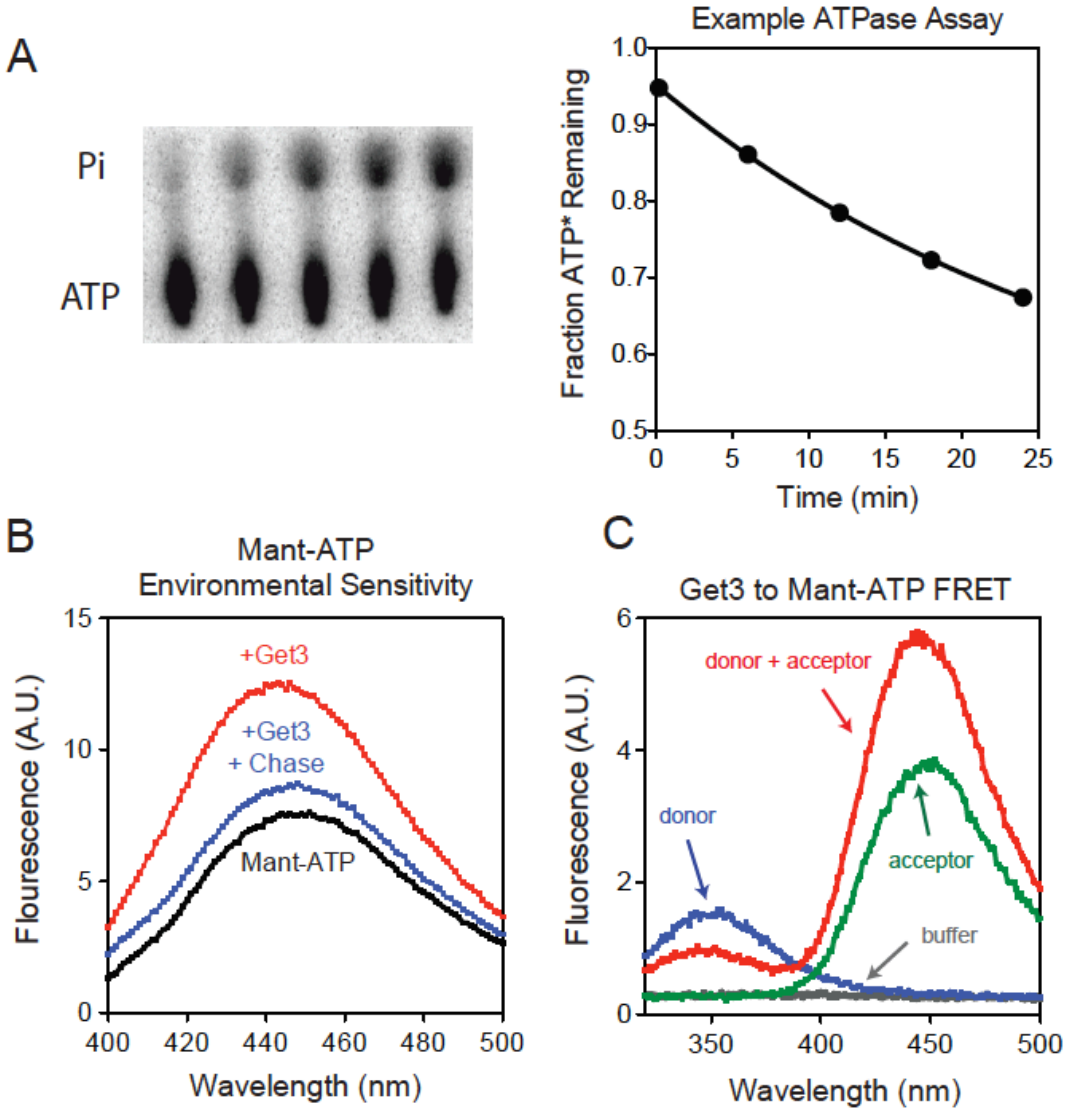

Figure 2.S1:
Assays for ATP binding and hydrolysis by Get3, related to Figure 1 and Figure 2. (**A**) Representative thin layer chromatography (TLC) analysis for monitoring the progress of a Get3 ATPase reaction (see Methods). Right panel shows quantification of the TLC data, which were fit to a single exponential function to obtain observed rate constants (k_{obsd}). (**B**) Fluorescence emission spectra of 0.4 μM mantATP with (red) or without (black) 35.8 μM Get3, and for the Get3-mantATP complex chased with 2 mM ATP (blue). (**C**)

Fluorescence emission spectra for 1.2 μM Get3 (donor, blue), 60 μM mantATP (acceptor, green), 1.2 μM Get3 incubated with 60 μM mantATP (donor + acceptor, red), or buffer (gray).

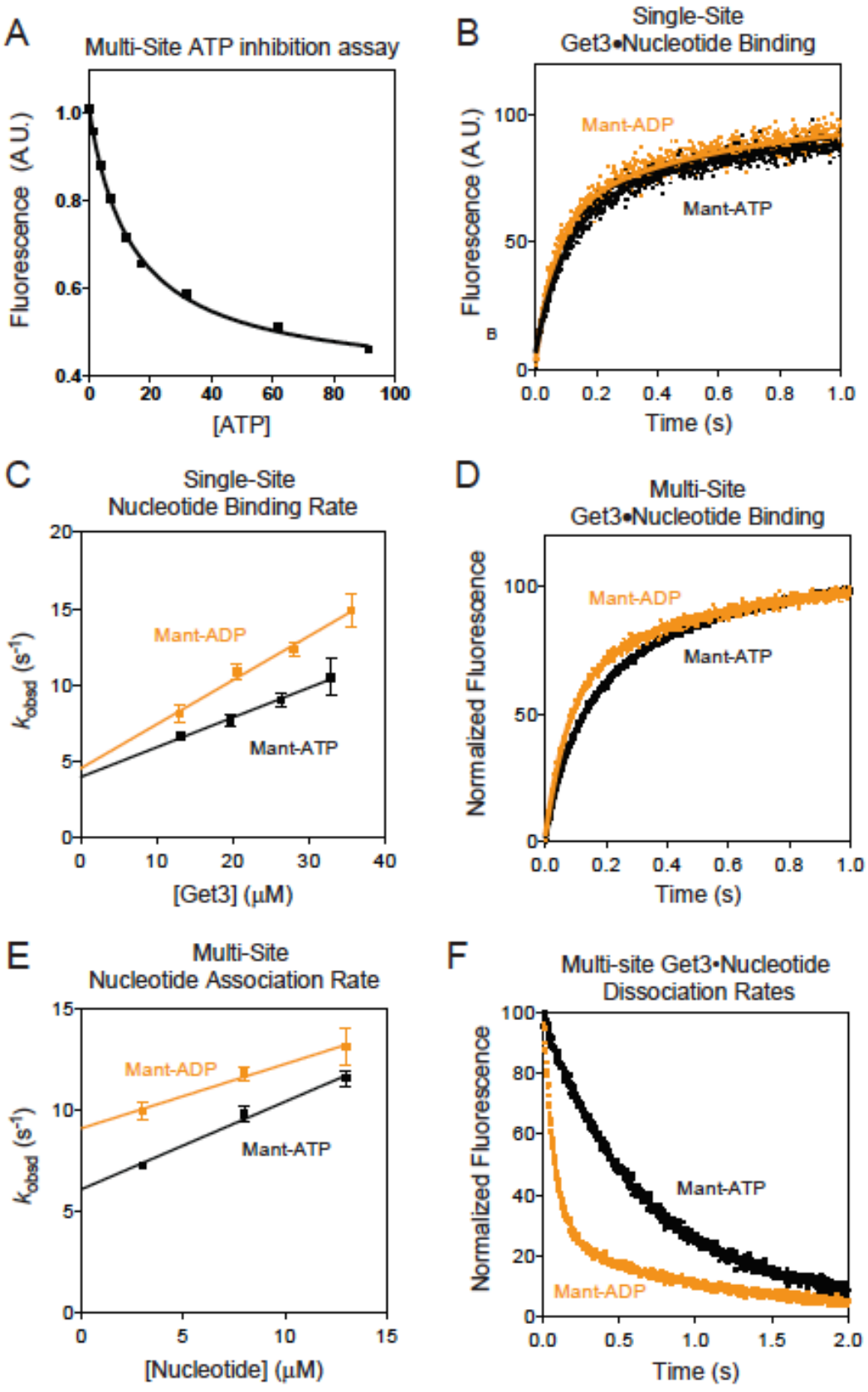
A
Multi-Site ATP inhibition assay
Fluorescence (A.U.)
1.0
0.8
0.6
0.4
0
20
40
60
80
100
[ATP]
B
Single-Site
Get3•Nucleotide Binding
Fluorescence (A.U.)
B
100
50
0
Mant-ADP
Mant-ATP
0.0
0.2
0.4
0.6
0.8
1.0
Time (s)
C
Single-Site
Nucleotide Binding Rate
k_{obsd} (s^{-1})
20
15
10
5
0
Mant-ADP
Mant-ATP
0
10
20
30
40
[Get3] (μM)
D
Multi-Site
Get3•Nucleotide Binding
Normalized Fluorescence
100
50
0
Mant-ADP
Mant-ATP
0.0
0.2
0.4
0.6
0.8
1.0
Time (s)
E
Multi-Site
Nucleotide Association Rate
k_{obsd} (s^{-1})
15
10
5
0
Mant-ADP
Mant-ATP
0
5
10
15
[Nucleotide] (μM)
F
Multi-site Get3•Nucleotide
Dissociation Rates
Normalized Fluorescence
100
80
60
40
20
0
Mant-ATP
Mant-ADP
0.0
0.5
1.0
1.5
2.0
Time (s)

Figure 2.S2:
Mant-ATP and mant-ADP binding and dissociation to Get3 related to Figure 1 and Figure 2. (**A**) Competition of mantATP binding to Get3 by ATP, performed with 1.5 μM Get3, 8 μM mantATP, and varying concentrations of ATP as indicated. The data were fit to Eq 2 in Methods, which gave a $K_{i,app}$ value of 4.5 μM. (**B**) Single-site time courses for mantATP (black) or mantADP (gold) binding to 37 μM Get3. (**C**) Single-site observed association rate constants were plotted as a function of Get3 concentration. Linear fits of the data (Eq 4) gave k_{on} values of 0.20 ± 0.01 and 0.29 ± 0.02 $\mu M^{-1}s^{-1}$ for ATP (black) and ADP (gold), respectively. The values reported are the mean ± SD, with n = 3. (**D**) Multi-site time courses for binding of 13 μM mantATP (black) or mantADP (gold) to 1.5 μM Get3 using the FRET assay (**E**) Multi-site observed nucleotide binding rate constants were plotted as a function of Get3 concentration. Linear fits of the data gave k_{on} values of 0.43 ± 0.04 $\mu M^{-1} s^{-1}$ for ATP (black) and 0.31 ± 0.03 $\mu M^{-1} s^{-1}$ for ADP (gold). (**F**) Time courses for mantATP (black) or mantADP (gold) dissociation from Get3 under multi-site conditions. The data were fit to double exponential functions. Rate constants derived from the fast phase are reported in the text and table S1.

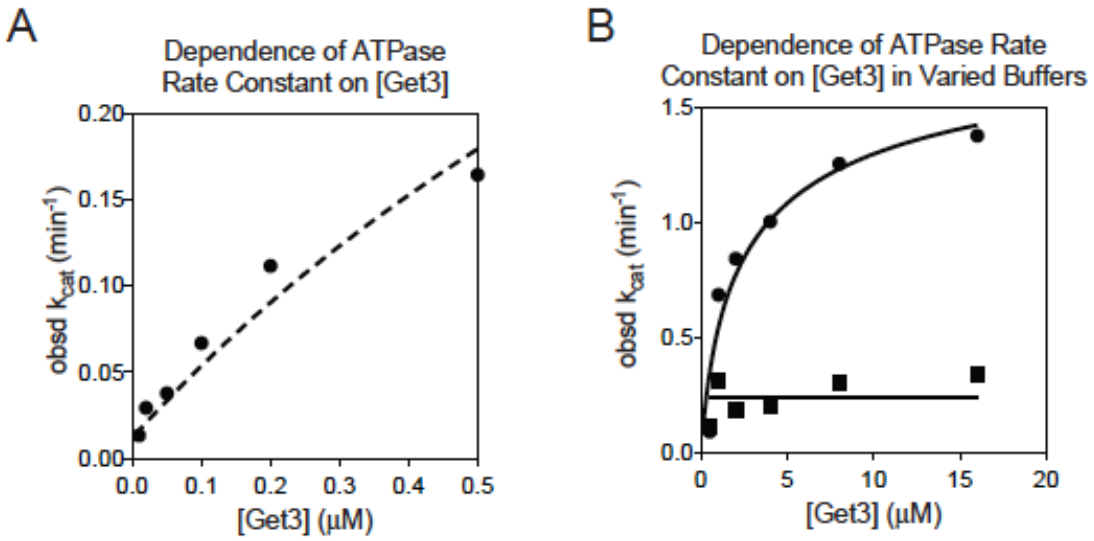

Figure 2.S3:
Controls for Get3 concentration-dependent ATPase stimulation, related to Figure 3. (**A**) Zoom-in of the dependence of observed k_{cat} values at low Get3 concentrations. Reactions were performed as in Figure 3A in the presence of 1mg/mL BSA (see methods). (**B**) Dependence of observed k_{cat} of Get3 in assay buffer (circles, see Methods) or purification buffer (squares; 10 mM Tris, pH 7.5, 150 mM NaCl, 1 mM $MgCl_2$).

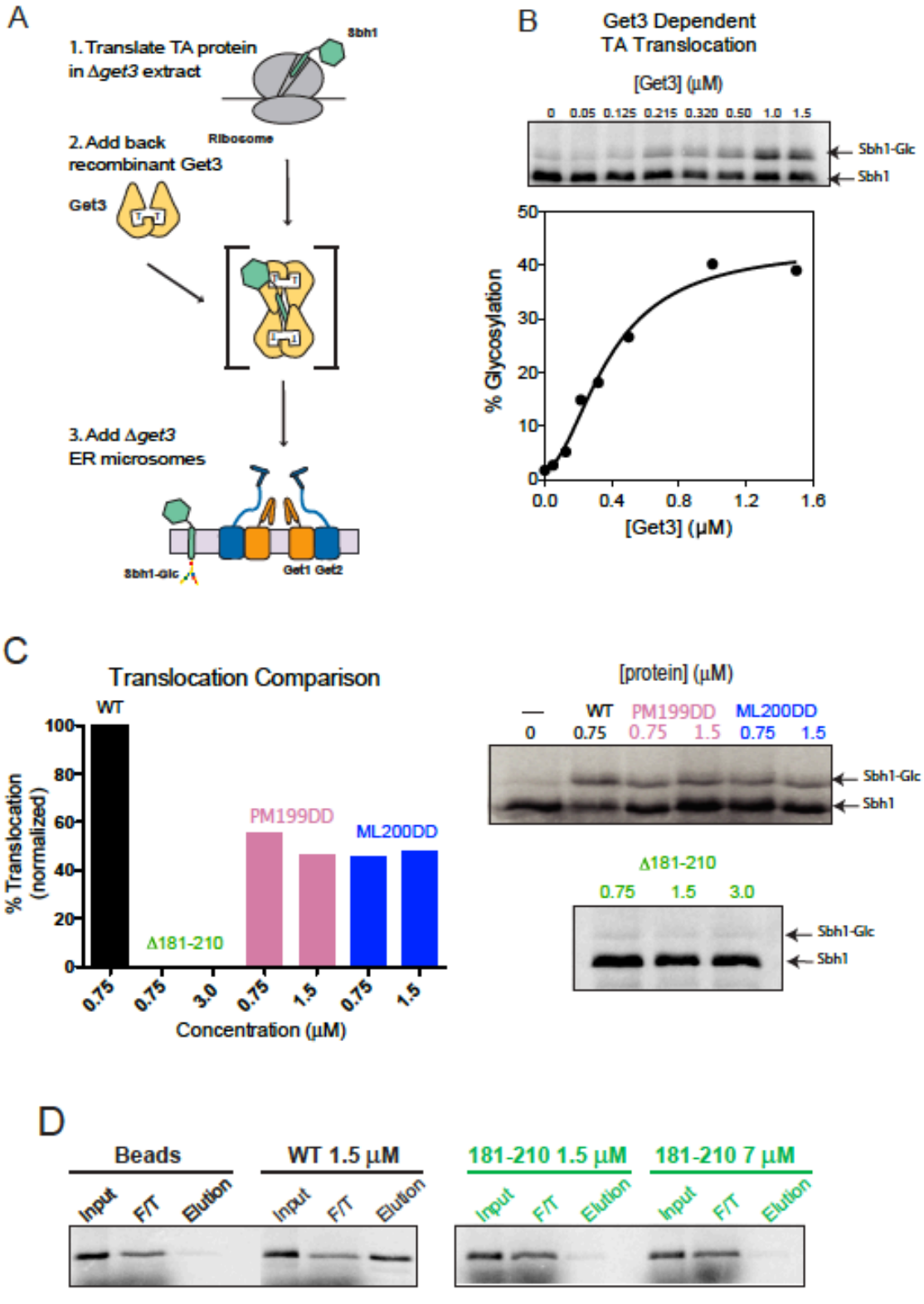
A
1. Translate TA protein in Δget3 extract
Sbh1
Ribosome
2. Add back recombinant Get3
Get3
3. Add Δget3 ER microsomes
Sbh1-Glc
Get1 Get2
B
Get3 Dependent TA Translocation
[Get3] (μM)
0 0.05 0.125 0.215 0.320 0.50 1.0 1.5
Sbh1-Glc
Sbh1
% Glycosylation
[Get3] (μM)
C
Translocation Comparison
% Translocation (normalized)
WT
PM199DD
ML200DD
Δ181-210
Concentration (μM)
[protein] (μM)
WT PM199DD ML200DD
0 0.75 0.75 1.5 0.75 1.5
Δ181-210
0.75 1.5 3.0
D
Beads
WT 1.5 μM
181-210 1.5 μM
181-210 7 μM
Input
F/T
Elution

Figure 2.S4:
Targeting and translocation of TA protein by wildtype and mutant Get3, related to Figure 3. (**A**) Cartoon diagram of the Get3 dependent TA targeting and translocation assay, as described in the Experimental Procedures and text. (**B**) Get3-dependent targeting and translocation of Sbh1p, performed under identical conditions to Figure 3C, but in an independent experiment on a separate day using different Get3 concentrations. The data were analyzed as in Figure 3C and gave a Hill coefficient of 2. (**C**) Sbh1p targeting and translocation by wildtype and mutants PM199DD, ML200DD, and Δ181-210 at high Get3 concentrations. Gels for the data are on the right panel. (**D**) Capture of Sbh1p by wildtype Get3 (left) and mutant (Δ181-210) (right), using pulldown of His_6-tagged Get3 by Ni-NTA beads as described in the Experimental Procedures.

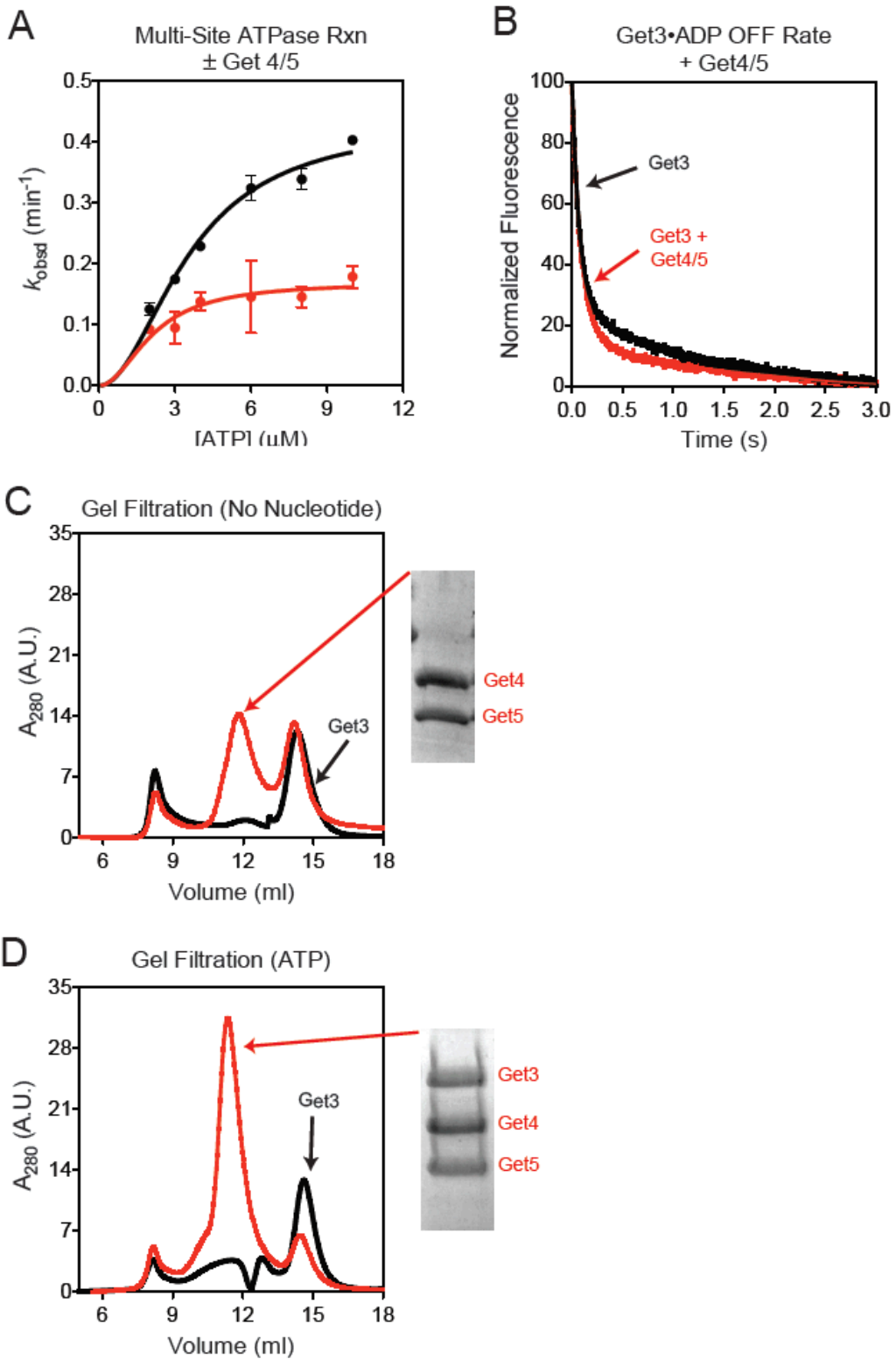

Figure 2.S5:
Get4/5 increases Get3's affinity for ATP, and vice versa. Related to Figure 4. (**A**) ATP concentration dependence of observed ATPase activity at 1 μM Get3, in the absence

(black) and presence (red) of 5 μM Get4/5. The data were fit to Eq 8 in the Extended Experimental Procedures, and gave average K_M values of 3.6 ± 0.01 and 2.2 ± 1.0 μM, and k_{cat} values of 0.43±0.003 and 0.18±0.04 min^{-1} with and without Get4/5, respectively. (**B**) Get3•mantATP dissociation kinetics, determined in the presence (red) or absence (black) of 3.0 μM Get4/5. Exponential fits of data gave dissociation rate constants of 14.4 s^{-1} and 11.3 s^{-1} with and without Get4/5, respectively. (**C**) Gel filtration chromatogram of apo-Get3 without (black) or with (red) Get4/5. Shown is a gel image for the fractions collected at ~11 ml. (**D**) Same as (C) but in the presence of saturating ATP.

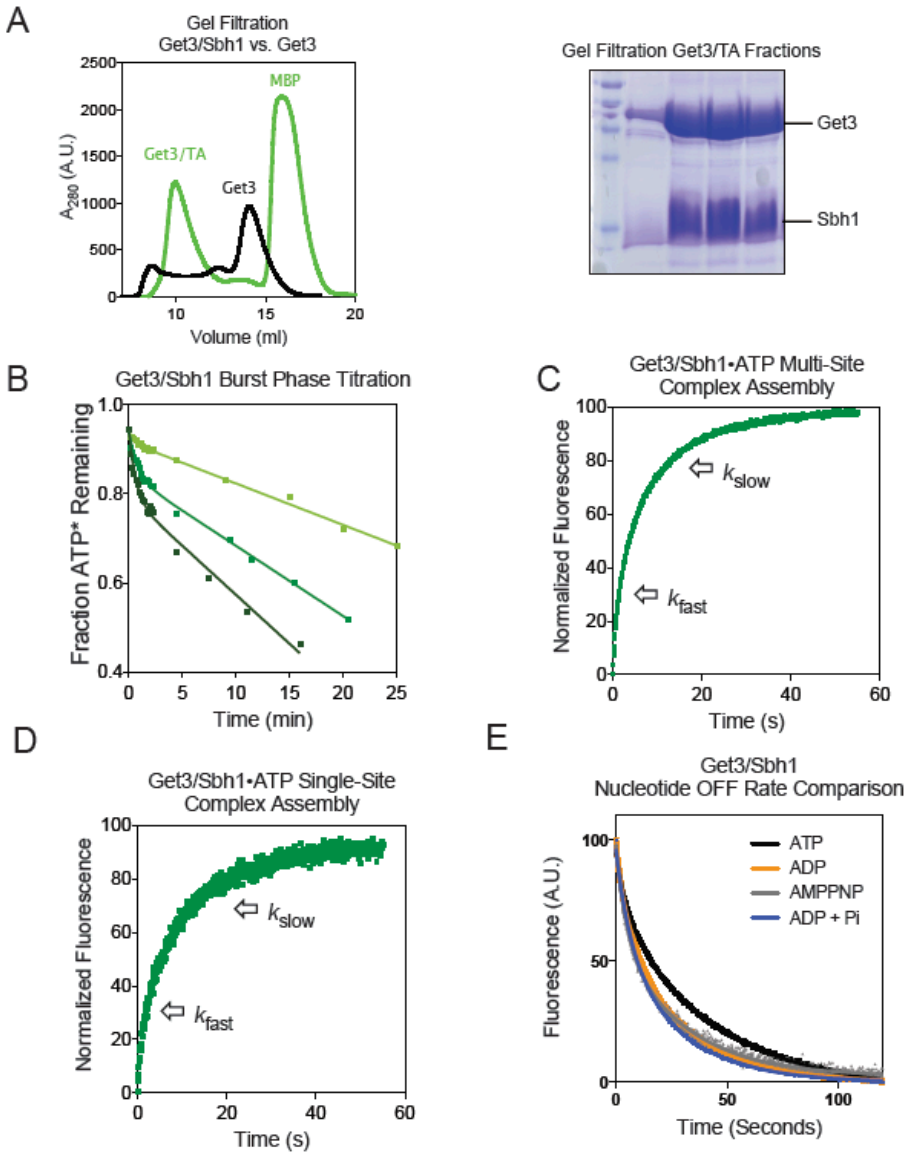

Figure 2.S6:
Purification and activity of the Get3/TA complex, related to Figure 5. (**A**) Purification of the recombinant Get3/TA complex over Superdex 200 (green). Maltose binding protein (MBP) was a cleavage product from MBP-tagged Get3 during the purification, as described in the Methods. Chromatogram for dimeric Get3 is shown in black. Right panel shows SDS-PAGE analysis of the elution peak at ~10 ml, which contain both Get3 and Sbh1p. (**B**) Pre-steady-state ATPase reaction from the Get3/TA complex, performed as in Figure 6A but with different ratios of Get3/TA complex relative to ATP: 1:10 (light green), 1:5 (green), 1:2.5 (dark green). Data were analyzed as in Figure 5A. (**C, D**) Representative time course for mantATP binding to the Get3/TA complex under multi-site (C) and single-site (D) conditions. Reaction in (C) used 2 μM Get3/TA complex and 13 μM mantATP and the obtained rate constants are plotted in Figure 6C. Reaction in (D) used 12.5 μM Get3/TA complex and 0.4 μM mantATP, and double exponential fit of the

data gave rate constants of 0.4 s^{-1} and 0.073 s^{-1}.(**E**) Dissociation rate measurements for the Get3/TA complex in various nucleotide states. 2 μM Get3/TA was preincubated with 20 μM of the following: mantATP (black), mantADP (gold), mantAMPPNP (grey), and ADP + 10 mM P_i (blue). Dissociation rate constants are reported in Table S2.

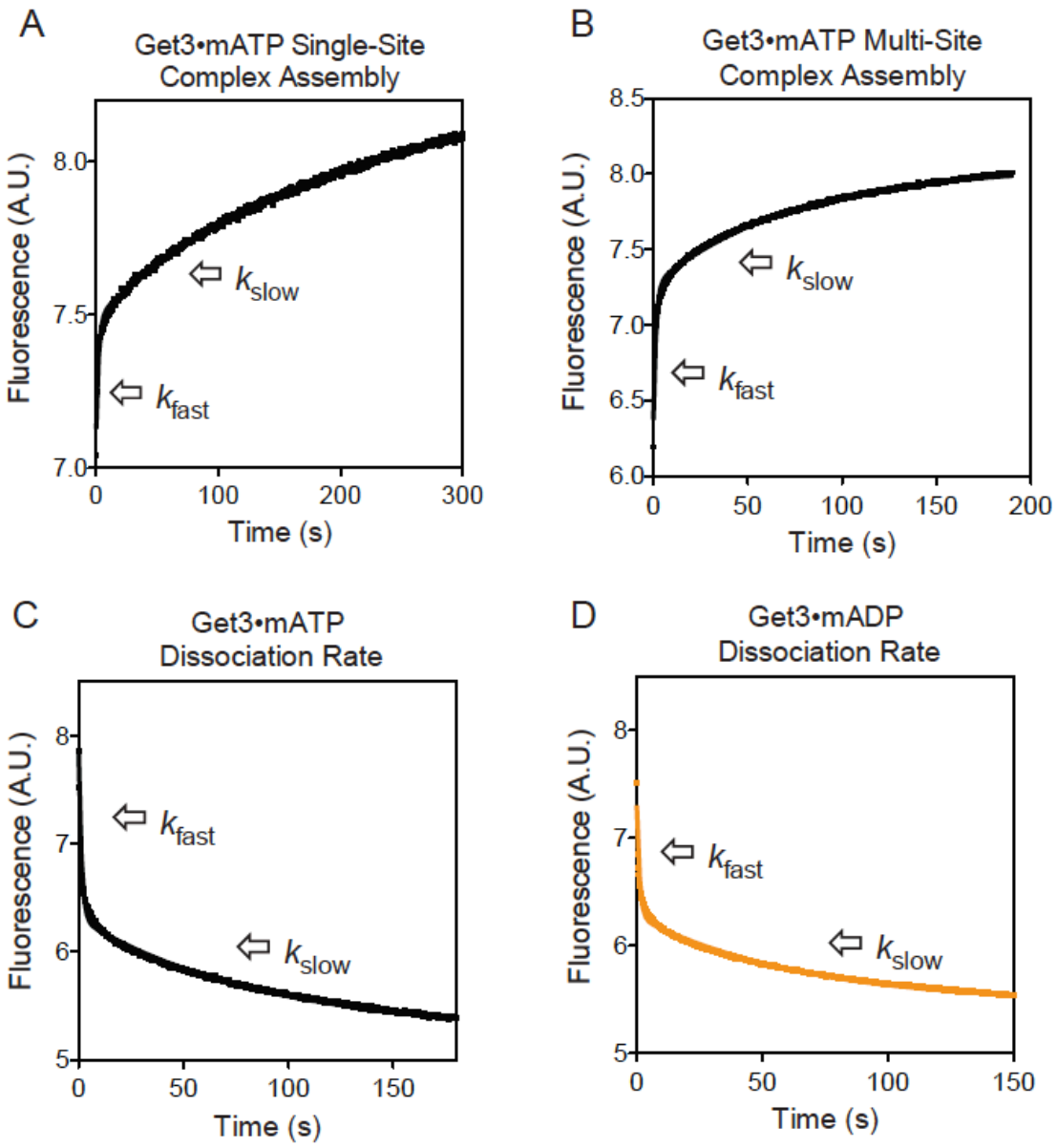

Figure 2.S7:
MantATP binding to Get3 is biphasic, related to Figure 2, and described in Extended Experimental Procedures. (**A, B**) Time course for mantATP binding to Get3 under single-site (A) and multi-site (B) conditions. The data were fit to double exponential functions. Rate constants derived from the fast phase are reported in the text. (**C, D**) Time courses for mantATP (C) or mantADP (D) dissociation from Get3 under multi-site conditions. The data were fit to double exponential functions. Rate constants derived from the fast phase are reported, as explained in the Extended Experimental Procedures.

Appendix B: Supplemental Data for Chapter 3

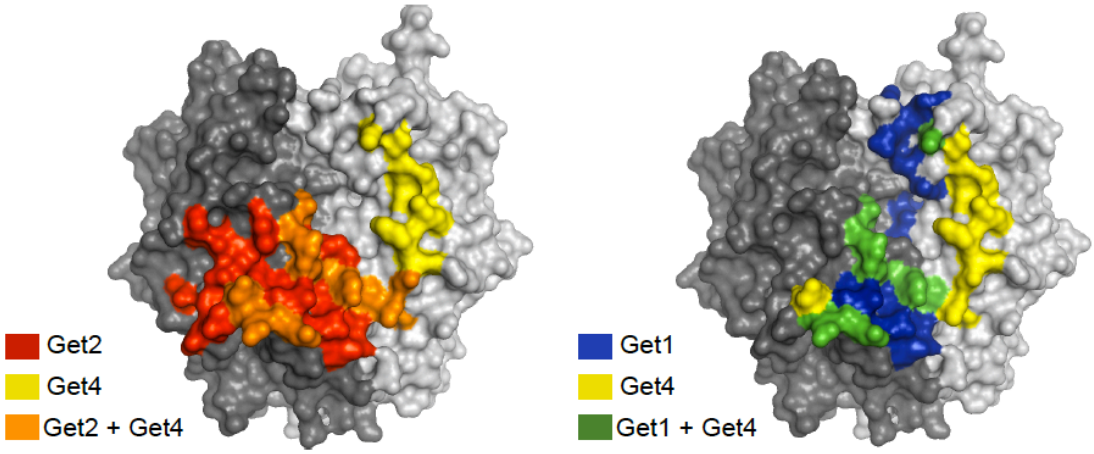

Figure 3.S1. Overlay of the binding sites of Get4 and Get2 (left), and Get4 and Get1 (right) on the Get3 dimer [48].

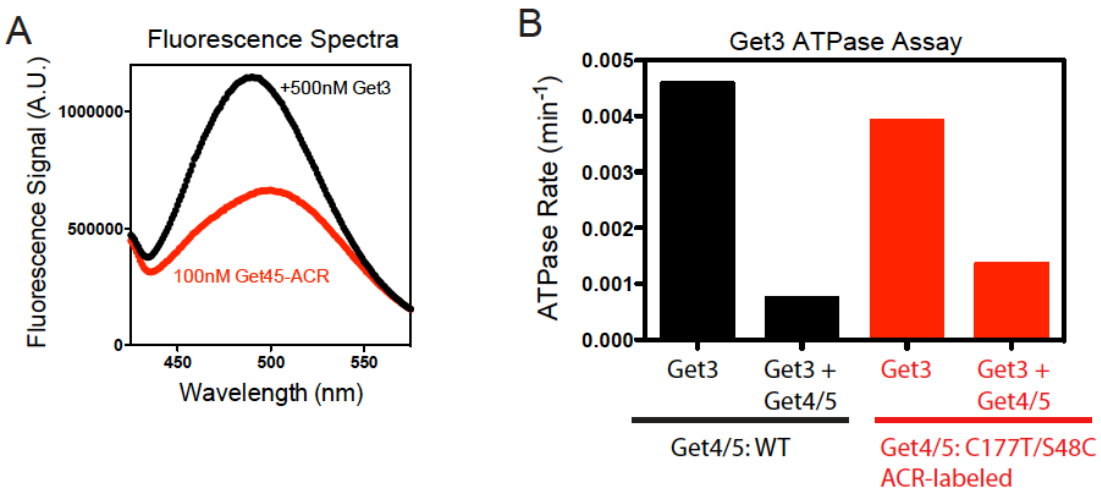

Figure 3.S2. Interaction of Get3 with Get4/5, related to Figure 1. (**A**) Fluorescence emission spectra of 100 nM acrylodan-labeled Get4/5 with (black) and without (red) 500 nM Get3. (**B**) Multi-turnover ATPase assay with 2.0 μM Get3 alone or in complex with 8.0 μM wild type (black) or acrylodan-labeled (red) Get4/5. All assays contained 200 μM ATP.

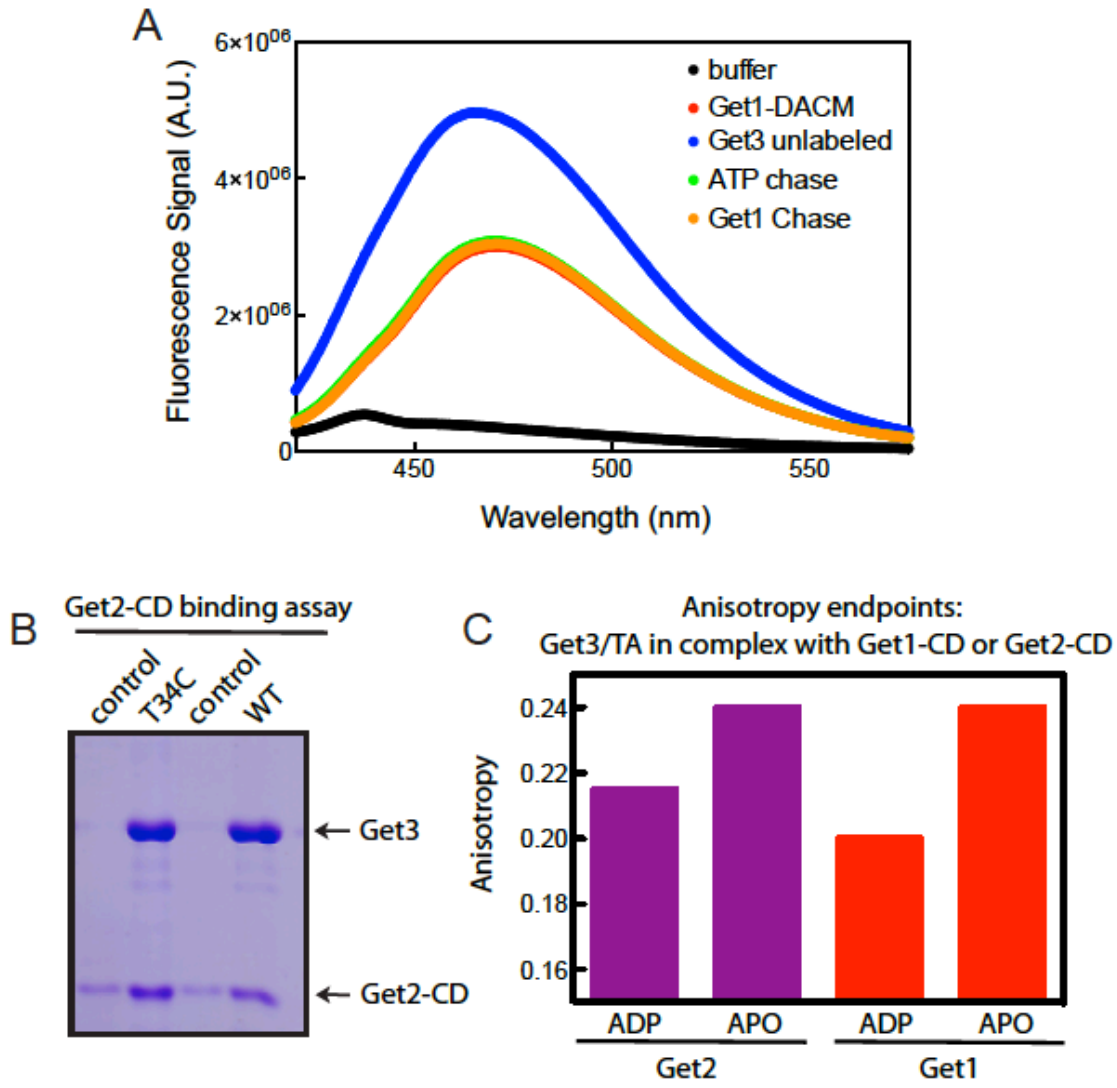

Figure 3.S3. The interaction of Get3 with Get1- and Get2-CD, related to Figs 3 and 4. (**A**) Fluorescence emission spectra of 150 nM DACM-labeled Get1 alone (red) or in the presence of the following: 400 nM Get3 present (blue), 400 nM Get3 and 2.3 mM ATP (green), or 400 nM Get3, 2.3 mM ATP and 17 μM unlabeled Get1 (orange). (**B**) Pull-down assay with His_6-tagged Get3 and untagged wildtype Get2 or Get2 T34C. Controls with no Get3-His_6 are shown for comparison. (**C**) Summary of the fluorescence anisotropy endpoints for the complexes of Get1-CD and Get2-CD with the Get3/TA complex in the ADP- or apo-states.

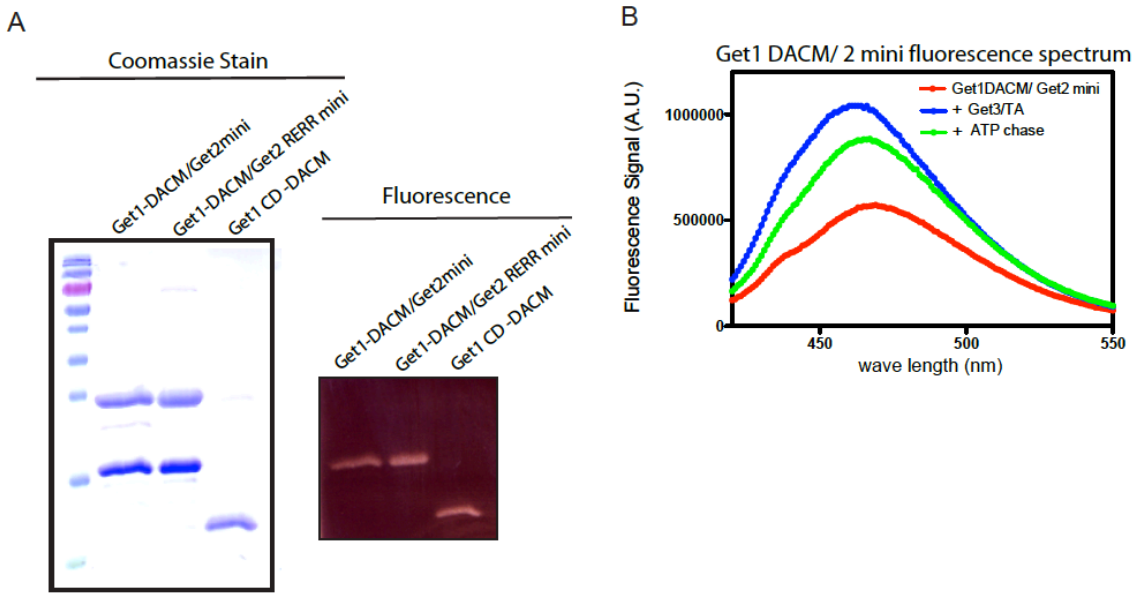

Figure 3.S4. The interaction of Get3 with mini-Get1/2, related to Figure 4. (**A**) Coomassie stained image (left) and UV-excited fluorescence image (right) of SDS-PAGE of DACM-labeled proteins: mini-Get1/2 (lane 1), mini-Get1/2RERR (lane 2), and Get1-CD (lane 3). (**B**) Fluorescence emission spectra of 150 nM DACM-labeled mini-Get1/2 alone (red) or in the presence of the following: 2 μM Get3/TA (blue), or 2 μM Get3/TA and 2.0 mM ATP (green).

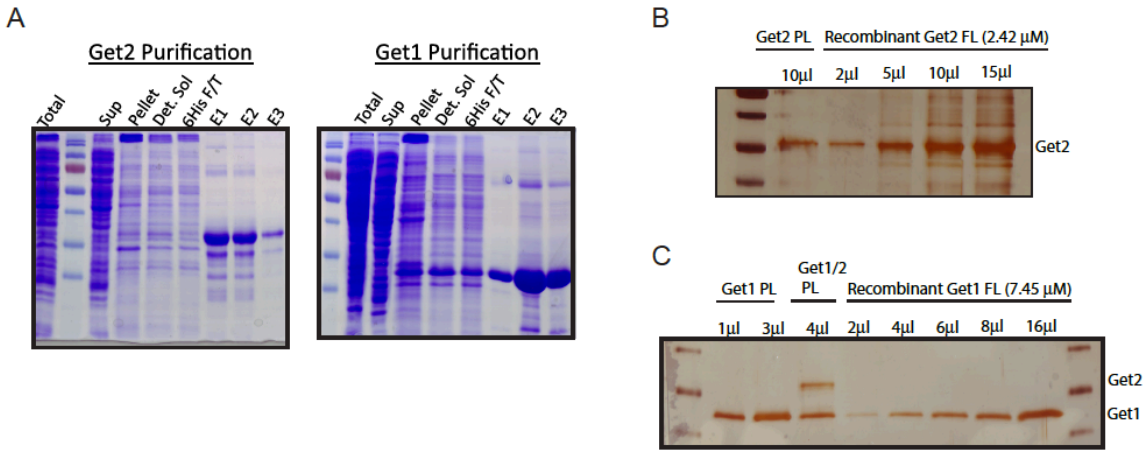

Figure 3.S5. Reagents for generating Get1/2-PL, related to Figure 5. (**A**) SDS-PAGE showing the purification of full-length Get1 and Get2 in detergent, as described in methods. (**B**) Silver-stained gel containing Get2-PL and increasing amounts of recombinant Get2. Band intensity of Get2 in PL was quantified using known amounts of recombinant Get2 as a standard for concentration determination. (**C**) same as (**B**) but using Get1-PL.

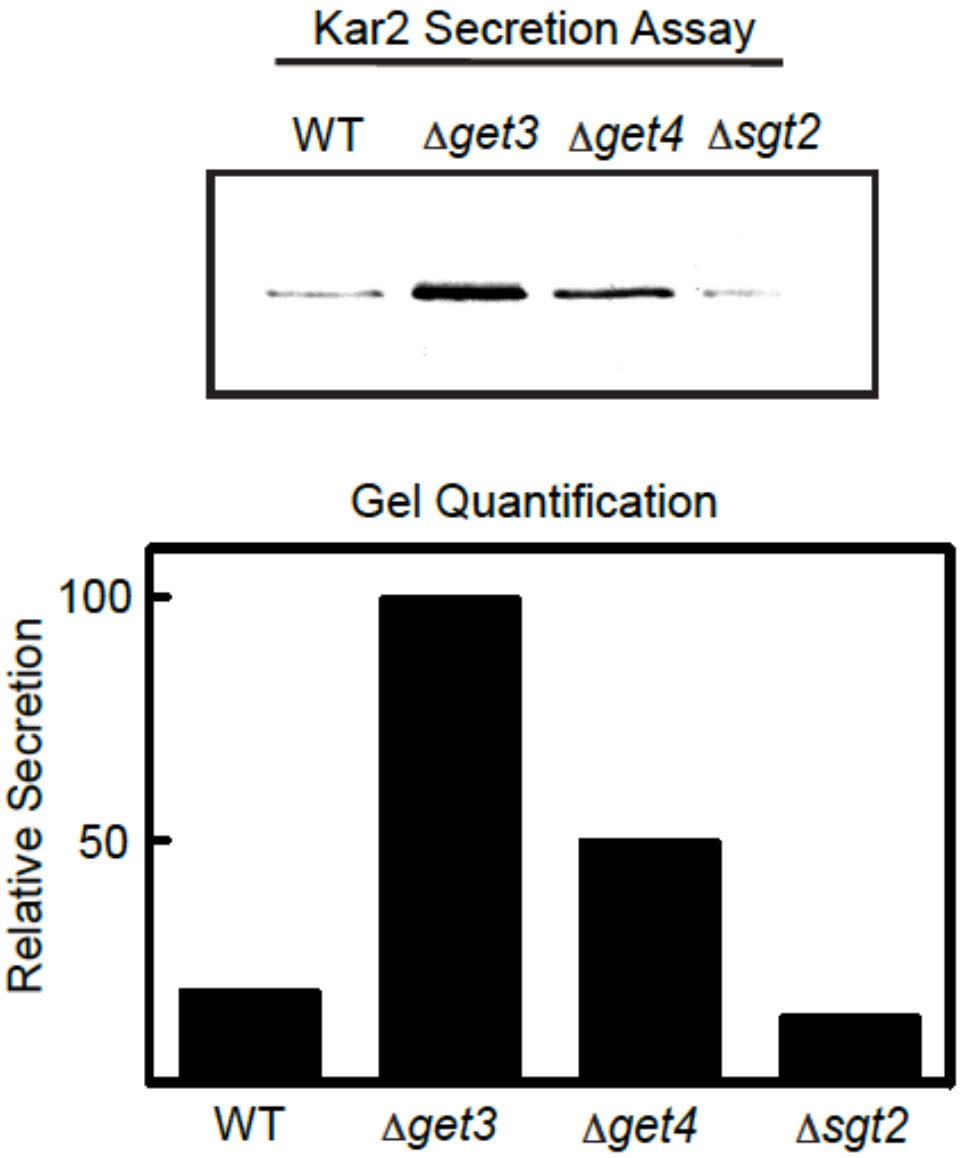

Figure 3.S6. *In vivo* assay for TA targeting based on Kar2p secretion, related to Figure 7. Western blot of secreted Kar2p from the indicated yeast strains (wild type, Δ*get3*, Δ*get4*, Δ*sgt2*), detected using an anti-Kar2p antibody. Quantification of secreted Kar2p is shown below the western blot.

Appendix C: Supplemental Data for Chapter 4

A

Component	MW	Relative abundance
Get4/5-FL	35935	100
Get4/5-FL-NEM	36060	61

B

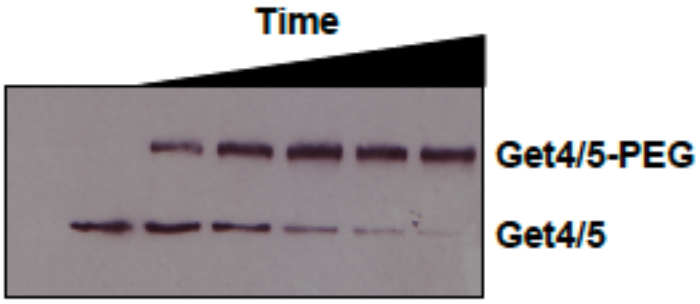

Figure 4.S1. Controls for accessibility experiment, related to Figure 2. (A) Molecular weight (determined by MSD) of the unmodified and modified (NEM-reacted) Get4 protein. (B) Time course for PEGylation of Q34C on Get4.

Bibliography

1. Hegde, R. S. & Keenan, R. J. Tail-anchored membrane protein insertion into the endoplasmic reticulum. *Nat Rev Mol Cell Biol* **12,** 787–798 (2011).
2. Chartron, J. W., Jr, W. M. C. & Suloway, C. J. The complex process of GETting tail-anchored membrane proteins to the ER. *Current Opinion in Structural Biology* **22,** 217–224 (2012).
3. Rome, M. E., Rao, M., Clemons, W. M. & Shan, S.-O. Precise timing of ATPase activation drives targeting of tail-anchored proteins. *Proc Natl Acad Sci USA* **110,** 7666–7671 (2013).
4. Wang, F., Brown, E. C., Mak, G., Zhuang, J. & Denic, V. A Chaperone Cascade Sorts Proteins for Posttranslational Membrane Insertion into the Endoplasmic Reticulum. *Mol Cell* **40,** 159–171 (2010).
5. Chartron, J. W., Gonzalez, G. M. & Clemons, W. M. A structural model of the Sgt2 protein and its interactions with chaperones and the Get4/Get5 complex. *Journal of Biological Chemistry* **286,** 34325–34334 (2011).
6. Schuldiner, M. *et al.* The GET complex mediates insertion of tail-anchored proteins into the ER membrane. *Cell* **134,** 634–645 (2008).
7. Wang, F., Whynot, A., Tung, M. & Denic, V. The Mechanism of Tail-Anchored Protein Insertion into the ER Membrane. *Mol Cell* 1–33 (2011). doi:10.1016/j.molcel.2011.07.020
8. Stefer, S. *et al.* Structural Basis for Tail-Anchored Membrane Protein Biogenesis by the Get3-Receptor Complex. *Science* **333,** 758–762 (2011).
9. Mariappan, M. *et al.* The mechanism of membrane-associated steps in tail-anchored protein insertion. *Nature* 1–9 (2011). doi:10.1038/nature10362
10. Mukhopadhyay, R., Ho, Y.-S., Swiatek, P. J., Rosen, B. P. & Bhattacharjee, H. Targeted disruption of the mouse Asna1 gene results in embryonic lethality. *FEBS Lett* **580,** 3889–3894 (2006).
11. Schuldiner, M. *et al.* Exploration of the function and organization of the yeast early secretory pathway through an epistatic miniarray profile. *Cell* **123,** 507–519 (2005).
12. Stefanovic, S. & Hegde, R. S. Identification of a targeting factor for posttranslational membrane protein insertion into the ER. *Cell* **128,** 1147–1159 (2007).
13. Mateja, A. *et al.* The structural basis of tail-anchored membrane protein recognition by Get3. *Nature* **461,** 361–366 (2009).
14. Suloway, C. J. M., Chartron, J. W., Zaslaver, M. & Clemons, W. M. Model for eukaryotic tail-anchored protein binding based on the structure of Get3. *Proc Natl Acad Sci USA* **106,** 14849–14854 (2009).
15. Bange, G. & Sinning, I. sinning. *Nature Structural & Molecular Biology* **20,**

776–780 (2013).
16. Suloway, C. J. M., Rome, M. E. & Clemons, W. M. Tail-anchor targeting by a Get3 tetramer: the structure of an archaeal homologue. *EMBO J* **31,** 707–719 (2012).
17. The transmembrane segment of a tail-anchored protein determines its degradative fate through dislocation from the endoplasmic reticulum. **285,** 20732–20739 (2010).
18. Kutay, U., Ahnert-Hilger, G., Hartmann, E., Wiedenmann, B. & Rapoport, T. A. Transport route for synaptobrevin via a novel pathway of insertion into the endoplasmic reticulum membrane. *EMBO J* **14,** 217–223 (1995).
19. Mariappan, M. *et al.* A ribosome-associating factor chaperones tail-anchored membrane proteins. *Nature* **466,** 1120–1124 (2010).
20. Comprehensive characterization of genes required for protein folding in the endoplasmic reticulum. **323,** 1693–1697 (2009).
21. Bozkurt, G. *et al.* Structural insights into tail-anchored protein binding and membrane insertion by Get3. *Proc Natl Acad Sci USA* **106,** 21131–21136 (2009).
22. The crystal structures of yeast Get3 suggest a mechanism for tail-anchored protein membrane insertion. **4,** e8061 (2009).
23. Yamagata, A. *et al.* Structural insight into the membrane insertion of tail-anchored proteins by Get3. *Genes to Cells* **15,** 29–41 (2010).
24. Kubota, K., Yamagata, A., Sato, Y., Goto-Ito, S. & Fukai, S. Get1 Stabilizes an Open Dimer Conformation of Get3 ATPase by Binding Two Distinct Interfaces. *J Mol Biol* 1–10 (2012). doi:10.1016/j.jmb.2012.05.045
25. Chartron, J. W., Suloway, C. J. M., Zaslaver, M. & Clemons, W. M. Structural characterization of the Get4/Get5 complex and its interaction with Get3. *Proc Natl Acad Sci USA* **107,** 12127–12132 (2010).
26. Kiekebusch, D., Michae, Essen, L.-O., Löwe, J. & Thanbichler, M. Localized dimerization and nucleoid binding drive gradient formation by the bacterial cell division inhibitor MipZ. *Mol Cell* **46,** 245–259 (2012).
27. Saraogi, I., Akopian, D. & Shan, S.-O. A tale of two GTPases in cotranslational protein targeting. *Protein Sci.* **20,** 1790–1795 (2011).
28. Wereszczynski, J. & McCammon, J. A. Nucleotide-dependent mechanism of Get3 as elucidated from free energy calculations. *Proc Natl Acad Sci USA* (2012). doi:10.1073/pnas.1117441109
29. Ghaemmaghami, S. *et al.* Global analysis of protein expression in yeast. *Nature* **425,** 737–741 (2003).
30. Chang, Y.-W. *et al.* Interaction surface and topology of Get3-Get4-Get5 protein complex, involved in targeting tail-anchored proteins to endoplasmic reticulum. *Journal of Biological Chemistry* **287,** 4783–4789 (2012).
31. Chartron, J. W., VanderVelde, D. G., Rao, M. & Clemons, W. M. Get5 carboxyl-terminal domain is a novel dimerization motif that tethers an extended Get4/Get5 complex. *Journal of Biological Chemistry* **287,** 8310–8317 (2012).
32. Classification and evolution of P-loop GTPases and related ATPases. **317,**

41–72 (2002).
33. Shan, S.-O., Schmid, S. L. & Zhang, X. Signal Recognition Particle (SRP) and SRP Receptor: A New Paradigm for Multistate Regulatory GTPases. *Biochemistry* **48,** 6696–6704 (2009).
34. Zhang, X., Schaffitzel, C., Ban, N. & Shan, S.-O. Multiple conformational switches in a GTPase complex control co-translational protein targeting. *Proc Natl Acad Sci USA* **106,** 1754–1759 (2009).
35. Gasper, R., Meyer, S., Gotthardt, K., Sirajuddin, M. & Wittinghofer, A. It takes two to tango: regulation of G proteins by dimerization. *Nat Rev Mol Cell Biol* **10,** 423–429 (2009).
36. G domain dimerization controls dynamin's assembly-stimulated GTPase activity. **465,** 435–440 (2010).
37. Role of SRP RNA in the GTPase Cycles of Ffh and FtsY †. **40,** 15224–15233 (2001).
38. Wu, C., Amrani, N., Jacobson, A. & Sachs, M. S. *Methods in Enzymology*. **429,** 203–225 (Elsevier, 2007).
39. Rothblatt, J. A. & Meyer, D. I. Secretion in yeast: reconstitution of the translocation and glycosylation of alpha-factor and invertase in a homologous cell-free system. *Cell* **44,** 619–628 (1986).
40. Zhang, X., Rashid, R., Wang, K. & Shan, S. O. Sequential Checkpoints Govern Substrate Selection During Cotranslational Protein Targeting. *Science* **328,** 757–760 (2010).
41. Interaction of myosin subfragment 1 with fluorescent ribose-modified nucleotides. A comparison of vanadate trapping and SH1-SH2 cross-linking. **29,** 3309–3319 (1990).
42. The kinetic mechanism of the SufC ATPase: the cleavage step is accelerated by SufB. **281,** 8371–8378 (2006).
43. Zhang, X., Kung, S. & Shan, S.-O. Demonstration of a multistep mechanism for assembly of the SRP x SRP receptor complex: implications for the catalytic role of SRP RNA. *J Mol Biol* **381,** 581–593 (2008).
44. Kalbfleisch, T., Cambon, A. & Wattenberg, B. W. A Bioinformatics Approach to Identifying Tail-Anchored Proteins in the Human Genome. *Traffic* **8,** 1687–1694 (2007).
45. Beilharz, T. Bipartite Signals Mediate Subcellular Targeting of Tail-anchored Membrane Proteins in Saccharomyces cerevisiae. *Journal of Biological Chemistry* **278,** 8219–8223 (2003).
46. Kriechbaumer, V. *et al.* Subcellular distribution of tail-anchored proteins in Arabidopsis. *Traffic* **10,** 1753–1764 (2009).
47. Kutay, U., Hartmann, E. & Rapoport, T. A. A class of membrane proteins with a C-terminal anchor. *Trends Cell Biol* **3,** 72–75 (1993).
48. Gristick, H. *et al. The structure of a tail-anchor membrane protein-binding complex reveals the regulation of Get3 by Get4*. (In Revision, NSMB, 2014).
49. Vilardi, F., Stephan, M., Clancy, A., Janshoff, A. & Schwappach, B. WRB and CAML Are Necessary and Sufficient to Mediate Tail-Anchored Protein Targeting to the ER Membrane. *PLoS ONE* **9,** e85033 (2014).

50. Yamamoto, Y. & Sakisaka, T. Molecular Machinery for Insertion of Tail-Anchored Membrane Proteins into the Endoplasmic Reticulum Membrane in Mammalian Cells. *Mol Cell* 1–11 (2012). doi:10.1016/j.molcel.2012.08.028
51. Schreiber, G. & Fersht, A. R. Rapid, electrostatically assisted association of proteins. *Nat. Struct. Biol.* **3,** 427–431 (1996).
52. Kleiger, G., Saha, A., Lewis, S., Kuhlman, B. & Deshaies, R. J. Rapid E2-E3 Assembly and Disassembly Enable Processive Ubiquitylation of Cullin-RING Ubiquitin Ligase Substrates. *Cell* **139,** 957–968 (2009).
53. Sandikci, A. *et al.* bukau paper. *Nature Structural & Molecular Biology* **20,** 843–850 (2013).
54. Chartron, J. W., VanderVelde, D. G. & Clemons, W. M., Jr. Structures of the Sgt2/SGTA Dimerization Domain with the Get5/UBL4A UBL Domain Reveal an Interaction that Forms a Conserved Dynamic Interface. *CellReports* 1–13 (2012). doi:10.1016/j.celrep.2012.10.010
55. Battle, A., Jonikas, M. C., Walter, P., Weissman, J. S. & Koller, D. Automated identification of pathways from quantitative genetic interaction data. *Molecular Systems Biology* **6,** 1–13 (2010).
56. Südhof, T. C. & Rothman, J. E. Membrane fusion: grappling with SNARE and SM proteins. *Science* **323,** 474–477 (2009).
57. Grosshans, B. L., Ortiz, D. & Novick, P. Rabs and their effectors: achieving specificity in membrane traffic. *Proc Natl Acad Sci USA* **103,** 11821–11827 (2006).
58. Wickner, W. Membrane Fusion: Five Lipids, Four SNAREs, Three Chaperones, Two Nucleotides, and a Rab, All Dancing in a Ring on Yeast Vacuoles. *Annu. Rev. Cell Dev. Biol.* **26,** 115–136 (2010).
59. Jun, Y., Xu, H., Thorngren, N. & Wickner, W. Sec18p and Vam7p remodel trans-SNARE complexes to permit a lipid-anchored R-SNARE to support yeast vacuole fusion. *EMBO J* **26,** 4935–4945 (2007).
60. Studier, F. W. Protein production by auto-induction in high-density shaking cultures. *Protein Expression and Purification* **41,** 207–234 (2005).
61. Nguyen, T. X. *et al.* Mechanism of an ATP-independent protein disaggregase: I. structure of a membrane protein aggregate reveals a mechanism of recognition by its chaperone. *J Biol Chem* **288,** 13420–13430 (2013).
62. Rome, L. H. & Kickhoefer, V. A. Development of the Vault Particle as a Platform Technology. *ACS Nano* **7,** 889–902 (2013).
63. Johnson, K. A., Simpson, Z. B. & Blom, T. Global kinetic explorer: a new computer program for dynamic simulation and fitting of kinetic data. *Anal Biochem* **387,** 20–29 (2009).